EFFECT OF CATIONIC SURFACTANT (CTAB) IN THE ELECTROKINETIC REMEDIATION OF DIESEL-CONTAMINATED SOILS

By

YUWEI QIAN

A Thesis

Submitted to the Faculty of Graduate Studies

in Partial Fulfilment of the Requirements

for the Degree of

MASTER OF SCIENCE

Department of Biosystems Engineering

University of Manitoba

August, 1998

THE UNIVERSITY OF MANITOBA

FACULTY OF GRADUATE STUDIES

*****

COPYRIGHT PERMISSION PAGE

EFFECT OF CATIONIC SURFACTANT (CTAB) IN THE ELECTROKINETIC REMEDIATION OF DIESEL-CONTAMINATED SOILS

BY

YUWEI QIAN

A Thesis/Practicum submitted to the Faculty of Graduate Studies of The University of Manitoba in partial fulfillment of the requirements of the degree

of

MASTER OF SCIENCE

Abstract

With the increase in knowledge about hydrocarbon contamination, concern over soil and groundwater contamination has grown. Hydrocarbon contaminated soil and groundwater is considered to be a leading cause for increased health risk and environmental contamination. Therefore, an efficient remediation technique needs to be developed. Surfactant flushing treatment coupled with the application of low-level electrical potential difference is a potential soil remediation technique for the removal of hydrocarbons from clayey soils. The goals of this research were to (a) evaluate the efficiencies of electrokinetic and surfactant-enhanced electrokinetic remediation methods by determining the removal of hydrocarbons from the contaminated clay soil in the laboratory; (b) determine the factors affecting the remediation technology; (c) select an efficient extraction technique during SPME-GC-FID analysis. The vibration enhanced SPME-GC-FID method was selected to analyze the samples.

Water-flushing and surfactant-flushing experiments were conducted on one-dimensional soil columns. The model diesel fuel was composed of a mixture of BTEX and three selected PAHs. In the water-flushing experiments, the application of an electrokinetic treatment was found to enhance the removal of model diesel fuel from the clay columns. In contrast, the application of an electrokinetic treatment coupled with surfactant-flushing retarded the movement of BTEX and the three selected PAHs in the clay columns. However, the flux through the electrokinetic columns during water flushing as well as surfactant flushing was higher than the flux due to hydraulic gradient

alone. The results also indicated that the location of weighted average of the residual diesel fuel components was a function of the solubility of hydrocarbons compounds.

The cationic surfactant cetyltrimethylammonium bromide (CTAB) was used in the surfactant-flushing treatments. The critical micelle concentration (CMC) of CTAB was determined as 9.0×10^{-4} M which is very close to the one reported in the literature. Molar solubilization ratio (MSR) and the micelle-water partition coefficient (K_{mic}) were also determined for BTEX and the three PAHs to show the effect of surfactant on the solubility of hydrocarbons. The relationship between solubility and the octanol-water partition coefficient (K_{ow}) was developed in an aqueous phase as well as in the surfactant solution to predict the solubility of other compounds based on the K_{ow} available in the literature. The relationship between K_{mic} and K_{ow} was developed to predict the surfactant effect for other compounds. The relationship between the organic carbon-water partition coefficient (K_{oc}) and K_{ow} was developed to account for the surfactant effect. The results indicate that the CTAB is more efficient on compounds with higher K_{ow} such as the PAHs during surfactant-flushing treatments. This research has expanded our knowledge about the role of cationic surfactants in electrokinetic remediation of hydrocarbon contaminated soils.

Acknowledgments

I wish to express my sincere gratitude to my supervisor, Dr. R. Sri Ranjan, for his guidance and support during my graduate study, as well as his help in my thesis writing. I would like to thank Dr. G.R.B. Webster and Dr. Q. Zhang, members of my advisory committee, for their advice and encouragement.

I would also like to thank Messrs. Leonard Sarna, Jack Putnam, Matt McDonald, and Dale Bourns for their excellent technical support. Thanks to the staff from the Department of Biosystems Engineering as well as from the Department of Soil Science for their help.

I am also greatly indebted to my husband, Chenyi Liu, for his love, encouragement, understanding, and moral support. I am also indebted to my daughter, Hanyun Liu, for her love and understanding.

Table of Contents

List of Tables

List of Figures

List of Symbols

A = cross-sectional area (cm^2)

C = the concentration at time t (ppm)

C_{aq} = the initial concentration of analyte in the aqueous phase

C_i = concentration of contaminant i dissolved in aqueous (mg/L)

C_o = the initial contaminant concentration (ppm)

C_{cmc} = critical micelle concentration (M)

C_{mic} = the concentration of surfactant in micellar form (M)

C_{mon} = the concentration of surfactant as monomers (M)

C_{surf} = surfactant concentration at which S_{abv} is evaluated (M)

$[CTAB^-]_{mic}$ = moles of CTAB in micellar form per liter of solution = $(C_{surf} - C_{cmc})$ (M)

D = hydrodynamic dispersion coefficient along the flow path (cm^2/sec)

D^* = diffusion coefficient (cm^2/sec)

D_i = the distance of each segment from the anode (cm)

D_0 = diffusion coefficient for a given hydrocarbons species whose concentration is C (cm^2/sec)

D_{wap} = the location of weighted average of the hydrocarbon from the anode (cm)

dC/dx = the concentration gradient (dimensionless)

dE/dx = uniform electric field strength (V/m)

F = the mass flux (g/cm^2. sec)

F_x = total mass of hydrocarbons per unit cross-sectional area per unit time in x direction (g/cm^2. sec)

f_{oc} = the weight fraction of organic compounds in the soil (dimensionless)

$f_{hc,\ mic}$ = the fraction of hydrocarbons in the surfactant micelles (dimensionless)

i_e = electrical potential gradient (V/cm)

i = - dh/dl = the hydraulic gradient (driven force)(dimensionless)

I = electricity (A)

K_d = distribution coefficient (L/kg)

$K_{d,cmc}$ = modified distribution coefficient due to the presence of surfactants (L/kg)

k_{eo} = coefficient of electroosmotic permeability (cm^2/s V)

K_f = the distribution constant of the analyte

K_h = hydraulic conductivity (cm/s)

k_i = electroosmotic water transport efficiency (cm^3/s A)

K_{mic} = mole fraction based micelle-water partition coefficient (dimensionless)

K_{mic}' = concentration based micelle-water partition coefficient (M^{-1})

K_{mon} = monomers-water partition coefficient (M^{-1})

K_{oc} = organic carbon-water partition coefficient (L/kg)

$K_{oc,cmc}$ = modified organic carbon-water partition coefficient (L/kg)

K_{ow} = octanol-water partition coefficient

M = initial mass of hydrocarbons in the system at x = 0 (μg)

MSR = molar solubilization ratio (dimensionless)

N = the mean occupancy number of the hydrocarbons in micelle solution at saturation

N_d = measure of deviation from linearity

n_e = the effective porosity

n_s = the number of moles of the analyte sorbed on the stationary phase

q = discharge (cm/s)

q_e = electroosmotic flow rate (cm^3/s)

R = retardation factor (dimensionless)

R_{cmc} = modified retardation factor taking into account micellar effects (dimensionless)

S = concentration of hydrocarbons in the solution (mg/L)

S_{abv} = concentration of hydrocarbons in micelle solution (mg/L)

S_{cmc} = apparent hydrocarbon solubility at the CMC (M)

S_i = the individual aqueous solubility

S_m = the aqueous solubility of a compound in the mixture

S_{mic} = apparent solubility of hydrocarbons at a particular surfactant concentration above the CMC (M)

S_{mic}' = the hydrocarbons solubility at the micelle concentration (mg/L)

S_s = concentration of hydrocarbons in soil (mg/kg)

S_{total} = the apparent hydrocarbons solubility at the total surfactant concentration (M)

S_w = the intrinsic solubility in pure water (M)

S_w' = the hydrocarbons solubility in water (mg/L)

t = hydrocarbons travel time (sec)

T = time (days)

V = average linear bulk flow velocity (cm/sec)

V_c = average pore water velocity with sorption reaction = the velocity of the C/C_o = 0.5 point on the concentration profile of contaminant with sorption reaction (cm/sec)

V_{eo} = electroosmotic velocity (m/sec)

V_{ep} = micelle velocity due to electrophoretic flow (m/sec)

V_s = the volume of the stationary phase

V_{total} = average linear water velocity due to advection

V_w = average pore water velocity without sorption reaction (cm/sec)

V_{mol} = the molar volume of water (0.01805 M^{-1} at 25°C)

x = distance along flowline (cm)

X_a = mole fraction of the compound in the aqueous phase

X_{im} = the mole fraction of individual compound in the mixture

X_m = mole fraction of the compound in the micellar phase

Y = the aggregation number of CTAB molecular in every CTAB micelle

Y_{ec} = electrical conductivity (ds/m)

α = dynamic dispersivity (or dispersivity) (cm)

τ = tortuosity of medium .

ρ_b = soil bulk density (g/cm^3)

ϕ = soil porosity (dimensionless)

τ = the tortuosity

σ = electrical conductivity (S/cm)

ε = permittivity of the pore fluid (~ 10^{-9} C/Vm for water)

ζ_s = uniform zeta potential of the surface corresponding to the surface charge (V)

η = viscosity of the liquid (10^{-3} Pa s for water at 20°C).

1.0 Introduction

1.1 Overview

With the increase in investigation of hydrocarbon-contaminated sites in recent years, public concern over soil and groundwater contamination has grown. The transport, processing and storage of refined petroleum products are frequently sited as sources responsible for environmental contamination and increased health risk. Benzene, toluene, ethylbenzene, xylenes (BTEX) and polycyclic aromatic hydrocarbons (PAHs) are selected as target organics at petroleum contaminated sites, because those compounds are highly bioavailable and carcinogenic (Brainard and Beck 1993). Besides, ingestion and dermal contact with chemicals in soil and ground pose the highest potential health risks (Brainard and Beck 1993). Contaminated soil and groundwater needs to be remedied to reduce the health risk to people. There are a number of remediation technologies that are commonly utilized in practice, including pump-and-treat, soil vapor extraction, in situ isolation/containment, chemical extraction or soil washing, in situ bioremediation (Kostecki and Calabrese 1993). However, those conventional remediation technologies have their limitations. Therefore, a fast, easy, and efficient remediation technique need to be developed.

1.2 Scope

In addition to conventional remediation techniques, electrokinetic remediation is also being used in practice (Alshawabkeh and Acar 1992; Acar *et al.* 1993a). Electrokinetic remediation is a process in which a low-level voltage potential gradient is applied to contaminated sites causing the contaminants to migrate along with bulk flow.

Electrokinetic remediation is achieved as a result of a combination of phenomena such as electroosmosis, electrophoresis, and electrolysis reactions. In a moist soil, the application of electrical potential gradient results in the movement of cations (positively charged ions) toward the negative electrode and anions toward the positive electrode. Electroosmosis occurs when the moving cations impart a larger viscous drag to the water causing it to move preferentially toward the cathode. Clay soils, due to their low permeability, cannot be easily remediated by conventional remediation techniques such as soil washing. However, electroosmosis can greatly increase the flow rate in very fine-grained clay soils. Electrophoresis is a process in which charged colloids such as surfactant micelles migrate toward the oppositely charged electrodes under the influence of an applied electrical potential gradient. The surfactant micelles present in the soil-water system cause hydrocarbons sorbed to them to migrate to the oppositely charged electrode. Therefore, electrophoresis becomes a critical process in decontamination (Pamucku and Wittle 1992). The electrokinetic remediation technique has a potential to enhance the efficiency of remediation of a contaminated site by using a combination of electroosmosis and electrophoresis. Since electrokinetic remediation is an *in situ* remediation technique, it is economical compared to other *ex situ* methods (Dzenitis 1997).

Since most hydrocarbons are non-polar organic compounds, their migration is restricted to the dissolved compounds. Therefore, the enhancement of solubility of organic compounds is a critical factor to increase the efficiency of remediation of hydrocarbon-contaminated sites. The presence of surfactants in the pore water increases

the apparent solubility of hydrocarbons by micelle formation and enhances their removal. When a cationic surfactant is used, micelles carry positive charges causing them to migrate toward the negative electrode. In electroosmosis the dissolved hydrocarbons migrate along with bulk flow, and in electrophoresis hydrocarbons dissolved in the micelles migrate toward the electrode. The removal of hydrocarbons in micelle form in the presence of an electrical potential gradient is called surfactant-enhanced electrokinetic remediation.

1.3 Objectives

The main goal of this research was to evaluate the efficiency of electrokinetic and surfactant-enhanced electrokinetic remediation of hydrocarbon-contaminated clay soils. Various remediation techniques were used such as water flushing, water flushing coupled with electrokinetic treatment, surfactant flushing, and surfactant-enhanced electrokinetic treatment. Solid-phase microextraction (SPME) coupled with gas chromatography (GC) and flame ionization detector (FID) was used to determine the concentrations of hydrocarbons in pore water samples, and monitor the movement of hydrocarbons in clay columns. In the surfactant-enhanced electrokinetic remediation, a cationic surfactant, cetyltrimethylammonium bromide (CTAB), was chosen to enhance the electrophoretic flow. The objectives of this research were to

(a) evaluate the efficiencies of electrokinetic and surfactant-enhanced electrokinetic remediation technology in the laboratory,

(b) determine the factors affecting the remediation technology, and

(c) select an efficient extraction technique for the SPME-GC-FID analysis.

2.0 Soil Remediation

2.1 Hydrocarbon compounds

Hydrocarbons are organic compounds composed of hydrogen and carbon atoms. They are the main components in refined petroleum products such as diesel, and important raw material in many industries (Kostecki and Calabrese 1993). Like other refined petroleum products, diesel is a complex mixture of hundreds of different hydrocarbons with the number of carbon atoms ranging from 10 to 19 (Stelljes and Watkin 1993).

The majority of the mixture is composed of aliphatic hydrocarbons and aromatic hydrocarbons. The aromatic hydrocarbons include BTEX (benzene, toluene, ethylbenzene, xylenes) and the polycyclic aromatic hydrocarbons (PAH) such as naphthalene, 2-methylnaphthalene, and phenanthrene (Stelljes and Watkin 1993). BTEX and PAHs were used as target analytes in the evaluation of various soil-remediation techniques since they are common soil and groundwater pollutants. Some physical and chemical properties of the hydrocarbon compounds of interest are presented in Table 2.1.

2.2 Conventional soil remediation techniques

Several methodologies are available for the remediation of petroleum contaminated soil and groundwater, including pump-and-treat, soil vapor extraction, *in situ* isolation/containment, chemical extraction or soil washing, and *in situ* bioremediation (Kostecki and Calabrese 1993). However, most of those remediation techniques are limited to soils with relatively high hydraulic conductivities (Acar 1992).

Table 2.1. Properties of hydrocarbons used in soil remediation experiments

Compound	Formula	Molecular weight	Aqueous solubility (mg/L)	Vapor pressure (mm Hg)	Henry's Constant (atm-m^3/mol)
benzene	C_6H_6	78.11	1.75E+03	9.52E+01	5.40E-03
toluene	C_7H_8	92.14	5.15E+02	2.20E+01	6.70E-03
ethylbenzene	C_8H_{10}	106.17	1.52E+02	7.08E+00	6.60E-03
p-xylene	C_8H_{10}	106.17	1.98E+02	8.76E+00	7.10E-03
m-xylene	C_8H_{10}	106.17	1.58E+02	8.29E+00	7.00E-03
o-xylene	C_8H_{10}	106.17	1.52E+02	1.00E+01	5.27E-03
naphthalene	$C_{10}H_8$	128.18	3.00E+01	5.40E-02	4.60E-04
2-methylnaphalene	$C_{11}H_{10}$	142.20	2.46E+01	NDA	NDA
phenanthrene	$C_{14}H_{10}$	178.24	1.00E+00	6.80E-04	3.90E-05

From Knox *et al.* (1993)

Pump-and-treat is the most widely used method for remediation of contaminated groundwater, by which the contaminated groundwater is pumped to the surface and remediated in an appropriate treatment system (Charbeneau *et al.* 1992; McCarty 1990). The contaminated groundwater is treated using air stripping, carbon adsorption, biological treatment, or other treatments above the ground surface (Charbeneau *et al.* 1992). However, if the aquifer is not homogeneous and contaminants consist of immiscible constituents such as an oily phase, a portion of contaminant would be trapped in the finer pores due to capillary forces while others would tend to sorb on the soil particles (McCarthy 1990; Lyman *et al.* 1992). Those trapped or sorbed contaminants

are not easily removed by pumping. Trapped and sorbed contaminants act as a source of contamination and continue to release dissolved components into the groundwater (McCarthy 1990). Such effects prolong remediation and result in longer treatment times. Some research has shown that even by increasing the pumping rate, the rate of release of trapped and sorbed contaminants is not increased beyond some point (McCarty 1990). In general, the pump-and-treat method is very effective for removal of contaminants in groundwater from within a homogeneous aquifer. However, the pump-and-treat method is unsatisfactory for groundwater contaminated with denser nonaqueous phase liquids (DNAPLs) or semivolatiles and groundwater within a heterogeneous aquifer (McCarty 1990; Kostecki and Calabrese 1993).

Soil vapor extraction is a remediation technique used to remove volatile chemical materials from contaminated soils in the vadose zone (Kostecki and Calabrese 1993; Charbeneau *et al.* 1992). The process uses an air stream which flows through the unsaturated soil matrix. The air stream vaporizes the light components and transports the contaminated air to a surface treatment system. This remediation method is usually effective and cost-efficient (Charbeneau *et al.* 1992). However, soil vapor extraction technology is less effective in clay soils because of their low permeability (Thomson 1996).

In situ isolation/containment is the process by which the contaminated region is separated from the rest of the environment using such devices as caps, grout curtains, and cut-off and slurry walls. The contaminants are immobilized within a given region and are prevented from migrating to other areas. However, the contaminants still remain in the

soil and are not destroyed (Charbeneau *et al.* 1992).

Chemical extraction or soil washing is the process by which excavated soils are washed using water containing solvents or surfactants to remove the contaminants. The wash water is then treated to acceptable environmental safety standards (Charbeneau *et al.* 1992). This method is effective in removal of heavy metals and radionuclides, as well as heavier organic compounds. However, it is relatively expensive and has a potential for further contamination (Pamucku and Wittle 1992).

In situ bioremediation is a widely used technique to remove or reduce the mobility and /or toxicity of the contaminants at a site (Charabeneau *et al.* 1992). It has the potential not only for removing but also for destroying toxic organic contaminants to form harmless inorganic end products such as carbon dioxide, water, and chloride (McCarty 1990). In general, this technique is cost-effective and can be used to treat large contaminated soil areas *in situ*. However, several factors affect the success of bioremediation such as toxicity of contaminants, water content of contaminants, oxygen, pH, water solubility of contaminants, temperature, and sorption (Charabeneau *et al.* 1992). The presence of water is essential for microbial activity. Soil with too low or too high a moisture content such as clays may lead to reduced microbial activity. At high moisture content, such as near saturation (about 35% for most soils), the pores of the soil are filled with water and diffusion of oxygen from the atmosphere is restricted (Charabeneau *et al.* 1992; Kostecki and Calabrease 1993). The optimum pH for microbial activity is around 7, generally in the range of 6 to 8. Nutrients, such as nitrogen and phosphorus, may be needed in the bioremediation process

(Charabeneau *et al.* 1992). Since microbial degradation is controlled by microbial enzymes, the contaminants that need to be degraded must be in contact with the microbes (Charabeneau *et al.* 1992). Many hydrocarbon contaminants are not water soluble and are tightly sorbed to the organic matter in soil. Therefore, *in situ* bioremediation is restricted to dissolved hydrocarbon contaminants (Kostecki and Calabrease 1993). Furthermore, it is believed that the presence of some organic compounds such as toluene, a common component of petroleum derived oils, inhibits microbial growth and reduces the efficiency of soil remediation (Frankenburger 1992).

2.3 Surfactant enhanced electrokinetic remediation

Because of the extremely low permeability of clayey soils, conventional techniques are not very effective in remediating hydrocarbon contamination. Therefore, an efficient remediation technique that is cost-effective and time-efficient needs to be developed for the remediation of contaminated clayey soils. Electrokinetic soil processing (electrokinetic remediation) is a technology which is used to remediate soils by the application of a low-level electrical potential difference. Under controlled conditions, it enhances contaminant desorption, transport, capture, and removal from fine-grained soils. The technique can be utilized in removing contaminants including organic and inorganic compounds from fine-grained soils. Alternatively, the technique can also retard the movement and contain the contaminant to a selected area. The construction of barriers against advective-dispersive transport of contaminants in soils, diversion schemes for waste plumes, and injection of grouts, microorganisms and nutrients into subsoils can all be achieved by appropriate electrokinetic methods

(Alshawabkeh and Acar 1992). Although this technique is less reported in the literature, it has the potential to remove hydrocarbons from contaminated soil faster and more effectively. The increased pore fluid flow rate leads to increased migration of hydrocarbons along with bulk flow thereby reducing the remediation time. This increased flow rate is important to the remediation of soils with low permeability such as clays. According to Helmholtz and Smoluchowski's electrokinetic theory (Alshawabkeh and Acar 1992), electroosmosis is not a function of soil pore size and pore distribution. Therefore, a heterogeneous soil mass with varying pore sizes and hydraulic conductivity has the same flow rate through the entire soil mass. This uniform flow distribution leads to high recovery of contaminants from within a region containing heterogeneous soils.

The removal of total petroleum hydrocarbons (TPH) was increased by 60% in the presence of surfactants compared to a treatment with water only (Peters *et al.* 1992). The presence of surfactants in the soil-water system dramatically increases the apparent solubility of hydrocarbons. The apparent solubility is increased due to increased micellar solubilization and reduction in interfacial tension between hydrophobic contaminants and the aqueous phase (Charabeneau *et al.* 1992; Pennell *et al.* 1993). With surfactants, more hydrophobic contaminants, including the sorbed and entrapped ones, are mobilized in the aqueous phase. Electrophoresis becomes a dominant phenomenon under electrical potential difference due to the presence of surfactants, which causes the migration of charged particles such as micelles towards the electrodes with an opposite charge. Therefore, it is believed that the surfactant-enhanced electrokinetic remediation has the potential to cause the enhanced migration of contaminants from contaminated soil.

The surfactant-enhanced electrokinetic method combines the advantages of both electrokinetic and surfactant remediation methods. While avoiding the high cost of excavation it also minimizes the human health risks (Dzenitis 1997).

2.4 Electrokinetic Processes

Electrokinetic remediation is the process by which a low-level electrical potential difference on the order of a few volts per centimeter across electrodes is applied to contaminated soils to remove inorganic and organic compounds (Alshawabkeh and Acar 1992; Acar and Alshawabkeh 1993b). Three main electrokinetic phenomena are involved, which are electroosmosis, electrophoresis, and electrolytic migration of ionic and polar species (Pamucku and Wittle 1992). Electroosmosis is a process by which porewater is dragged along with the moving ions. Electrophoresis is a process by which charged colloids such as micelles move towards an oppositely charged electrode under the influence of an applied electrical potential gradient. Electrolytic migration is a process by which ion species present in the pore fluid such as H^+ (produced at the anode) and OH^+ (produced at the cathode) migrate towards the opposite electrode (Pamukcu and Wittle 1992). Streaming potential or sedimentation potential is also generated by the movement of charged particles with water moving under a hydraulic gradient or gravitational forces, respectively (Acar and Hamed 1991). Several phenomena are presented in Table 2.2.

Table 2.2. Summary of electrokinetic processes

Process	Definition	Cause
Electroosmosis *	pore fluids are dragged with cations towards cathode.	Water surrounding ions is dragged with the movement of ionic species at the electrical double layer.
Electrophoresis *	charged colloids such as micelles migrate towards the opposite electrode as a group.	charged colloids such as micelle under applied electrical potential difference.
Electrolytic migration	ionic species migrate towards the opposite electrode.	ionic species such as H^+ and OH^- migrate under the electrical potential difference.
Electrolysis *	H^+ and OH^- are produced at anode and cathode respectively.	acid and base fronts produce at anode and cathode respectively.
Streaming potential **	a current is generated by the movement of ions with water under a hydraulic gradient.	ions move with water under an applied hydraulic gradient
Sedimentation potential **	a current is generated by the settling of particles under gravitational forces.	particles move under gravitational forces.

* From Pamukcu and Wittle (1992); ** From Acar and Hamed (1991).

2.4.1 Electroosmosis

Transport of pore fluid due to electroosmosis is associated with an electrical double layer of negative and positive ions at the solid-liquid interface in clay or silt soils. An excess concentration of cationic species is present in porewater which migrates under the influence of an electrical potential gradient. The water molecules surrounding cationic species are thus dragged with them towards the cathode. This phenomenon is also referred to as electroosmotic advection. Electroosmosis can lead to an increase in the flow rate of porewater causing the enhancement of removal of dissolved hydrocarbons from contaminated sites (Acar 1992). Therefore, soil and groundwater remediation is enhanced.

According to Helmholtz and Smoluchowski's electrokinetic theory, flow rate caused by electroosmosis is independent of soil fabric (pore size and distribution). It is unlike the flow rate caused by a hydraulic gradient that is dependent on the type of soil. This factor is important for remediation of heterogeneous soil. According to Helmholtz-Smoluchowski's law, the velocity of pore fluid through a soil under the influence of an applied electrical potential gradient can be theoretically described by (Shapiro and Probstein 1993)

$$V_{eo} = \frac{\varepsilon \zeta_s}{\eta} \frac{dE}{dx} \qquad (2.1)$$

where

V_{eo} = electroosmotic velocity (m/sec),

ε = permittivity of the pore fluid (~ 10^{-9} C/Vm for water),

ζ_s = uniform zeta potential of the surface corresponding to the surface charge (V),

dE/dx = uniform electric field strength (V/m), and

η = viscosity of the liquid (10^{-3} Pa ·s for water at 20 °C).

In equation 2.1, the permittivity, ε, is a parameter used to describe the ability of a fluid to transport charges, and the zeta potential, ζ_s, is the potential drop across the mobile part of the double layer (Stumm and Morgan 1981).

Similar to the hydraulic pore fluid flow described by Darcy's law, electroosmotic flow rate can be expressed by (Acar Hamed 1991; Eykholt Daniel1994)

$$q_e = k_{eo}\, i_e A = k_i I = \frac{k_{eo}}{\sigma} I \qquad (2.2)$$

where

q_e = electroosmotic flow rate (cm^3/s),

i_e = electrical potential gradient (V/cm),

k_{eo} = coefficient of electroosmotic permeability (cm^2/s V),

A = cross-sectional area (cm^2),

k_i = electroosmotic water transport efficiency (cm^3/s A),

I = current (A), and

σ = electrical conductivity (S/cm).

The coefficient of electroosmotic permeability k_{eo} is a function of zeta potential, viscosity of pore fluid, porosity, and electrical permittivity of the pore water. The electroosmotic permeability k_{eo} is defined as (Acar and Alshawabkeh 1993b; Eykholt Daniel 1994)

$$k_{eo} = \frac{\varepsilon \zeta_s n_e \tau}{\eta} \qquad (2.3)$$

where

n_e = the effective porosity,

τ = the tortuosity,

ε = permittivity of the pore fluid (~ 10^{-9} C/V/m for water),

ζ_s = uniform zeta potential of the surface corresponding to the surface charge (V), and

η = viscosity of the liquid (10^{-3} Pa s for water at 20°C).

Several researchers have reported that the zeta potential, ζ_s, is affected by the pH of the pore water, generally decreasing with a drop in pH. During the electrokinetic process, the pH value drops due to the movement of the acid front through the column, which causes a reduction in the coefficient of electroosmotic permeability (k_{eo}) (Acar and Alshawabkeh 1993b; Lorenz 1969). Therefore, the pore fluid flow decreases due to a reduction in k_{eo}. The k_{eo} varies in time, and is controlled by the chemical reaction associated with application of an electrical potential gradient though a soil column. The values of k_{eo} measured at earlier stages of processing range within one order of magnitude for all soils,

10^{-5} to 10^{-4} cm^2/s V, the higher values being at higher water contents (Acar *et al.* 1993a; Eykholt and Daniel 1994). For most clayey soils, the value of k_{eo} is near 5×10^{-5} cm^2/s V. However, it is important to note that k_{eo} is not a function of pore size.

Acar *et al.* (1993a) reported that electrical conductivity, σ, at the anode showed higher values than at the cathode due to the sweep of the acid front generated at the anode. Such a phenomenon is associated with different pH values across the soil specimen which leads to diverse electroosmotic flows through the soil, higher at the cathode and lower at the anode (Acar and Alshawabkeh 1993b). In fined-grained soils (hydraulic conductivity, $K_h < 10^{-6}$ cm/s), insufficient pore fluid flows towards the cathode leading to a drop in water content at the cathode. The above phenomena could also have been due to the electrolytic reactions at the electrodes. The electrolytic reactions result in the generation of an alkaline and an acidic medium at the cathode and the anode, respectively. An acidic medium migrates towards the cathode over time, and the pH of the pore water changes due to the advance of an acid front. Based on the above, it is believed that electrokinetic remediation is a superior method for fined-grained and/or heterogeneous contaminated soil in which most of the traditional remediation methods are limited (Bruell *et al.* 1992). Electroosmosis becomes a significant process in fine-grained soils where flow caused by hydraulic gradient is minimal.

2.4.2 Electrophoresis

Electrophoresis is another electrokinetic phenomenon in which charged colloids such as charged micelles migrate to the opposite electrodes under an influence of applied

electrical potential difference. The hydrocarbons present in diesel are non-polar compounds and have no ability to migrate under an influence of applied electrical potential difference. However, those non-polar organic compounds can sorb into charged micelles and migrate with them towards the opposite electrode in the presence of the surfactant micelle in pore water. With an application of surfactant to pore water, the electrophoresis may become a critical electrokinetic process in the decontamination of hydrocarbon contaminated site (Pamukcu and Wittle 1992). The surfactant enhanced electrokinetic remediation has the potential to remove non-polar organic compounds more effectively from contaminated soils.

2.4.3 Electrolytic migration

The application of an electrical potential gradient via electrodes embedded in a soil and water system leads to electrolytic reactions at the electrodes. As a result, the H^+ and OH^- are transported to the opposite electrodes. Such a phenomenon is referred to as electrolytic migration in which ions as well as H^+ and OH^- are moved causing a current flow in soil and groundwater system (Pamukcu and Wittle 1992). During electrolytic migration, water molecules surrounding the ions are dragged towards the electrodes (Pamukcu and Wittle 1992). Since the relative mobility of H^+ is 18 times faster than the mobility of OH^-, the pore fluid flow rate due to migration of ions is enhanced by electroosmosis (Pamukcu and Wittle 1992). The higher concentration of ions is responsible for the increased electrolytic migration. During ionic species movement through the soil and water system, values of pH change in time and varies spacially

across the system. However, this change in pH may affect electroosmosis.

The faster H^+ ion movement is an important factor for soil remediation with metal contamination (Pamukcu and Wittle 1992). During soil remediation for the removal of metals, the metal ions adsorbed onto soil surfaces are replaced by a relatively large amount of faster moving H^+ ions. Those replaced contaminants are dissolved in the pore water which is transported towards the cathode. However, hydrocarbon contaminants are usually not charged, and migrate only in the dissolved form transported by the pore fluid movement. Therefore, electrolytic migration is of less importance to transport organic compounds through the soil and water system.

2.4.4 Electrolysis

During the application of an electrical potential difference on the soil and water system, electrolysis is responsible for the formation of H^+ and OH^- at the anode and cathode, respectively. The acid front (H^+) and base front (OH^-) migrate through the soil specimen to the opposite electrode, which changes the pH in soil and water system and affects the electrokinetic processing. At the same time, hydrogen and oxygen gases are produced at the cathode and anode, respectively (Acar and Alshawabkeh 1993b). The primary electrode reactions of electrolysis can be described by

Anode:

$$2\,H_2O - 4e^- \Rightarrow O_2 \uparrow + 4\,H^+ \qquad (2.4)$$

Cathode:

$$4\,H_2O + 4e^- \Rightarrow 2\,H_2 \uparrow + 4\,OH^- \qquad (2.5)$$

The pH values can reach 3 and above 11 at the anode and cathode, respectively (Eykholt and Daniel 1994). Since the acid and base fronts migrate to the cathode and anode respectively, referred to as electrolytic migration, the pH of the soil and water system changes over time. However, the soil and water system finally becomes acidic, because H^+ movement is about 18 times faster than OH^- movement. Many researchers report that the zeta potential, ζ_s, is affected by the pH of the soil and water system, generally decreasing with a drop in pH. The decrease in zeta potential leads to a reduction of the coefficient of electroosmotic permeability, k_{eo}, which lowers the electroosmotic flow and even stops and reverses the electroosmotic flow (Acar and Alshawabkeh 1993b; Lorenz 1969). However, many models have been developed to predict the pH changes in the soil and water system during electrokinetic processing.

2.5 Surfactant theory

Surfactants, or surface active agents, have both polar and nonpolar chemical groups that exhibit hydrophilic (water-compatible) and hydrophobic (water-repellant) properties, respectively (Karsa, 1987; Kostecki and Calabrese 1993). The classification of surfactants is based on chemical structure of the hydrophilic group. The surfactant can be classified as cationic (positively charged), anionic (negatively charged), nonionic (uncharged), and amphoteric (both positively and negatively charged) (Porter 1991). In soils contaminated with hydrophobic hydrocarbons, the presence of surfactant enhances the mobilization of the hydrocarbons by micellar solubilization and interfacial tension reductions (Pennell *et al.* 1993).

2.5.1 The critical micelle concentration (CMC)

When the concentration of surfactants increases to a critical level, called the critical micelle concentration (CMC), several physical and chemical properties such as electrical conductivity, interfacial tension, and detergency dramatically change (Kostecki and Calabrese 1993). The solubility of hydrocarbons is greatly increased if the concentration of surfactant is above the CMC. At this concentration, the polar and nonpolar groups become oriented and organized to form clusters in the solution, referred as micelles. The hydrophilic groups point outwards from within the micelles, and the hydrophobic groups point inwards within the micelles and often have hydrocarbon character. This arrangement is a result of the minimization of the free energy of the oil-water interface (Kostecki and Calabrese 1993). The CMC of the surfactant is affected by several factors such as the number of carbons in the hydrophobic chain, the charge status of the hydrophilic groups, pH of the solution, the electrolytes in ionic surfactants, and the presence of organic additives in solution (Porter 1991; Myers 1992). The critical micelle concentration (CMC) of a surfactant decreases with an increase in the number of carbons in the hydrophobic chain. The addition of an anionic salt or the presence of an organic compound decreases the CMC of the surfactant solution (Pennel *et al.* 1993; Porter 1991; Myers 1992; Karsa 1987). Also, a surfactant with a charged hydrophilic group has a higher CMC compared to a non-ionic surfactant. The CMC usually ranges from 0.1 to 10 mmol/L (West and Harwell 1992).

The solubility of a surfactant increases with increasing temperature of the aqueous solution. As a result, the CMC is also temperature dependent. The temperature of the

solution should be at a certain point, known as the Kraft point, before CMC can be attained (Porter 1991; West and Harwell 1992). Above the Kraft temperature, the surfactant has an ability to form the micelles. It is important in the application of surfactants in the field because the temperature of groundwater may be lower than the Kraft temperature causing a reduction of remediation efficiency. It is possible to reduce the Kraft temperature to enhance micelle formation in the field. A reduction of Kraft temperature can be brought about by increasing the hydrophilic character of the surfactant or by reducing the hydrophobic character, such as branching the hydrocarbon tails, or using a co-solvent (Porter 1991; West and Harwell 1992).

2.5.2 Micellar solubilization

When surfactants are present in the pore water, hydrocarbons become more mobile leading to a decrease in the hydrocarbons sorbed on the soil particles. Such effects result from micellar solubilization of non-aqueous phase liquids (NAPLs). In addition, in the presence of a surfactant, entrapped NAPLs become solubilized due to a reduction in interfacial tension between NAPL and the aqueous phase (Lyman *et al.* 1992; Pennell *et al.* 1993). With surfactants in the aqueous phase, the hydrocarbon distribution coefficient (K_d) and the partition coefficient of the hydrocarbon between organic carbon and the aqueous phase (K_{oc}) decrease due to an increase in solubility of the organic compounds.

The micelles are capable of solubilising hydrocarbon compounds in the hydrophobic interiors because a nonpolar environment is created within the center of the micelles. The interior of micelle is capable of attracting nonpolar organic compounds and

dissolved organic contaminants (Karsa 1986; Kostecki and Calabrese 1993). This effect is usually called micellar solubilization (West and Harwell 1992). Valsaraj *et al.* (1988) reported that cationic micelles have a larger capacity to solubilize hydrophobic compounds compared to anionic micelles. The size of the micelle and the number of micelles affect the apparent solubility of hydrocarbon compounds; the larger the size of the micelle the more ability to solubilize hydrocarbon compounds. Therefore, in general, non-ionic surfactants are good at solubilising hydrocarbons compared to anionic or cationic surfactants (Porter 1991). Many researchers have reported that surfactants at concentrations below the CMC have minimal effect on the solubility of most organic compounds (Kile and Chiou 1989; Pennel *et al.* 1993; Valsaraj *et al.* 1988). However, the solubility of some organic compounds, such as DDT, also exhibit significant enhancement at surfactant concentration below CMC (Kile and Chiou 1989).

The micellar solubilization can be determined by the molar solubilization ratio (MSR). Molar solubilization ratio is defined as the ratio of the number of moles of hydrocarbon solubilized to the number of moles of surfactant in the micellar form (Pennell *et al.* 1993; Edwards *et al.* 1991). Several researchers have found that there is a linear relationship between solubility of hydrocarbons and the surfactant concentration at concentrations above CMC. Therefore, in the presence of excess hydrophobic organic compounds, the MSR can be obtained from the slope of straight line of a plot of hydrocarbon solubility versus surfactant concentrations expressed as moles/litre (M). The molar solubilization ratio is thus described by (Edwards *et al.* 1991; Ponnell *et al.* 1993)

$$MSR = \frac{(S_{mic} - S_{cmc})}{(C_{surf} - C_{cmc})} = \frac{(S_{mic} - S_{cmc})}{[CTAB^-]_{mic}} \qquad (2.6)$$

where

MSR = molar solubilization ratio (dimensionless),

S_{mic} = apparent solubility of hydrocarbons at a particular surfactant concentration above the CMC (M),

S_{cmc} = apparent hydrocarbon solubility at the CMC (M),

C_{surf} = surfactant concentration at which S_{abv} is evaluated (M),

C_{cmc} = critical micelle concentration (M), and

$[CTAB^-]_{mic}$ = moles of CTAB in micellar form per liter of solution = $(C_{surf} - C_{cmc})$ (M).

The micelle-water partition coefficient (K_{mic}) is another measure of the solubilization capability. Since the micelle-water partition coefficients have been reported as both mole fraction based K_{mic} (dimensionless) and concentration based (K_{mic}'), we must be careful to choose the micelle-water partition coefficient from the literature. In the literature, the octanol-water partition coefficient is treated as being equal to the micelle-water partition coefficient expressed in either the mole fraction based form or the concentration based form. The mole fraction based micelle-water partition coefficient can be calculated from MSR and has been described by (Edwards *et al.* 1991)

$$K_{mic} = \frac{X_m}{X_a} = \frac{1}{S_{cmc} V_w} \frac{MSR}{(1 + MSR)} \qquad (2.7)$$

where

K_{mic} = micelle-water partition coefficient (dimensionless),

X_m = mole fraction of the compound in the micellar phase,

X_a = mole fraction of the compound in the aqueous phase,

S_{cmc} = apparent hydrocarbon solubility at the CMC (M),

V_{mol} = the molar volume of water (0.01805 M^{-1} at 25°C), and

MSR = molar solubilization ratio (dimensionless).

However, some researchers have reported that the concentration based micelle-water partition coefficient K_{mic}' that can be characterized as follows (Kostecki and Calabrese 1993; Kile and Chiou 1989; Jafvert 1991)

$$S_{total} = 1 + C_{mon}K_{mon} + C_{mic}K_{mic}' \qquad (2.8)$$

where

S_{total} = the apparent hydrocarbons solubility at the total surfactant concentration (M),

S_w = the intrinsic solubility in pure water (M),

Cmon = the concentration of surfactant as monomers (M),

K_{mon} = monomers-water partition coefficient (M^{-1}),

C_{mic} = the concentration of surfactant in micellar form (M), and

K_{mic}' = micelles-water partition coefficient (M^{-1}).

In general, the presence of surfactants at concentrations above CMC greatly increases the apparent solubility of organic compounds in the aqueous phase. The

micellar term, $C_{mic}K_{mic}$, in equation 2.8, plays a dominant role in enhancing the solubility of organic compounds. Considering only the concentration of surfactants above CMC, the micelle-water coefficient can be defined as (Jafvert 1991)

$$K_{mic}' = \frac{S_{mic}'}{S_w'} \frac{1}{(C_{surf} - C_{cmc})} = \frac{S_{mic}'}{S_w'[CTAB^-]_{mic}} \qquad (2.9)$$

where

K_{mic}' = micelles-water partition coefficient (M^{-1}),

S_{mic}' = the hydrocarbons solubility at the micelle concentration (mg/L),

S_w' = the intrinsic solubility in pure water (mg/L), and

$[CTAB^-]_{mic}$ = moles of CTAB in micellar form per liter of solution = $(C_{surf} - C_{cmc})$ (M).

Kile and Chiou (1989) developed the method which can be used to determine the K_{mon} and K_{mic}'. The relationship between apparent hydrocarbon solubility S_{total} and the total concentration of surfactants can be plotted. In the plot, two linear lines are shown that represent K_{mon}, ranging from zero to CMC, and K_{mic}', ranging above CMC, respectively. Two distinct slopes are represent K_{mon} and K_{mic}' for a given hydrocarbons-surfactant system (Kile and Chiou, 1989).

The micelle-water partition coefficient is used as a measure of the hydrophobicity of hydrocarbons, as is the octanol-water partition coefficient K_{ow}. These parameters increase with increasing hydrophobicity of hydrocarbon contaminants (Valsaraj *et al.* 1988). The micelle-water partition coefficient slightly increases with an increase in

temperature (Valsaraj *et al.* 1988).

The conversion of the mole fraction- and the concentration- based micelle-water partition coefficients is defined as (Thomas 1996a and Jafvert 1991)

$$K_{mic}' = K_{mic} V_{mol} \frac{(Y+N)}{Y} \qquad (2.10)$$

where

K_{mic}' = concentration based micelle-water partition coefficient (M^{-}),

K_{mic} = mole fraction-based micelle-water partition coefficient (dimensionless)

V_{mol} = the molar volume of water ($0.01805 M^{-}$ at 25°C),

N = the mean occupancy number of the hydrocarbons in micelle solution at saturation, and

Y = the aggregation number of CTAB molecular in every CTAB micelle.

2.5.3 Properties of CTAB as a surfactant

A surfactant is selected to enhance the apparent solubility of hydrocarbons that are dissolved in the aqueous phase and those that are entrapped/sorbed on the soil particles. Several factors should be considered in the selection of a surfactant. The factors include the type of soil, type and concentration of hydrocarbons, cost and toxicity of surfactants, solubilization power of surfactants (Kostecki and Calabrese 1993; Thomas 1996a). In addition, the impact on electrokinetic properties should be taken into account if this remediation technique is to be applied.

Peters *et al.* (1992) reported that cationic surfactants are effective in removing diesel fuel from contaminated soil compared to nonionic surfactants (or no surfactants at

all) in the aqueous phase. The migration of hydrocarbons, enhanced by the surfactants, is governed by the advection-dispersion equation. However, if the electrokinetic phenomenon is taken into account, the bulk flow is either increased or decreased depending on the direction of the electroosmotic flow. When the anode is located at the higher hydraulic head, the flow rate is increased since the flow due to both advective-dispersive transport and electroosmosis are in the same direction. The pore water flow due to the hydraulic head and electroosmosis is from anode (higher hydraulic head) to cathode (lower hydraulic head). Under such conditions, the electroosmotic phenomenon increases the total flow rate and enhances the migration of hydrocarbons through the contaminated soil. It was presumed that electroosmotic flow will enhance the hydraulic gradient effects in this research project. Another electrokinetic phenomenon affecting the movement of hydrocarbons is electrophoresis in which charged particles, such as micelles, are translocated to the electrode having the opposite charge. Thus, the hydrocarbons that are held within the interior of micelles will also be transported. A cationic surfactant such as cetyltrimethylammonium bromide (CTAB) leads to the formation of positively charged micelles. Therefore, the micelles are expected to preferentially move towards the cathode during electrophoresis. If the anode is placed on the high hydraulic gradient side of the soil column, the direction of movement of the micelles will be the same as the one due to electroosmosis, as well as advection and dispersion. Since CTAB is a common cationic surfactant used as a detergent and/or an antiseptic and it results in great enhancement of solubility of organic compounds, it was

chosen for the remediation of hydrocarbon contaminated columns (Jungermann 1970; Kile and Chiou 1989). Table 2.3 lists the properties of the surfactant CTAB.

2.6 Migration and fate of hydrocarbon contaminants during remediation

The migration and fate of hydrocarbon contaminants are controlled by several processes such as advection due to hydraulic gradient, electroosmosis, hydrodynamic dispersion due to concentration and microscopic variations, and chemical reactions (CCME 1994). The migration of contaminants is numerically described by advective-dispersive-adsorption equation. The presence of surfactants in the soil-water system, however, has an effect on the solubility of organic compound, and thus influence the migration of organic contaminants. Therefore, this effect due to the presence of surfactants is accounted for by modifying the retardation factor.

Table 2.3 Properties of cetyltrimethylammonium bromide

Formula	$C_{19}H_{42}BrN$
Molecular weight	364.45
Melting point	237-243°C
CMC ($\times 10^{-4}$M)	9.2 (Soma and Papadopoulos, 1997)
	9.9 or (361mg/L) (Kile and Chiou (1989))
	9.0 (from experimental results)

2.6.1 Sorption interaction

During the migration of contaminants, they are subjected to sorption interaction (adsorption and desorption) and co-solvation (enhanced solubility due to the presence of

another contaminant). Sorption interaction results in the transfer of contaminant mass between the liquid and solid phases or conversion of dissolved species from one form to another (Walton 1991). Desorption plays a major role in surfactant enhanced soil remediation.

2.6.1.1 Distribution coefficient

At equilibrium, the relationship between the sorbed and solution phase concentration can be described by the Freundlich isotherm (Lyman *et al.* 1992; Walton 1991)

$$S_s = K_d (S_w')^{N_d} \qquad (2.11)$$

where

S_s = concentration of hydrocarbons in soil (mg/kg),

S_w = the hydrocarbons solubility in water (mg/L),

K_d = distribution coefficient (L/kg), and

N_d = measure of deviation from linearity.

If the hydrocarbon concentration is below one-half of the solubility limit of the compound, the relationship is linear (N=1) (Charbeaneau *et al.* 1992). For dilute solutions such as those normally encountered in natural environments, the relationship is considered to be linear and represented by

$$S_s = K_d S_w \qquad (2.12).$$

If the contaminant source contains different hydrocarbons, it is commonly assumed that the migration of each contaminant is independent of its neighbors and can be calculated separately. However, this assumption is valid only for the contaminants at very low concentrations (Walton 1991). The unit of K_d is generally reported as mL/g, and the commonly encountered values of K_d range from near zero to 10^3 mL/g or greater (Freeze and Cherry 1979; Walton 1991). If the K_d values are orders of magnitude greater than one, the hydrocarbons are considered to be immobile(Walton 1991). The contaminant with a high value of K_d has low solubility in the aqueous phase and a strong affinity for sorption to soil particles (CCME 1994). However, soluble and mobile contaminants generally have lower K_d. The distribution coefficient, K_d, is found to be a function of the hydrophobicity of the organic compound and the amount of organic matter present, which is described by (Charbeneau *et al.* 1992)

$$K_d = K_{oc} \times f_{oc} \qquad (2.13-1)$$

$$K_{oc} = \frac{K_d}{f_{oc}} = \frac{S_s}{S_w f_{oc}} \qquad (2.13-2)$$

where

K_d = distribution coefficient (L/kg),

f_{oc} = the weight fraction of organic compounds in the soil (dimensionless),

K_{oc} = organic carbon-water partition coefficient (L/kg),

S_s = concentration of hydrocarbons in soil (mg/kg), and

S_w' = the hydrocarbons solubility in water (mg/L).

The equation above is valid only for f_{oc} larger than 0.001 (Charbeneau *et al.* 1992). The K_{oc} is the partition coefficient which is used to describe the degree of hydrophobicity of the hydrocarbons, and can be used to predict K_d (Walton 1991). Since K_{oc} is largely independent of the soil properties, it can be estimated from the other physical properties of contaminants such as their aqueous solubility or their octanol/water partition coefficients (Charbeneau *et al.* 1992).

When surfactants are applied in aqueous phase, the amount of hydrocarbon contaminants sorbed to the soil would be decreased due to the transfer of contaminants to the micellar form. A decrease in the sorbed contaminants also decreases the distribution coefficient, K_d. The modified distribution coefficient $K_{d,cmc}$ due to the presence of surfactants in aqueous phase can be described as (Jafvert 1991)

$$K_{d,cmc} = \frac{S_s}{S_w' + S_{abv}} \qquad (2.14)$$

where

$K_{d,cmc}$ = distribution coefficient (L/kg),

S_s = concentration of hydrocarbons in soil (mg/kg),

S_w' = the hydrocarbons solubility in water (mg/L), and

S_{abv} = concentration of hydrocarbons in micelle solution (mg/L).

While the surfactants cause a reduction in contaminants sorbed to soil particles there is a corresponding increase in the dissolved amount. Contaminants in water are either dissolved in the aqueous phase due to the solubility of contaminants or exist within the interior of micelles.

The combination of equation 2.9 (micelle-water partition coefficient concentration-based units K_{mic}'), equation 2.13 (organic carbon-water partition coefficient, K_{oc}), and equation 2.14 results in $K_{d,cmc}$ which is a function of K_{oc}, f_{oc}, K_{mic}', and $[CTAB^-]_{mic}$, expressed as

$$K_{d,cmc} = \frac{K_{oc} f_{oc}}{1 + K_{mic}'[CTAB^-]_{mic}} \qquad (2.15)$$

where,

$K_{d,cmc}$ = modified distribution coefficient due to the presence of surfactants (L/kg),

f_{oc} = the weight fraction of organic compounds in the soil (dimensionless),

K_{oc} = organic carbon-water partition coefficient (L/kg),

K_{mic}' = concentration-based micelles-water partition coefficient (M^{-1}), and

$[CTAB^-]_{mic}$ = moles of CTAB in micellar form per liter of solution = $(C_{surf} - C_{cmc})$ (M).

Equation 2.10 can be used in the unit conversion of mole fraction-based and concentration-based micelle-water partition coefficients to the modified distribution coefficient which is described by

$$K_{d,cmc} = \frac{K_{oc} f_{oc}}{1 + K_{mic} V_{mol} \frac{(Y+N)}{Y} [CTAB^-]_{mic}} \qquad (2.16)$$

where

$K_{d,cmc}$ = modified distribution coefficient due to the presence of surfactants (L/kg),

f_{oc} = the weight fraction of organic compounds in the soil (dimensionless),

K_{oc} = organic carbon-water partition coefficient (L/kg),

K_{mic} = mole fraction-based micelles-water partition coefficient (dimensionless),

$[CTAB^-]_{mic}$ = moles of CTAB in micellar form per liter of solution = $(C_{surf} - C_{cmc})$ (M),

N = the mean occupancy number of the hydrocarbons in micelle solution at saturation,

V_{mol} = the molar volume of water (M^-) (0.01805 L/mol at 25°C), and

Y = the aggregation number of CTAB molecular in every CTAB micelle.

However, the aggregation number of CTAB molecules in every CTAB micelle (Y) and the mean occupancy number of the hydrocarbons in micelle solution (N) are not yet available in the literature. Therefore, the conversion of the mole fraction-based and concentration-based micelle-water partition coefficients cannot be accomplished.

2.6.1.2 Retardation factor (R)

During the migration of contaminants, the velocity of contaminant movement decreases due to adsorption to soil particles. The ratio of the rate of advance of a contaminant without adsorption to the rate of advance with adsorption is referred to as retardation factor R and it is given by (Gillham and Cherry 1982)

$$R = \frac{V_w}{V_c} = 1 + \frac{K_d \rho_b}{\phi} \qquad (2.17)$$

where

R = retardation factor (dimensionless),

V_w = average pore water velocity without sorption reaction (cm/sec),

V_c = average pore water velocity with sorption reaction = the velocity of the $C/C_o = 0.5$ point on the concentration profile of contaminant with sorption reaction (cm/sec),

K_d = distribution coefficient (cm^3/g),

ρ_b = soil bulk density (g/cm^3),

ϕ = soil porosity (dimensionless),

C = the concentration at time t (ppm), and

C_o = the initial contaminant concentration (ppm).

The retardation factor R is commonly used in contaminant migration studies. The physical significance of the retardation factor is that it measures how much more slowly the hydrocarbons migrate relative to the aqueous phase without sorption (Charbeneau *et al.* 1992). A retardation factor of 1 or 2 has been reported for many organic chemicals in contaminant migration studies (Walton 1991). The effective velocity (V_w/R) reduced by sorption interactions is introduced to describe the retardation of the movement of a contaminant without sorption interaction (V_w).

When surfactants are applied to soil-water systems, the amount of hydrocarbons sorbed to the soil particles decreases and the apparent solubility of hydrocarbons

increases especially at surfactant concentrations above CMC. Therefore, the migration of contaminants is less affected by the sorption which is described by the retardation factor R. In general, the application of surfactants may reduce the effect of retardation and reduce the retardation factor. Therefore, the retardation factor must be modified to account for the increase of apparent solubility of the hydrocarbons caused by the application of surfactants in the soil-water system. The retardation factor R_{cmc} modified by surfactant effects can be measured by combining equation 2.15 and equation 2.17, which is given by

$$R_{cmc} = 1 + \frac{K_{oc} f_{oc} \rho_b}{\phi\left\{1 + K_{mic}^{'}\left[CTAB^{-}\right]_{mic}\right\}} \qquad (2.18)$$

where

R_{cmc} = modified retardation factor taking into account micellar effects (dimensionless),

K_{oc} = organic carbon and water partition coefficient (L/kg),

f_{oc} = weight fraction of organic carbon (dimensionless),

ρ_b = dry bulk density (kg/L) or (g/cm^3),

ϕ = porosity (dimensionless),

K_{mic}' = micelles-water partition coefficient (M^{-1}), and

$[CTAB^-]_{mic}$ = moles of CTAB in micellar form per liter of solution = $(C_{surf} - C_{cmc})$ (M).

The modified retardation factor is related to the mole fraction-based micelle-water partition coefficient and is given by combining equation 2.10 and equation 2.18

$$R_{cmc} = 1 + \frac{K_{oc} f_{oc} \rho_b}{\phi\left\{1 + K_{mic} V_{mol} \left[CTAB^-\right]_{mic} \left(\frac{Y+N}{Y}\right)\right\}} \qquad (2.19)$$

where

K_{mic} = mole fraction-based micelles-water partition coefficient (dimensionless),

N = the mean occupancy number of the hydrocarbons in micelle solution at saturation,

V_{mol} = the molar volume of water (M^-) (0.01805 L/mol at 25°C), and

Y = the aggregation number of CTAB molecules in every CTAB micelle.

2.6.2 The traditional advection-dispersion-sorption equation

During soil and groundwater remediation, the migration of contaminants is driven by the advection-dispersion-sorption equation. Advection, dispersion, and adsorption processes are summarized in Table 2.4. The advection is the process by which the hydrocarbons are transported by the bulk water movement due to the hydraulic gradient and can be defined by the Darcy's law (Freeze and Cherry 1979)

$$q = K_h\, i \qquad (2.20)$$

where

q = discharge (cm/s),

i = - dh/dl = the hydraulic gradient (driven force)(dimensionless), and

K_h = hydraulic conductivity (cm/s).

Table 2.4 Summary of advection-dispersion-adsorption

Processes	Definition
Advection	The process by which the hydrocarbons are transported with the water movement through a geologic formation in response to a hydraulic gradient (dh/dx). The advection is the most important way of transporting the hydrocarbons away from sources.
Hydrodynamic Dispersion	a) Molecular Diffusion ---- The process by which the hydrocarbons spread due to molecular diffusion in response to concentration gradients. b) Mechanical Dispersion ---- The process by which the hydrocarbons spread due to the velocity variations in the pore channels and the tortuous nature of flow in the porous medium.
Adsorption	Sorption of hydrocarbons from the aqueous phase by soil particles (mineral or organic solids).

From CCME (1994).

The advective transport is due to the hydraulic gradient and is affected by several factors including the intrinsic permeability of the material, mass density of the fluid, the gravitational constant, and the viscosity of the fluid. The permeability (k) is a function

only of the medium, which depends on the porosity, pore size distribution, and possible other factors (Charbeneau *et al.* 1992). The value k of clay soil ranges from 10^{-15} to 10^{-12} cm^2 (Freeze and Cherry 1979). The fluid properties such as the dynamic viscosity and density are sensitive to temperature variations (Charbeneau *et al.* 1992).

Hydrodynamic dispersion resulting in the dilution of hydrocarbons includes two components, molecular diffusion due to the thermal-kinetic energy of the hydrocarbons particles and mechanical dispersion (or hydraulic dispersion) due to mechanical mixing during fluid advection (Freeze and Cherry 1979). Mechanical dispersion is the process by which the hydrocarbons spread in the direction of bulk flow (longitudinal dispersion) and in the direction perpendicular to the flow (transverse dispersion). The molecular diffusion takes place due to the migration of the contaminants from high concentration regions to low concentration regions until equilibrium is reached. Such diffusion happens even in the absence of groundwater flow (Walton 1991). Dispersion is generally much slower than the advective transport, and is only important where fluids are essentially not moving or moving slowly. The Fick's first law governs the molecular diffusion

$$F = -D\frac{dC}{dx} \qquad (2.21)$$

where

F = the mass flux (g/cm^2. sec),

D = diffusion coefficient (cm^2/sec),

C = the hydrocarbons concentration (g/cm^3), and

dC/dx = the concentration gradient (dimensionless).

However, Fick's law is assumed to govern the hydrodynamic dispersion phenomenon in developing the hydrocarbon transport equations (Knox *et al.* 1993). During the migration of contaminants, sorption reactions retard the movement of contaminants. Taking into account the effect of sorption, the advection-dispersion-adsorption equation can be described by (Freeze and Cherry 1979; Walton 1991; and Charabeneau *et al.* 1992)

$$R\frac{\partial C_i}{\partial t} = D\frac{\partial^2 C_i}{\partial x^2} - V\frac{\partial C_i}{\partial x} \qquad (2.22)$$

where

C_i = concentration of contaminant i dissolved in aqueous phase (mg/L),

D = hydrodynamic dispersion coefficient along the flow path (cm^2/sec),

V = average linear bulk flow velocity (cm/sec),

x = distance along flow line (cm),

R = retardation factor (dimensionless),

t = time (sec).

The equation is based on the assumption of conservative hydrocarbons in saturated, homogeneous, isotropic materials under steady state, uniform, one-dimensional flow. The left-hand side term gives the concentration change at a given location including the mass in solution as well as the sorbed mass. The first right-hand side term accounts for the concentration change associated the dispersion including mechanical dispersion and

molecular diffusion. The second right-hand side term accounts for the change in concentration associated with the advection.

In the left-hand side term, the retardation factor R is included to account for sorption. The R can calculated by equation 2.19 (in the absence of surfactants), the concentration-based equation 2.20 (in the presence of surfactants), and the mole fraction-based equation 2.21 (in the presence of surfactants).

In the diffusion term, the hydrodynamic dispersion coefficient can be described in terms of two components

$$D = \alpha V + D^* \qquad (2.23)$$

and

$$D^* = \tau D_o \qquad (2.24)$$

where

D = hydrodynamic dispersion coefficient along the flow path (cm^2/sec),

D* = diffusion coefficient (cm^2/sec),

D_0 = diffusion coefficient for a given hydrocarbons species whose concentration is C (cm^2/sec),

α = dynamic dispersivity (or dispersivity) (cm),

V = average linear bulk flow velocity (cm/sec), and

τ = tortuosity of medium .

The dispersivity is the parameter that characterizes the property of the porous medium which is dependent on the grain size distribution but independent of the grain shape. The average linear water velocity is equal to the specific discharge divided by the effective porosity (q/ϕ). The dispersivity and water velocity, and the molecular diffusion coefficient of the contaminant are properties that control the dispersion process. Molecular diffusion coefficient values of 10^{-11} to 10^{-10} m^2/s are typical for chemical species in clay like materials (Freeze and Cherry 1979). From the above equation, the diffusion coefficient D* is assumed to be negligible relative to the mechanical dispersion. However, at low groundwater velocities such as in unfractured silty or clayey deposits, molecular diffusion is the dominant component and controls the contaminant migration (Walton 1991; Knox *et al.* 1993).

2.6.3 The modified advection-dispersion-adsorption equation

The advection-dispersion-adsorption equation needs to be modified if taking into account of the effects of applied electrical potential gradient and/or surfactants. When the eletrokinetic treatment is applied on contaminated soil, several phenomena are involved in which electroosmotic and electrophoresis are two main process (Pamucku and Wittle 1992). Electroosmosis affects the classic advection-dispersion-adsorption equation by increasing the advective flow. Therefore, the rate of advective transport equal to the average linear fluid velocity (V_{total}) is the sum of the hydraulic (V) and electroosmotic (V_{eo}) velocities. The electrophoresis due to the application of surfactants with concentration above CMC affects the movement of organic compounds by migrating micelles towards to the opposite electrolyte. For the cationic surfactant (CTAB) used in

the experiment, the electrophoretic flow of micelles is in the same direction of advective flow. The rate of advective transport (V_{total}) is defined as the specific discharge q divided by the porosity ϕ, which is driven by a hydraulic gradient and electroosmosis. The mass of hydrocarbon per unit volume of solution can be characterized by the concentration of the hydrocarbons. Therefore, the mass of hydrocarbons per unit volume of porous media is equal to the concentration of the hydrocarbons, S, times the porosity ϕ. The total mass of the hydrocarbons, due to advective (hydraulic and electroosmotic) flow, electrophoretic flow, and dispersion, per unit cross-sectional area per unit time are transported in the one-dimension direction (x direction) and can be described as (Freeze and Cherry 1979)

$$F_x = V_{total}\phi S + V_{ep}\phi S_{mic} - \phi D\frac{\partial S}{\partial x} \qquad (2.25)$$

where

F_x = total mass of hydrocarbons per unit cross-sectional area per unit time in x direction ($g/cm^2 \cdot s$),

V_{total} = average linear water velocity due to hydraulic and electroosmotic flow (cm/s) = $V + V_{eo}$,

V_{ep} = micelle velocity due to electrophoretic flow (cm/s),

ϕ = the porosity (dimensionless),

D = hydrodynamic dispersion coefficient (cm^2/sec),

S = the concentration of hydrocarbons in the solution (mg/L),

x = distance along flow line (cm), and

S_{mic} = the concentration of hydrocarbons in the micelle solution (mg/L).

The above equation is similar to the one given by Thomas (1996a). The terms on the right-hand side, from the first term to the third term, represent the mass transported by the hydraulic and electroosmotic flow, electrophoresis, and dispersion in one-dimension (x-direction), respectively. Since the directions of water movement due to advection under hydraulic and electroosmotic flow and micelle movement are in the same direction, the signs before three terms are positive.

The dispersion term is derived from Fick's first law, in which the negative sign indicates the contaminants move from the zone with high concentration to the one with low concentration (Freeze and Cherry 1979). The difference of mass entering and leaving in the element is described as (Freeze and Cherry 1979)

$$\frac{\partial F_x}{\partial x} dx\, dy\, dz \qquad (2.26)$$

The rate of mass change in the element while taking into account the effect of interaction is

$$-R\phi \frac{\partial C}{\partial t} dx\, dy\, dz \qquad (4.27).$$

Therefore, the complete conservation of mass can be expressed as

$$\frac{\partial F_x}{\partial x} = -R\phi \frac{\partial S}{\partial t} \qquad (2.28).$$

By combining equation 2.25 and equation 2.28, the modified one-dimensional advection-dispersion-adsorption equation due to the application of electricity in the system can be expressed as

$$R\frac{\partial S}{\partial t} = D\frac{\partial^2 S}{\partial x^2} - V_{total}\frac{\partial S}{\partial x} - V_{ep}\frac{\partial S_{mic}}{\partial x} \qquad (2.29)$$

where

R = the retardation factor (dimensionless),

D = hydrodynamic dispersion coefficient in x direction (cm^2/s),

V_{total} = the sum of hydraulic and electroosmotic velocities = $V + V_{eo}$ (cm/s),

V_{ep} = the velocity of micelles due to electrophoresis (cm/s),

S = the concentration of contaminants in the solution (mg/L), and

S_{mic} = the concentration of contaminants in the micelle solution (mg/L).

The concentration of contaminants in the solution S is equal to the sum of concentrations of contaminants in the aqueous S_w and in the micelles S_{mic} expressed as

$$S_w = S - S_{mic} \qquad (2.30).$$

Rearranging equation (2.9), the relationship of the concentration of the hydrocarbons in aqueous and in the micelle solution is showed in terms of the concentration-based micelle-water coefficient expressed as

$$S_{mic} = K'_{mic}\,[CTAB^-]_{mic}\,S_w \qquad (2.31)$$

where

S_{mic} = the concentration of the hydrocarbons in surfactant micelles (mg/L),

S_w = the concentration of the hydrocarbons in aqueous phase (mg/L),

K_{mic}' = micelles-water partition coefficient (M^{-1}), and

$[CTAB^-]_{mic}$ = moles of CTAB in micellar form per liter of solution = $(C_{surf} - C_{cmc})$ (M).

Substituting equation 2.30 with equation 2.31, the relationship of the concentration of hydrocarbons in solution and in the surfactant micelles is shown in the following

$$(1 + K_{mic}[CTAB^-]_{mic})S_{mic} = K_{mic}[CTAB^-]_{mic}S \qquad (2.32).$$

The fraction of hydrocarbons in the surfactant micelles is defined as

$$f_{hc,mic} = \frac{S_{mic}}{S} = \frac{K_{mic}[CTAB^-]_{mic}}{1 + K_{mic}[CTAB^-]_{mic}} \qquad (2.33).$$

Substituting and rearranging equation 2.26 and equation 2.30, and taking into account the effect of surfactants, the modified advection-dispersion-adsorption equation can be expressed as

$$\frac{\partial S}{\partial t} = \frac{D}{R_{cmc}}\frac{\partial^2 S}{\partial x^2} - \frac{V_{total}}{R_{cmc}}\frac{\partial S}{\partial x} - \frac{V_{ep} f_{hc,mic}}{R_{cmc}}\frac{\partial S}{\partial x} \qquad (2.34).$$

The migration of hydrocarbon contaminants, taking into account the effect of the presence of cationic surfactant (CTAB) and the presence of electricity, is expressed in the

modified advection-dispersion-adsorption equation 2.31.

The modified advection-dispersion-adsorption equation can be solved by assuming the initial condition of an instantaneous source at x = 0 with initial mass M_o, as reported by Baetsle (1969). The contaminant concentration at a given distance x and time t can thus be expressed as (Baetsle 1969)

$$S(x,t) = \frac{M_o}{2\sqrt{\frac{\pi Dt}{R_{cmc}}}} \exp\left(-\frac{X^2}{\frac{4Dt}{R_{cmc}}}\right) \qquad (2.35)$$

where

$$X = x - \frac{V_{total}}{R_{cmc}} t - \frac{V_{ep} f_{hc,mic}}{R_{cmc}} t,$$

S = the concentration of contaminants in the solution (mg/L),

x = distance from the source (cm),

V_{total} = the sum of hydraulic and electroosmotic velocities = $V + V_{eo}$ (cm/s),

R_{cmc} = the retardation factor (dimensionless),

$f_{hc,mic}$ = the fraction of hydrocarbon concentration in surfactant micelles (dimensionless),

V_{ep} = the velocity of micelles due to electrophoresis (cm/s) ,

D = hydrodynamic dispersion coefficient in x direction (cm^2/s),

M_o = initial mass of hydrocarbons in the system at x = 0 (μg), and

t = hydrocarbons travel time (s).

2.7 SPME-GC-FID analysis

To monitor the movement of hydrocarbon contaminants during remediation as well as to determine the remaining hydrocarbon contaminants in the remediated soil, automated solid-phrase microextraction (SPME) with gas chromatography (GC) coupled with a flame ionization detector (FID) was used. SPME is a rapid, inexpensive, solventless, portable, and easily automated technique to extract volatile and nonvolatile compounds from both liquid and gaseous samples onto the special coating on the fibre (Chai *et al.* 1993; Shirey *et al.* 1993).

Solid-phrase microextraction (SPME) utilizes a fused-silica fibre coated with an organic stationary phase such as polydimethylsiloxane to extract hydrocarbons from contaminated aqueous or gaseous samples by exposing the fibre directly or in the headspace over samples. The fibre is contained in a specially designed syringe to protect the fibre between extractions. In using SPME analysis, two processes are involved, i.e., the adsorption of organic compounds onto a fibre from the samples and desorption of concentrated organic compounds adsorbed onto the coating of fibre into gas chromatography (GC) to be analyzed. In the first process, a fibre is exposed directly to the aqueous sample or to the headspace over the sample to extract the hydrocarbons onto the coating. Figure 2.1 shows the fibre immersed in an aqueous sample allowing the hydrocarbons partitioning from the water into the stationary phase until equilibrium has been reached. The fibre with concentrated target organics is withdrawn into the syringe, and automatically moved from the sample to a gas chromatography injector for thermal desorption. Target hydrocarbons are then thermally desorbed from the stationary phase

into GC column to be analyzed. The detector response from SPME-GC-FID can be quantified by using calibration curves, which shows the relationship between the concentration of aqueous samples and the detector responses, to determine the concentration of target hydrocarbons in the sample.

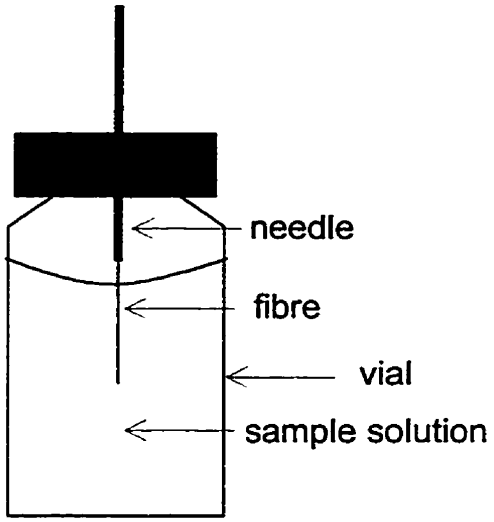

Figure 2.1 The fibre is exposed to the aqueous sample during extraction. The analytes are sorbed to the fibre coating from the aqueous phase in a 2-mL vial.

The amount of analyte sorbed onto the coated fibre at a given time is affected by three major factors: (1) the distribution constant of the analyte, (2) the volume of the stationary phase and (3) the initial sample concentration (Sarna *et al.* 1994). When the analytes sorbed onto the coating reach a maximum level over time, equilibrium between the concentration of the analytes in solution and the concentration in the coating of the fibre is attained. At equilibrium, a linear relationship exists between the amount of analyte sorbed to the stationary phase and the concentration of analyte in the sample. The linear relationship is described by (Arthur *et al.* 1992a; Sarna *et al.* 1994)

$$n_s = K_f V_s C_{aq} \qquad (2.28)$$

where

n_s = the number of moles of the analyte sorbed on the stationary phase,

K_f = the distribution constant of the analyte,

V_s = the volume of the stationary phase, and

C_{aq} = the initial concentration of analyte in the aqueous phase.

The number of moles of the analyte sorbed on the stationary phase (n_s) can be quantified from the standard curve, which shows the relationship of the moles of analytes injected into GC column and its detector response. The distribution constant (K_f) increases with the increase in molecular weight and boiling point of the analytes (Shirey *et al.* 1993). Arthur (1992b) reported the distribution constants of benzene, toluene, ethylbenzene, and *o*-xylene as 126, 340, 528, and 654 respectively by using a 56μm methylsilicone fibre.

The distribution constants K_f for the water-fibre system are very similar to the octanol-water partition coefficient K_{ow}, when the fibre used is coated with polydimethylsiloxane (Chai *et al.* 1993). Therefore, the distribution constant K_f can be predicted based on the known octanol-water partition coefficient. The larger distribution constant results in the longer equilibrium time, because the analytes with large distribution constant have to diffuse more material through the static layer to reach the fibre (Arthur *et al.* 1992b; Chai *et al.* 1993). To increase the extraction efficiency and reduce the equilibrium time, the sample must be agitated during extraction or modified by the addition of salt. The pH could be changed to decrease the time to reach equilibrium. All these methods result in the reduction of distribution constant (Shirey *et al.* 1993).

2.7.1 Dilution protocol

In general, remediation projects encountered in many contaminated sites contain free-phase or high concentrations of BTEX and PAHs (Thomas S.P. *et al.* 1996b). To determine the concentration of hydrocarbons using SPME, the solution with free-phase concentration of contaminants must be diluted to ensure complete dissolution of the hydrocarbons. The linearity of hydrocarbon response was reported to be less than 3000 ppb (w/v) using SPME with 56-μm methyl silicone fibre (Arthur *et al.* 1992b). At higher concentrations the response of fibre decreases and becomes nonlinear as a result of the absorption and desorption dynamics (Arthur and Pawliszyn 1990). The decrease in the amounts of desorption resulted from the change in porosity and chemical properties of the surface of the stationary phase due to the swelling of the stationary phase by solvents.

To determine the hydrocarbon concentration using SPME, the sample has to be diluted to meet the requirement of the linear response.

The solubility of hydrocarbons is another factor requiring the dilution of the sample prior to using SPME, since the presence of other organic compounds in a solution reduces the solubility of individual organic compounds (Arthur *et al.* 1992a; Sanemasa *et al.* 1987; Shirey *et al.* 1993; Thomas 1996a). The hydrocarbon-contaminated sites seldom contain a single compound, which usually involve tens or hundreds of contaminants which commonly include benzene, toluene, ethylbenzene, three isomers (*para-, meta-, and ortho-*) (BTEX) and PAHs. Therefore, the solubilities of hydrocarbons in a complex mixture are reduced, which can be predicted by Raoult's law according to the solubility of individual compound and mole fraction of compounds (Lane and Loehr 1992; Sanemasa *et al.* 1987; Thomas 1996a). Raoult's law is described by

$$S_m = X_{im}S_i \qquad (2.29)$$

where

S_m = the aqueous solubility of a compound in the mixture ,

X_{im} = the mole fraction of individual compound in the mixture, and

S_i = the individual aqueous solubility.

Prior to using automated SPME-GC-FID to analyze the sample, the sample had to be diluted to ensure all the hydrocarbons are dissolved in the solution. Since contaminants

in the contaminated sites are a mixture of many hydrocarbons, the standard solution and model diesel fuel were prepared by mixing nine commonly encountered hydrocarbons. There are a lot of time and effort advantages in using a complex mixture compared to the analysis of individual compounds on the gas chromatography as well as the entire experiment.

The presence of co-solvent in the solution is another factor affecting the accuracy of hydrocarbon analysis using SPME with a polydimethylsiloxane coating fibre. However, Arthur (1992a) indicated the limitation of co-solvent concentration at or below 1% in which the accuracy was not affected. Therefore, to maintain high accuracy of analysis, the sample must be diluted to ensure the concentration of co-solvent at or below 1% in the aqueous phase. The co-solvent such as acetone was introduced in the experiment to increase the solubility of hydrocarbons. The solution with high concentration of co-solvent must be diluted at least by a factor of 100 to ensure the concentration of co-solvent at or below 1% (Thomas S.P. *et al.* 1996b).

In conclusion, the linearity, solubility, and the co-solvent effect requires the dilution of the sample prior to using SPME to determine the concentration of hydrocarbons.

2.7.2 Limits of detection

The limits of detection (LOD) and linear ranges are affected by several factors in which the volume of the fibre coating is one of the main factors (Potter and Pawliszyn 1994). Thicker films result in a larger volume of coating and a lower limit of detection because more analytes can be extracted (Arthur *et al.* 1992c). In general, thin films are used to absorb analytes with higher K_f values, and thick films are used to absorb the

analytes with lower K_f values (Arthur *et al.* 1992c). The amount of analyte extracted is limited by the rate of diffusion of analyte through the water (Louch *et al.* 1992). The limitation of detection (LOD) can be improved by using an agitation technique during extraction (Arthor *et al.* 1992a; Thomas 1996a). The LOD in the presence of agitation ranged from 47.8-526 pg/mL rather than 117-661 pg/mL in the static solution, when the fibre used in the experiments was coated with 100-μm polydimethylsiloxane (Thomas 1996a).

2.7.3 Agitation and static extraction

Solid-phrase microextraction (SPME) has been shown to be a fast, simple, and low-cost method for analysis of organic compounds in water (Arthur *et al.* 1992b; Shirey *et al.* 1993). However, the amount of an analyte sorbed to the fibre coating depends on its solubility in water compared with its sorption onto the fiber coating (Shirey *et al.*).

The extraction efficiency can be enhanced by promoting larger amount of the analytes to be partitioned onto the fibre coating or by a reduction in the equilibrium time. Agitating the sample is one of enhanced methods (Arthur *et al.* 1992a; Arthur *et al.* 1992b; Arthur *et al.* 1992c; Louch *et al.* 1992; Shirey *et al.*; Thomson 1996a; Zhang and Pawliszyn 1993). Although different agitation techniques have been available to choose such as using of magnetic stir bar and sonification, they have their own disadvantage. The use of magnetic stir bar for agitating the sample may cause the sample to lose the vapor of volatile organic compounds to the environment (Arthur *et al.* 1992a; Arthur *et al.* 1992b; Arthur *et al.* 1992c; Louch *et al.* 1992; Zhang and Pawliszyn 1993). The

sonification technique is another available agitation technique to enhance the extraction efficiency, which requires expensive equipment (Zhang and Pawliszyn 1993).

An innovative agitation technique is required. The sample carousel agitation device (SAMCAD) was designed in our lab as an adjustment to the Varian 8200 autosampler. It vibrated the sample carousel only when the SPME fibre was exposed to the sample during extraction. The SAMCAD agitation technique has the potential to enhance the efficiency of extraction response and leads to a reduction of the equilibrium time. Two optical sensors are mounted on the autosampler to control agitation on/off time to ensure agitation of the sample only during extraction. The sample carousel agitation device is easy to work with automated extraction.

3.0 Materials and Methods

Section 3.1 presents the methods which were used to determine the properties of cationic surfactant (CTAB) used in this study. The properties include the critical micelle concentration (CMC), molar solubilization ratio (MSR), and micelle-water partition coefficient K_{mic}.

The soil remediation methods used in this study are described in Section 3.2. This section presents the experimental set-up in the laboratory, the preparation of clay columns, the preparation of model diesel fuel, and the contamination of test columns. The experimental methodology is also introduced, including the experimental conditions, the measurement of several parameters which are critical for the evaluation of the efficiency of soil remediation techniques. The parameters measured include flow rate, voltage drop and current flow, contaminant concentrations, bulk density, water content, and pH.

In Section 3.3, a description of the solid-phase microextraction method combined with GC and FID analysis is provided. The method for determining the linear response range is developed. A method for selecting an efficient extraction technique is also described.

3.1 Methods for the determination of surfactant properties

3.1.1 Determination of critical micelle concentration (CMC)

The Critical Micelle Concentration (CMC) of cetyltrimethylammonium bromide (CTAB) is the concentration of surfactant at which the rate of increase of electrical conductivity as a function of concentration is zero or proceeds at a much lower rate

(Paker 1984). The CMC of CTAB was obtained by measuring the electrical conductivity of the surfactant at different concentrations.

Surfactant solutions, at concentration ranging from 0% to 2.62%, were prepared for determining the CMC of CTAB. The surfactant concentrations of 0%, 0.03%, 0.05%, 0.07%, 0.11%, 0.14%, 0.16%, 0.20%, 0.26%, 0.33%, 0.45%, 0.70%, 0.90%, 0.95%, 0.99%, 1.00%, 1.07%, 1.10%, 1.23%, 1.51%, 1.72%, 2.03%, 2.34%, and 2.62% were obtained by dissolving known masses of CTAB in 100 mL of distilled water. The surfactant solutions were stirred using a magnetic stir bar for over 24 h until completely dissolved. When the solution appeared to be clear with no residues settling at the bottom an electrical conductivity meter was used to measure the electrical conductivity of the solution. When the concentration was above 0.7%, the CTAB was found to dissolve less in distilled water at a temperature of 20°C.

3.1.2. Determination of MSR and K_{mic}

Molar solubilization ratio (MSR) and micelle water partition coefficients (K_{mic}) are parameters that were used to determine the ability to solubilize BTEX and PAHs in micelles. When the concentration of surfactant is above the CMC, there is a linear relationship between the solubility of hydrocarbon compounds and the concentration of the surfactant Edwards *et al.* 1991; Gannon *et al.* 1989; Rouse *et al.* 1993; Valsaraj *et al.* 1988). The solubility of hydrocarbons increases linearly with an increase in concentration of surfactant solutions. The MSR was determined by finding the slope of

the linear relationship between solubility and surfactant concentration at concentrations above CMC.

Five CTAB solutions, at concentrations ranging from 0, 1.37, 13.49, 20.58, and 27.44 mmol/L, were prepared to dissolve the compounds in the BTEX and three selected PAHs. A volume of 1.6-mL each of benzene, toluene, ethylbenzene, and the three xylene isomers (BTEX) were added separately to 100-mL of solutions at five different concentrations. The solutions were stirred for two days, to ensure the maximum solubility of the organic compounds, after which they were poured into separator funnels. Since densities of compounds in the BTEX are smaller than the density of water, free-phase compounds were found to float to the top of the solution in the separator funnels. A 5-mL aliquot was taken from the bottom of each separator funnel to determine the solubility of hydrocarbons in surfactant solution. Prior to the analysis of the solution, the aliquot was diluted by 100 times. An aliquot of 1.5-mL of diluted solution was taken and placed in a 2-mL screw-cap vial for SPME-GC-FID analysis. The MSRs, of the compounds in BTEX, was obtained by calculating the slope of the linear relationship between the solubility and surfactant concentrations.

Similar tests were also carried out with 0.8 g each of naphthalene, 2-methylnaphthalene, and phenanthrene. The solution was stirred for two days as before. Since the densities of PAHs are slightly higher than the density of water, free-phase hydrocarbon compounds settled to the bottom of the flasks. An aliquot of 5-mL containing the dissolved hydrocarbons was taken from the top of the flasks and diluted 100 times before SPME-GC-FID analysis.

The effect of micelles on solubility of organic compounds can also be characterized by the micelle-water partition coefficient (K_{mic}). Equation 2.7 was used to calculate K_{mic} from MSRs.

3.1.3 Preparation of surfactant solution for soil remediation

The surfactant used in this remediation experiments is cetyltrimethylammonium bromide (CTAB) with a critical micelle concentration of 0.9 (mmol/L). The concentration of CTAB solutions used in the surfactant-enhanced remediation is 1.5 %. The surfactant solution was flushed through three hydraulic and three electrokinetic hydrocarbon-contaminated clay columns.

The solution with 1.5% concentration was prepared by adding 1.5g of CTAB into 100 mL of distilled water. The solubility of a surfactant in water increases with increasing temperature in a similar way to most organic molecules (Porter 1991). Therefore, the solution was slightly warmed to reduce the dissolving time and to ensure CTAB was completely dissolved in distilled water. The above steps were replicated to prepare 3 L of surfactant solution needed during the course of this experiment.

3.2 Soil remediation experiments

3.2.1 Experimental set up for soil remediation

The laboratory set-up for remediation of hydrocarbon-contaminated clay columns included six specially designed glass columns, a constant hydraulic head supply device, a flow-rate measuring system, a DC power supply, and a voltage measuring system. The

voltage measuring system designed in our lab consisted of a data acquisition system controlled by a computer, a voltmeter, and a 24-channel multiplexer shown in Figure 3.1.

The clay soil was packed into 30-cm long, 5.08-cm O.D., 4.76-cm I.D. (cross sectional area 17.8 (cm^2)) glass columns, which were specially designed in our lab. During soil remediation experiments, six clay columns were used simultaneously to evaluate the efficiency of various soil remediation techniques. Three of them were subjected to water flushing treatment or surfactant flushing, referred to as hydraulic columns. The other three columns were subjected to water flushing or surfactant flushing coupled with electrokinetic treatment, referred to as electrokinetic columns. The electrokinetic remediation was achieved by applying a low-level DC electrical potential gradient across the length of the column. The glass columns, packed with clay soils, were placed between two Teflon-backed plexiglass endcaps which were held together with 3 stainless steel tie rods. Thin nylon mesh and glass beads were used to separate the clay soils from the endcaps as shown in Figure 3.2. During the soil remediation experiments, the six columns were mounted in the horizontal position on a wooden rack.

The glass column had two rows of ports made by fusing 2-mL screw cap vials along the length of the column. One row of ports, referred to as current and voltage drop monitoring ports, consisted of eight ports placed 3-cm apart starting at 4.5 cm from the end of the column. The other row of ports, referred to as sampling ports, consisted of five ports located at 2, 8.5, 15, 21.5, and 28-cm from the end of the column.

The voltage measuring ports had platinum electrodes that were connected to a voltage measuring system to record the current flow and the voltage drop along the length

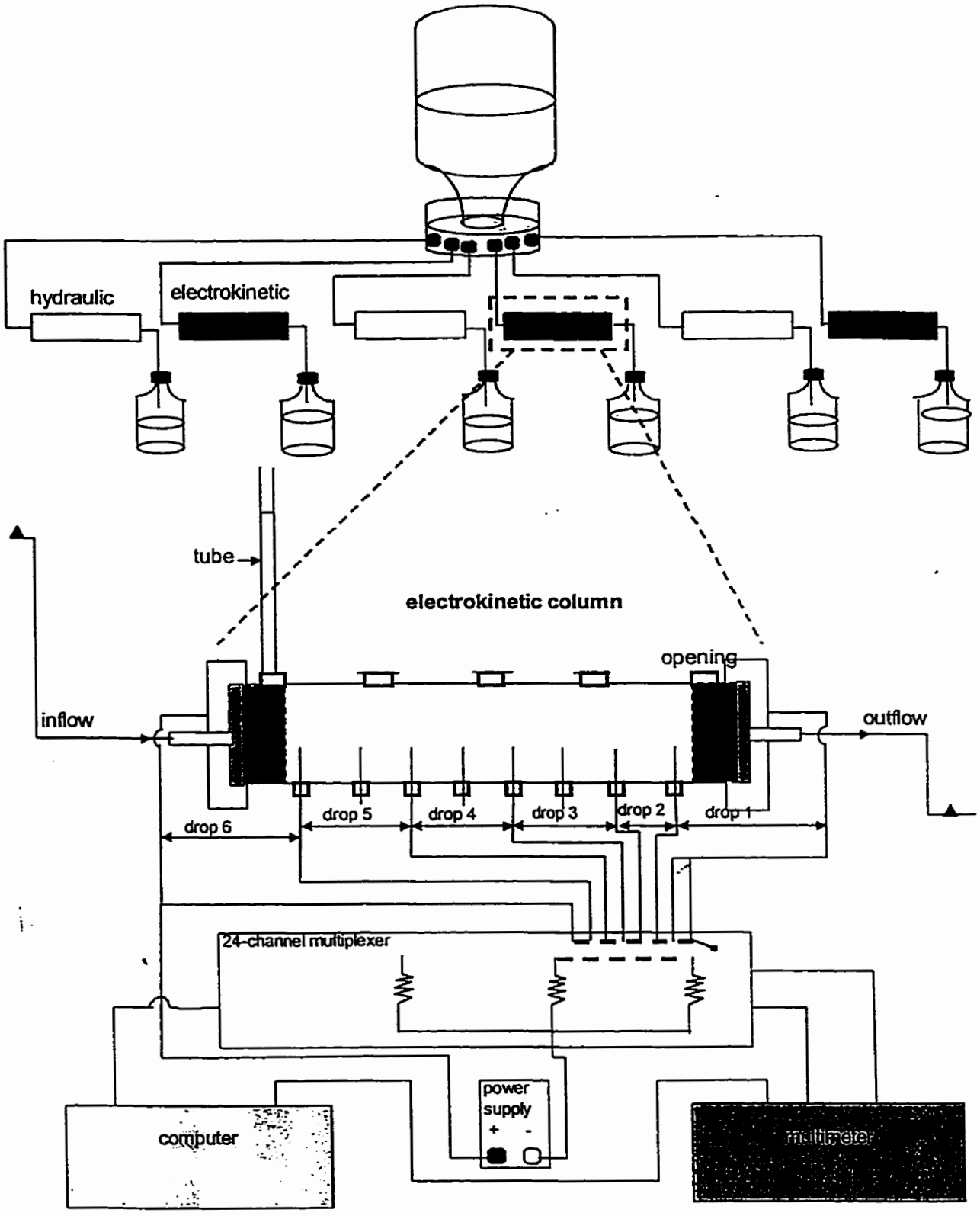

Figure 3.1 Laboratory set up for soil remediation.

of the columns during soil remediation. The sampling ports were used to obtain pore water samples for monitoring the movement of organic compounds in the contaminated columns during soil remediation. The contaminated pore fluids were analyzed by SPME-GC-FID.

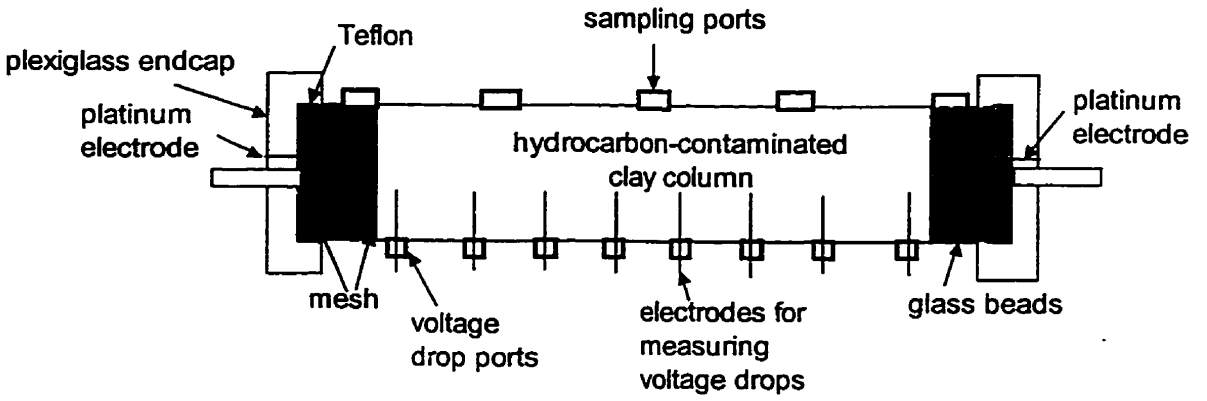

Figure 3.2 Test clay soils packed in the glass column.

An inverted carboy placed over a cylindrical container was used as the constant hydraulic head device. The cylindrical container had six separate tubes attached on its vertical wall which supplied the water or surfactant solutions to the sample at a constant hydraulic gradient. The level of the water in the cylindrical container was used as a reference to measure the applied hydraulic head.

The flow rate measuring system consisted of a flask connected to the outflow end of the column as shown in Figure 3.1. The effluent was collected in a flask over time for each of columns during remediation. Therefore, the flow rate can be calculated by

dividing the volume of the effluent by the time of the collection. The flask had rubber stoppers with two holes, one of which was used to connect the outflow tube from the clay column and other was used to balance the air pressure with the atmosphere. The outflow tubes were made of Teflon. A small diameter tube was chosen to balance the inside and outside air pressures. Since this tube had a small diameter, the vapor loss from the effluent could be neglected.

A BK Precision DC Power Supply 1610 was used to apply a constant voltage gradient on the test columns. In the experiment, 0.51-mm diameter platinum wire was used as electrodes to apply the voltage drop across the ends of the electrical columns. Platinum wire was also used to measure current and voltage drop along the length of the columns.

The current and voltage measuring system consisted of a voltmeter, a 24-channel multiplexer, a data acquisition system controlled by a computer program. The 24-channel multiplexer is the device to control channel switches for voltage drop and current measurements during soil remediation. Voltage on/off time on three electrokinetic columns were controlled by channels 1, 9, and 17. Channels 8, 16, 24 were separately used to measure the voltage drop over a 1000 ohm resistor on each electrokinetic column. The current in the column was then determined based on Ohm's Law. The remaining channels were used to measure the voltage drops along the column. The 24-channel multiplexer and the data acquisition system were controlled by a computer program (Thomas 1996a). The voltmeter used in the experiment was a Hewlett Packard 34410A.

3.2.2 Preparation of the test columns

3.2.2.1 Preparation of the clay columns

The clay soils used in the water flushing and water flushing coupled with electrokinetic treatments were provided by Manitoba Hydro. They. were identified as Pine Falls: Forebay PF009, Sec'A', S-3, S-4, S-6, S-7; Forebay PF009, Sec'B', S-7; Forebay, PF009, Sec'C', S-1, S-2; Forebay, PF011, Sec'C', S-6.

The dry bulk density of each of the cores was determined. Clay cores were placed separately in 600-mL labeled beakers and oven dried at 105°C for over 24 hours. After oven drying, the beaker with the clay core was cooled in a desiccator to prevent moisture gain from the atmosphere. The volume of the clay cores were calculated from measured dimensions. The dry bulk density and water content (w/w) are calculated using equation 3.1

$$\text{dry bulk density} = \frac{(\text{Wt. oven dried clay} + \text{tare}) - \text{tare}}{\text{volume of clay}} \qquad (3.1).$$

After measuring the dry bulk density of each of the cores, they were ground into particles small enough to pass through 60 - 100 mesh sieve. Distilled water was then added to the mixed clay soil until it became a paste with a water content of about 60%. The clay paste was spooned into the glass columns, held vertically on a stand, over a nylon mesh that was used to separate the clay from the glass beads. To minimize air entrapment in the columns and to ensure a uniform bulk density, a tamping tool was used to slightly tamp the soil down during packing of the clay columns. Since gas is produced at the anode and

cathode during electrokinetic remediation, glass beads were placed between the endcap and the first sampling port on either side of the columns to allow the gas to escape.

The clay soil used in the surfactant flushing experiments was obtained from a construction area located near the agriculture building at the University of Manitoba. The dry bulk density of the clay from near the agriculture building was calculated using equation 3.1. Prior to packing the columns with this clay soil, it was tested for hydrocarbon contamination and pH. This clay soil was not found to be contaminated by BTEX and selected PAHs (naphthalene, 2-methylnaphthalene, and phenanthrene). The porosity of the clay soil was 62% which was similar to that of the one from Manitoba Hydro. Both porosities, from Manitoba Hydro and from the construction area at the University of Manitoba, were found to be in the typical porosity range of 40-70% for clay soils (Freeze and Cherry 1993).

3.2.2.2 Model diesel fuel composition

Petroleum hydrocarbons are one of the most frequent sources of groundwater and soil contamination. Among petroleum products, diesel is one of the most common petroleum products, composed of hundreds hydrocarbons generally in the range of C_{10} through C_{19} (Kostecki and Calabrese 1993). Although diesel is a complex mixture of hundreds of hydrocarbons, depending on the refining method and feed and blending stocks, the majority of the mixture is composed of aliphatic hydrocarbons and aromatic compounds such as BTEX, naphthalene, 2-methylnaphthalene, and phenanthrene. BTEX is a mixture of benzene, toluene, ethylbenzene, *o*-xylene, *p*-xylene, and *m*-xylene.

The composition of the model diesel fuel, including BTEX and three common PAHs (naphthalene, 2-methylnaphthalene, and phenanthrene), matches a typical mixture of diesel fuel and is listed in Table 3.2. The selected composition is based on the average concentrations of the respective compounds found at diesel contaminated sites (Kostecki and Calabrese 1993). The BTEX was chosen because they are somewhat soluble in water, highly mobile in the environment, and represents the most volatile and soluble components of diesel. Naphthalene, 2-methylnaphthalene, and phenanthrene were chosen because they are prevalent in diesel, and represent the heavier or less volatile components of diesel. In addition, BTEX and naphthalene, 2-methylnaphthalene, and phenanthrene are also known animal carcinogens (Kostecki and Calabrese 1993).

Table 3.1 Composition and properties of model diesel fuel

Compound	Concentration (ppm)		Solubility (ppm) †	Specific Gravity †	Molecular Weight †	Solubility (ppm) †
benzene	500	82*	1750	0.87	78.11	1159
toluene	500	800*	515	0.87	92.14	401
ethylbenzene	500	800*	152	0.88	106.17	175
p-xylene	500	800*	198	0.86	106.17	138
m-xylene	500	800*	158	0.86	106.17	135
o-xylene	500	800*	152	0.88	106.17	160
naphthalene	2000	2,730*	30	1.15	128.18	106
2-methylnaphalene	6000	6,700*	25	1.01	142.20	94
phenanthrene	1500	1,500*	1	1.18	178.24	1

† From: (Knox *et al.* 1993); * From: (Kostecki and Calabrese 1993)

The model diesel fuel was prepared by adding 5.8 μL each of benzene, toluene, ethylbenzene, *o*-xylene, *p*-xylene, *m*-xylene, 20 mg of naphthalene, 60 mg of 2-methylnaphthalene, and 15 mg of phenanthrene into 100 mL acetone. The acetone was chosen as a co-solvent because all of the above organic compounds are miscible with acetone and acetone itself is miscible with water.

3.2.2.3 Contamination of clay columns with the model diesel fuel

Prior to conducting the model remediation experiments, the clay columns, both hydraulic and electrokinetic, were contaminated by adding 10 mL of model diesel. The first voltage drop port of each column near the anode at the inflow end was used for the injection of the model diesel by syringe. To minimize the cracking and physical disturbance of the clay soils, the model diesel was slowly injected over two hours.

3.2.3 Experimental methodology

3.2.3.1 Water-flushing experiments

In water flushing and water flushing coupled with electrokinetic remediation, six columns contaminated by the model-diesel fuel were used simultaneously. Three of them were remediated only under the influence of an applied hydraulic gradient, referred to as hydraulic columns. The other three were remediated under a hydraulic gradient coupled with the application of an electrical potential difference, referred to as electrokinetic columns. To ensure a similar water flow, all six clay columns were placed in the horizontal orientation on a rack and were flushed with distilled water under a hydraulic gradient of 2.8 for several weeks

A constant low-level voltage potential difference of 7.5V was applied to the electrokinetic columns. The anode was located at the inflow end of the column, which facilitated the electrophoretic flow of positively charged micelles, electoosmotic flow, and hydraulic flow in the same direction towards the cathode at the outflow end. During the electrokinetic remediation, oxygen and hydrogen were being produced at the anode (inflow) and cathode (outflow) electrodes, respectively. If the gases produced at the electrodes were allowed to accumulate in the clay columns, the gases would generate enough back pressure to retard water flow and thus reduce the efficiency of remediation. The hydrogen gas produced at the cathode could be released by opening the last sample port (near the cathode) to the atmosphere directly. Water did not flow out through the last sample port because of the low hydraulic head at the cathode end. Releasing the gas produced at the anode was found to be difficult because of the high hydraulic head near anode end. Therefore, a long vertical tube was connected to the first sample port located near the inflow end of the column allow for gas egress as shown in Figure 3.1.

To monitor the movement of hydrocarbons during remediation, the pore fluid was sampled at each sampling port along the length of the column and analyzed by SPME-FID-GC once every three days. The voltage drop and current in each electrokinetic column were measured every 15 minutes. After the experiment had been allowed to run for 55 days, all six columns were disconnected. The soil sample was cooled in a refrigerator overnight and the sample was pushed out from the glass column and segmented for SPME-GC-FID analysis. This was done to determine the remaining

hydrocarbons in the clay sample and thus evaluate the efficiency of the soil remediation techniques.

3.2.3.2 Surfactant-flushing treatments

Six columns, three hydraulic and three electrokinetic, were flushed with a surfactant solution, made with 1.5% (w/w) of CTAB, under a hydraulic gradient of 2.8. A constant voltage of 7.5V was applied to the electrokinetic columns.

The anode was located at the inflow end of column. During the remediation, oxygen and hydrogen were produced at the anode (inflow) and at the cathode (outflow), respectively. The method used to release the gases was the same as the one in the water flushing experiments. During the soil remediation, pore fluid was sampled from the sample ports. The voltage drop and current were measured from the voltage-drop-measurement ports. Effluent was collected to measure the flow rate through the columns. The electrical conductivity and pH of the effluent was also measured. The experiment lasted 53 days after which the samples were sectioned for the extraction of the hydrocarbon contaminants. A summary of water-flushing and surfactant-flushing experimental conditions is shown in Table 3.3.

3.2.4 Flow rate measurement

The flow rate is one of the critical parameters that is needed to evaluate the efficiency of soil remediation techniques. The flow rate of each column, in either water flushing or surfactant flushing with or without the application of electrical potential gradient, was measured by collecting effluent volume over time. The effluent was collected in a graduated flask, as shown in Figure 3.1, which had a specially designed cap

to minimize the evaporation of the effluent.

3.2.5 Monitoring contaminant movement

Pore water samples were collected from the columns to monitor the movement of hydrocarbons in the soil columns during the experiments. Solid-phase microextraction (SPME) with gas chromatography (GC) coupled with a flame ionization detector (FID) was used to determine the hydrocarbon concentration in the pore water samples. The pore liquid was sampled and analyzed every three days. In hydraulic columns, the pore

Table 3.2 Summary of the experimental conditions

Conditions	Hydraulic gradient (dh/dx)	Voltage applied (V)	% CTAB (w/w)	Test time (days)	Diesel injected
Water flushing	2.8	0	0	55	10 mL of BTEX and PAHs
Water flushing with voltage	2.8	7.5	0	55	10 mL of BTEX and PAHs
CTAB flushing	2.8	0	1.5	55	10 mL of BTEX and PAHs
CTAB flushing with voltage	2.8	7.5	1.5	55	10 mL of BTEX and PAHs

liquid could be sampled from each sampling port, except one sampling port closer to the outflow end near the cathode. For electrokinetic columns, the pore liquid was sampled starting from the second sampling port, because the first port was used to release the gaseous oxygen produced at the anode. In the sampling port near the outflow end, no pore liquid was sampled from the column.

Since the amount of pore fluid in the sampling ports was low it was difficult to collect from the sampling ports. Since clay particles clogged the needle of the syringe, the syringe was found to be unsuitable for collecting the pore fluid directly. To solve the clogging problem encountered, a glass tube was used to create a cylindrical cavity at each sampling port in the clay column. At the end of each sampling, distilled water was filled into the openings and allowed to come into equilibrium with the surrounding pore fluid. Since the volume of pore fluid available for removal from the ports was different the samples were diluted based on the volume withdrawn prior to SPME-GC-FID analysis.

3.2.6 Sectioning of the columns for contaminant analysis

After soil remediation, the columns were disconnected, sealed at both ends and chilled in a refrigerator at 4°C for a day. The clay core was then pushed out of the anode end of the glass column. The length and diameter of the clay core was 26 cm and 2.54 cm, respectively. The clay core was cut into nine equal segments by using a piece of dental floss. Each segment was individually mixed thoroughly to distribute the contaminant uniformly within each segment. However, this was done quickly to prevent evaporation of the contaminants. Two samples of clay, each weighing 5.0 g, were taken

from the mixed clay segment and placed into 25-mL vials separately and stored in a deep freezer (-20°C) until extraction was performed. The remaining portion of each clay segment was used to determine the gravimetric water content and pH. The gravimetric water content is given by

$$\text{water content} = \frac{(\text{Wt.of wet clay + tare}) - (\text{Wt.of oven dried clay + tare})}{(\text{Wt.of oven dried clay + tare}) - \text{tare}} \times 100\% \quad (3.2).$$

An extraction procedure was developed to extract the analytes from the clay samples prior to analysis. A 10 mL volume of acetone was added to the 5 g clay sample contained in the 25-mL vial. The vial was then sealed with a Teflon-lined screw cap to prevent the loss of hydrocarbons during the extraction procedure. The sample was then vibrated by a wrist-action shaker for 3 h. Prior to decanting the supernatant part of the extract from the 10-mL vial, the sample was set without agitation to allow the clay particles to settle down. The extract was diluted with HPLC grade water by a factor of 100 to meet the concentration limit of the co-solvent. Prior to analyzing the sample, the diluted solution was stirred with a magnetic stir bar to obtain a homogeneous distribution. Three 1.5 mL aliquot replicates were taken from the diluted solution and placed in 2-mL vials for SPME analysis.

3.2.7 Electrical conductivity measurement

The conductance is defined as the inverse of resistance and its unit is given in ds (Parker 1984). A YSI model 32 conductance meter was used to measure the conductance of a solution. The conductivity, used to express the ability of a solution to conduct electrical current, can be given by the conductance reading (ds) multiplied by the cell

constant of the conductivity cell (1/m or 1/cm). Therefore, the unit of conductivity is given in ds/m or ds/cm.

3.3 SPME

3.3.1 Standard solution preparation

A standard solution was used to determine the calibration curve, sorption-time profiles, and standard curve. The standard solution was prepared by adding BTEX (benzene, toluene, ethylbenzene, *p*-xylene, *o*-xylene, and *m*-xylene) and three selected polycyclic aromatic hydrocarbons (naphthalene, 2-methylnaphthalene, and phenanthrene) to acetone. This mixture was stirred using a magnetic stirrer for 12 h. The hydrocarbon and acetone mixture was then diluted to meet the requirements of linearity, solubility, and the concentration limit of the co-solvent. The acetone was chosen as a co-solvent to ensure all the hydrocarbons dissolved completely into the solution. The solution was then diluted at least by a factor of 100 to ensure the concentration of the acetone at or below 1%.

The standard solution was prepared by adding 58 mL each of BTEX and 5 mg each of naphthalene, 2-methylnaphthalene, and phenanthrene into the acetone. The solution was stirred using a magnetic stir bar over half a day to obtain a homogeneous solution containing 500 ppm BTEX and 50 ppm PAHs. The solution was then diluted with HPLC grade water by at least a factor of 100 to meet the requirement of the concentration limit of the co-solvent.

3.3.2 Determination of linear response limits

Various concentrations of standard solutions ranging from 0 to 50 ppm of BTEX and 0 to 5 ppm of PAHs were prepared to determine the linear responses of SPME with gas chromatography (GC) coupled with a flame ionization detector. The solutions with 5000 ppm of BTEX and 500 ppm PAHs in acetone were prepared and diluted with HPLC grade water by factors of 100 000, 50 000, 20 000, 10 000, 5 000, 2 000, 1 000, 500, 200, and 100, in which the maximum concentration of co-solvent was at or below 1%. Three 1.4-mL aliquots of the solution were taken and placed into 2-mL screw cap vials with silicone Teflon-backed septa for SPME-GC-FID analysis.

The adsorption and desorption time in the procedure were 30 and 2 minutes, respectively. The 2-minute desorption time was chosen based on the results from preliminary experiments showing the FID responses of 2-, 10-, and 15-minute desorption in the GC column which showed no significant difference. Therefore, the 2-minute time was chosen to desorb the analytes from the fibre coating into the GC column for analysis. The 30-minute was chosen as the extraction time, because most selected hydrocarbon compounds in the model diesel fuel seem to reach equilibrium within 30 minutes (as shown in Figure 4.8 and Figure 4.9). Although some selected polycyclic compounds reach the equilibrium in around 45 min, the response of those compounds at 30 min was not significantly different from the response at 45 min in the application of the agitation extraction. Therefore, the extraction time was chosen as 30 min, taking into account the effects of the equilibrium and exposure time.

3.3.3 Static and agitation extraction sorption-time profiles

The static and agitation extraction sorption-time profiles were developed to determine the efficiency of static and agitating extraction methods during the SPME-GC-FID analysis. The sorption-time profiles were developed with extraction times up to 60 min for benzene, toluene, ethylbenzene, three xylene isomers, and three PAHs (naphthalene, 2-methylnapthalene, and phenanthrene). The desorption time was 2 min during thermal desorption in GC. From the sorption-time profile, the equilibrium time can be obtained for both static and agitation extraction. In addition, the detector responses from the static and agitation extractions can be compared. Therefore, the more efficient extraction technique can be determined based on the equilibrium time and the detector response.

A standard solution containing 500 ppm BTEX and 50 ppm PAHs in acetone was prepared and diluted with HPLC grade water by a factor of 1000 to obtain the solution of 0.5 ppm BTEX and 0.05ppm PAHs. Six 1.4-mL aliquots of samples with a concentration of 0.5 ppm BTEX and 0.05 ppm PAHs were taken and placed into the vials for SPME-GC-FID analysis. Three of the vials were agitated during extraction while the other three were extracted without agitating the solution. To obtain sorption-time profiles, extraction times were chosen as 1, 5, 10, 15, 30, 45, and 60 min for both static and agitation extractions. The desorption time was chosen as 2 min.

3.3.4 Calibration curve and standard curve

The calibration curves for BTEX and PAHs were developed only using agitation extraction because of the efficiency of this method. A solution containing 5 000 ppm of BTEX and 500 ppm of PAHs in acetone was prepared and diluted with HPLC grade water by factors of 100 000, 50 000, 20 000, 10 000, 5 000, 2 000, 1 000, 500, 200, and 100. Three 1.4-mL aliquots were taken from the above diluted solution and placed into 2-mL screw cap vials with silicon Teflon-backed septa for SPME-GC-FID analysis.

The standard curve was developed to calculate the number of moles of analyte in the test sample. The various concentrations of the standard solutions prepared in acetone ranged from 5 000, 4 000, 3 500, 3 000, 2 750, 2 500, 1 400, 900, 500, 395, to 250 ppm of BTEX and PAHs. A disposable syringe was used to take 1 μL from the above solutions and directly injected into the gas chromatography for analysis. Three replicate injections were done for each of the above solutions.

3.3.5 Analysis of hydrocarbons by using SPME-GC-FID

To determine the hydrocarbon residues in the remediated clay soil, and monitor the movement of hydrocarbons during soil remediation, SPME-GC-FID was used. The hydrocarbons in the aqueous sample were extracted by a 100-μm polydimethylsiloxane fibre. The hydrocarbons sorbed on the fibre were thermally desorbed in a gas chromatography (GC) column. All separations were done using a Varian 3400 gas chromatography (GC) equipped with a flame ionization detector (FID). The separation was conduced using a Supelco 30-m × 0.32-mm I.D. carbon-layer open tubular (CLOT)

column. The FID was operated with He carrier gas plus make-up gas at a flow rate of 30 mL/min, air at 300 mL/min, and H_2 at 30 mL/min.

The determination of hydrocarbon residues in these experiments was performed with 30 min of adsorption of analytes from an aqueous sample and 2 min of thermal desorption into the GC column. The temperatures run as follows: detector of 250 °C; injector of 200 °C; column 40 °C (hold 2 min), 5 °C/min to 220°C, 2 °C/min to 280 °C, hold 2 minutes.

3.4 Experimental materials

Nine hydrocarbon compounds and one co-solvent were used in these experiments. Benzene and ethylbenzene were purchased from Caledon Laboratories, Inc., Georgetown, Ontario, Canada. Naphthalene (catalog No. 18, 450-0), 2-methylnaphthalene (catalog No. M5, 700-6), phenanthrene (catalog No. P1, 140-9), *p*-xylene (catalog No. 29,633-3), *m*-xylene (catalog No.29, 632-5), *o*-xylene (catalog No. 29, 588-4), and cetyltrimethylammonium bromide (CTAB) (catalog No. 85,582-0) were obtained from Aldrich Chemical Company Inc., Milwaukee, Wisconsin, USA. HPLC grade water was purchased from Mallinckrodt, ChromAR, Paris, Kentucky, USA. Toluene (catalog No. GD-9165) and acetone (catalog No. GD-1050) were obtained from Anachemia, Toronto, Ontario, Canada).

The fibre coated with 100-μm polydimethylsiloxane used for the solid-phase microextraction (SPME) was obtained from Supelco, Bellefonte, Pennsylvania, USA. Disposable 1-mL syringes were obtained from B-D (Fisher Scientific Co., catalog No. 14-823-2F). The pH 7.00 buffer solution was from Mallinckrodt Specialty Chemical

Company (Lot 0098 KMDB) and the 4.63 buffer solution was from Fisher Scientific Company (Lot 704100).

4.0 Results and Discussion

Since it is important to understand the properties of the surfactant before it can be used in soil remediation, many laboratory measurements were done. Section 4.1 describes the results of the experiments carried out to determine the surfactant properties. The efficiency of soil remediation is ascertained by analyzing the clay columns for hydrocarbon residues after a period of remediation treatment. Since a new analytical technique, SPME-GC-FID, was used to analyze the soil for residues, more experiments were carried out to test the analytical methods. The results of these tests are presented in Section 4.2. Finally, Section 4.3 presents the residual hydrocarbon remaining in the clay columns at the end of the 50-day remediation period.

4.1 Surfactant properties

The properties of the surfactant presented here include the critical micelle concentration (CMC), molar solubilization ratio (MSR), and micelle-water partition coefficient (K_{mic}). This section develops the relationships between the solubility of hydrocarbons as a function of octanol-water partition coefficient (K_{ow}) both in the aqueous phase as well as in a surfactant solution. The micelle-water partition coefficient (K_{mic}) as a function of K_{ow} is also presented. In addition, the organic carbon-water partition coefficient (K_{oc}) was calculated. The modified retardation factor (R) was determined to account for the effect of micelles in solution.

4.1.1 Critical micelle concentration (CMC) of CTAB

The critical micelle concentration (CMC) was determined as the concentration at

which there was a change in the rate of increase of the electrical conductivity. Figure 4.1 shows a bi-linear response of electrical conductivity with an increase in the concentration of the surfactant. The critical micelle concentration, concentration of surfactant at the intersection of the bi-linear line, was found to be 9.0×10^{-4}M (0.03%) for the CTAB. This experimentally determined CMC of CTAB is very close to the one reported by Soma and Papadopoulos (1997) and Kile and Chiou (1989) which are 9.2×10^{-4}M and 361 mg/L ($= 9.9 \times 10^{-4}$M), respectively. Since the value of CMC of the surfactant is temperature dependent, the critical micelle concentration (CMC) was also determined at the room temperature of 20°C.

4.1.2 MSR and K_{mic}

The individual solubility of selected compounds was measured in the aqueous phase and in surfactant solutions at CMC. The solubility, shown in two different units, is listed in Table 4.1. The solubility in the unit of mg/L was measured from the experiments in both aqueous phase and surfactant solution. The solubility in the unit of mmol/L was calculated. BTEX shows higher apparent solubility in either water or surfactant solution at CMC compared to the selected PAHs. Among them, benzene shows the highest solubility followed by toluene, ethylbenzene, and the three isomers. Of the nine hydrocarbons of interest, phenanthrene shows the lowest solubility, even in the presence of a surfactant solution at CMC. Table 4.1 also shows that the solubilities of individual hydrocarbon compounds are increased in the presence of surfactants at the CMC.

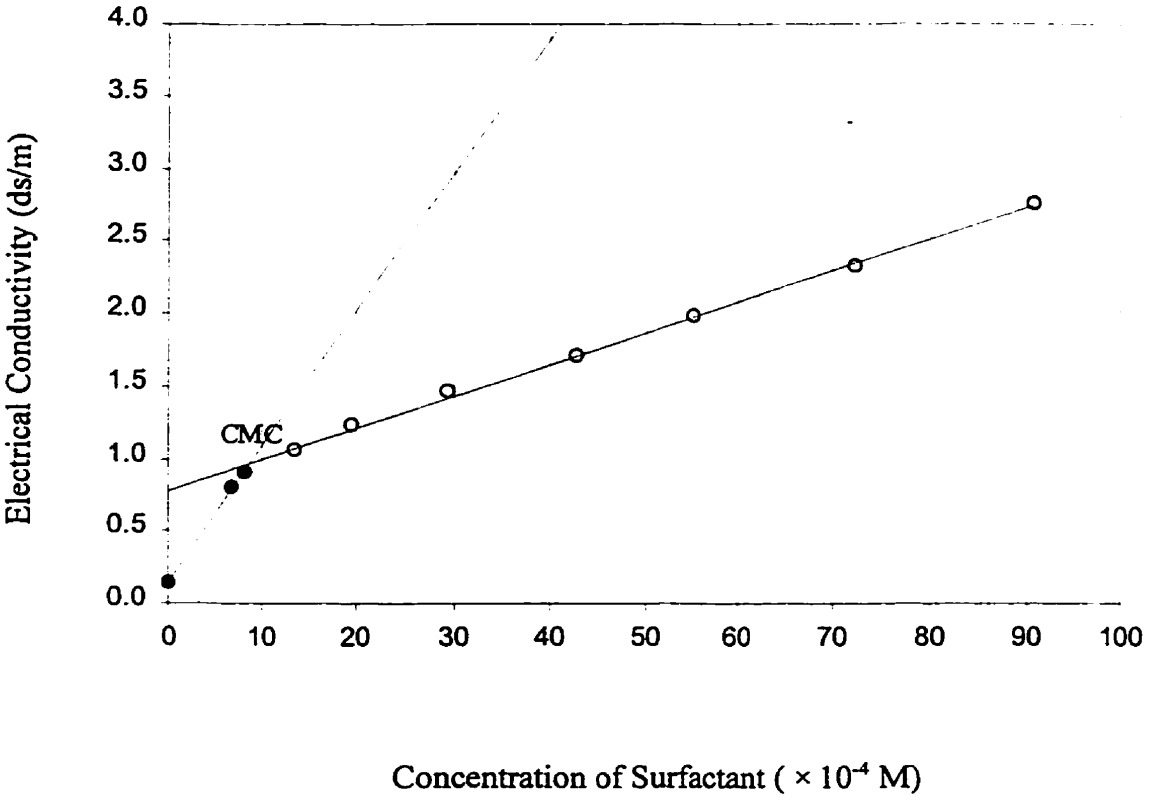

Figure 4.1 The critical micelle concentration (CMC) of CTAB is the concentration of surfactant at the intersection of the bi-regression lines. The CMC is 9.0×10^{-4} M.

Table 4.1 Experimental MSRs and micelle-water partition coefficients of CTAB

Compounds	Aqueous solubility		Solubility at CMC		MSR	r^2	log K_{mic}
	mmol/L	mg/L	mmol/L	mg/L			
benzene	14.84	1159	16.11	1258	1.39	0.91	3.30
toluene	4.35	401	6.26	577	0.78	0.90	3.59
ethylbenzene	1.65	175	4.00	425	1.93	0.91	3.96
p-xylene	1.30	138	2.40	255	0.95	0.87	4.05
m-xylene	1.27	135	2.39	254	0.88	0.87	4.03
o-xylene	1.51	160	2.40	255	0.75	0.94	4.00
naphthalene	0.35	45	2.24	287	1.14	0.92	4.12
2-methylnaphthalene	0.22	31	1.00	142	0.99	0.76	4.44
phenanthrene	0.01	1	0.38	68	0.50	0.95	4.69

The enhanced apparent solubility in the presence of a surfactant solution at the CMC was contributed by the effect of micellar solubilization. The solubility of selected hydrocarbons linearly increased with increasing surfactant concentrations above the CMC as shown in Figure 4.2. The higher r^2 values indicate that most of the compounds showed very strong linear relationships between the solubilities of hydrocarbons and the concentrations of surfactant CTAB.

To determine the effect of the presence of micelles on solubility, the molar solubilization ratio (MSR) is used. The apparent solubility of hydrocarbon increases with increasing concentration of a surfactant. Figure 4.2 shows linear relationships between the solubility and surfactant concentrations above CMC. The slope of each regression line indicates the molar solubilization ratio (MSR) of individual BTEX and selected

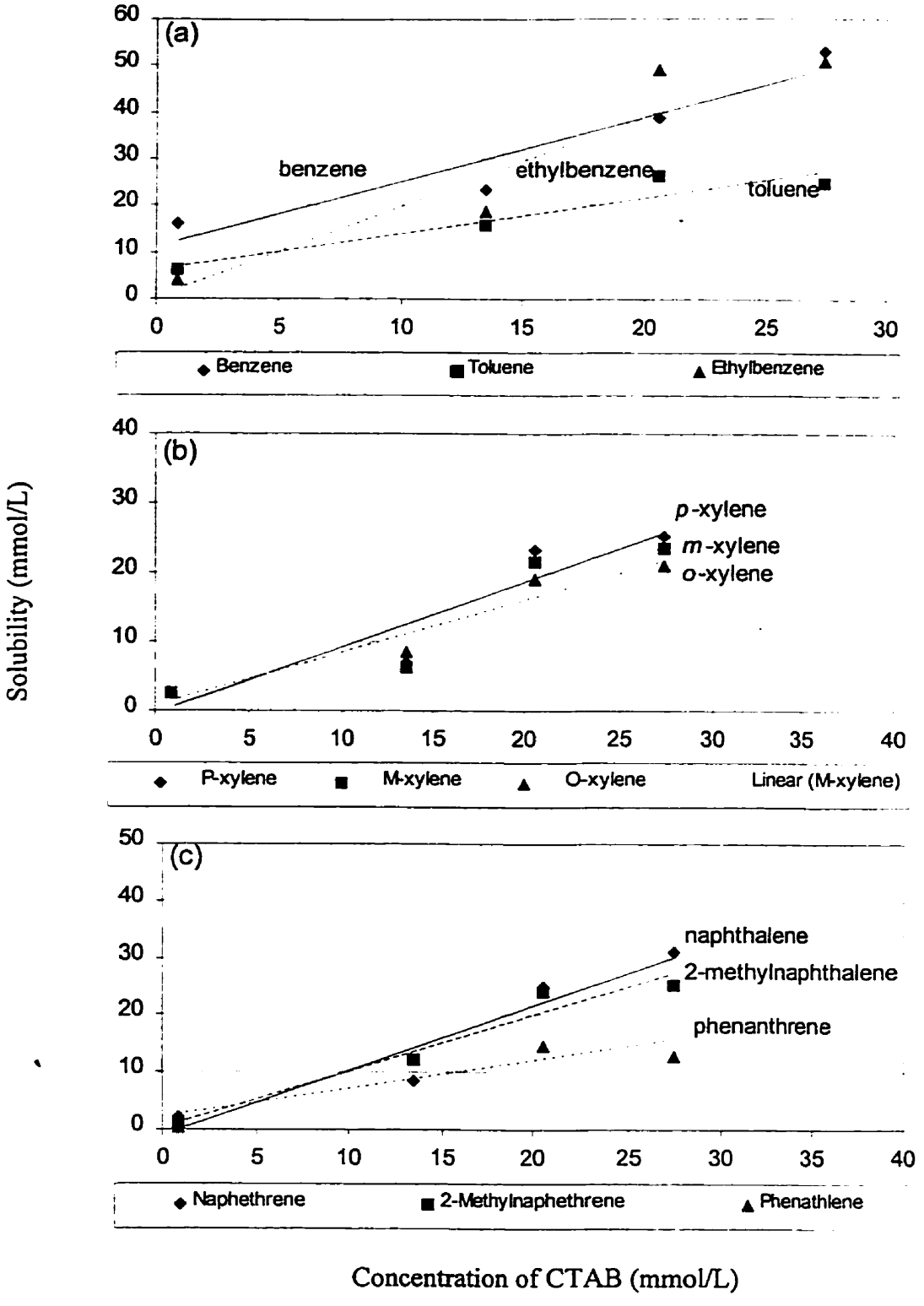

Figure 4.2 The MSRs are indicated by the slopes of the regression lines.

PAHs (naphthalene, 2-methylnaphthalene, and phenanthrene) is presented in Table 4.1. Among the nine selected hydrocarbons, ethylbenzene has the highest MSR followed by benzene, naphthalene, the three xylenes, toluene, and phenanthrene. Based on the MSR, the surfactant-enhanced remediation may be more efficient for the removal of ethylbenzene and benzene compared to remediation without the surfactant.

The micelle-water partition coefficient (K_{mic}) is another common approach for the evaluation of surfactants in solubilizing hydrocarbons. The micelle-water partition coefficient can be calculated by equation 2.7 based on the calculated MSR. The calculated values of micelle-water partition coefficients (log K_{mic}) for the nine selected hydrocarbons are also presented in Table 4.1. With an increase in K_{mic} of the hydrocarbon, the hydrophobicity also increases. Therefore, benzene and toluene with a lower K_{mic} are more hydrophilic compared to the three selected PAHs, with a higher K_{mic}.

4.1.3 Relationship between solubility and K_{ow}

The octanol-water partition coefficient (K_{ow}) used to evaluate the hydrophobicity of hydrocarbons is another parameter that is available in the literature. The linear relationship between K_{ow} and solubility in the aqueous phase as well as in the surfactant solution are shown in Figures 4.3a and 4.3b, respectively. The regression line ($r^2 = 0.89$), representing the relationship between the K_{ow} and the aqueous solubility is given the equation

$$\log S_w = -1.1382 \log K_{ow} + 5.6409 \qquad (4.1)$$

where

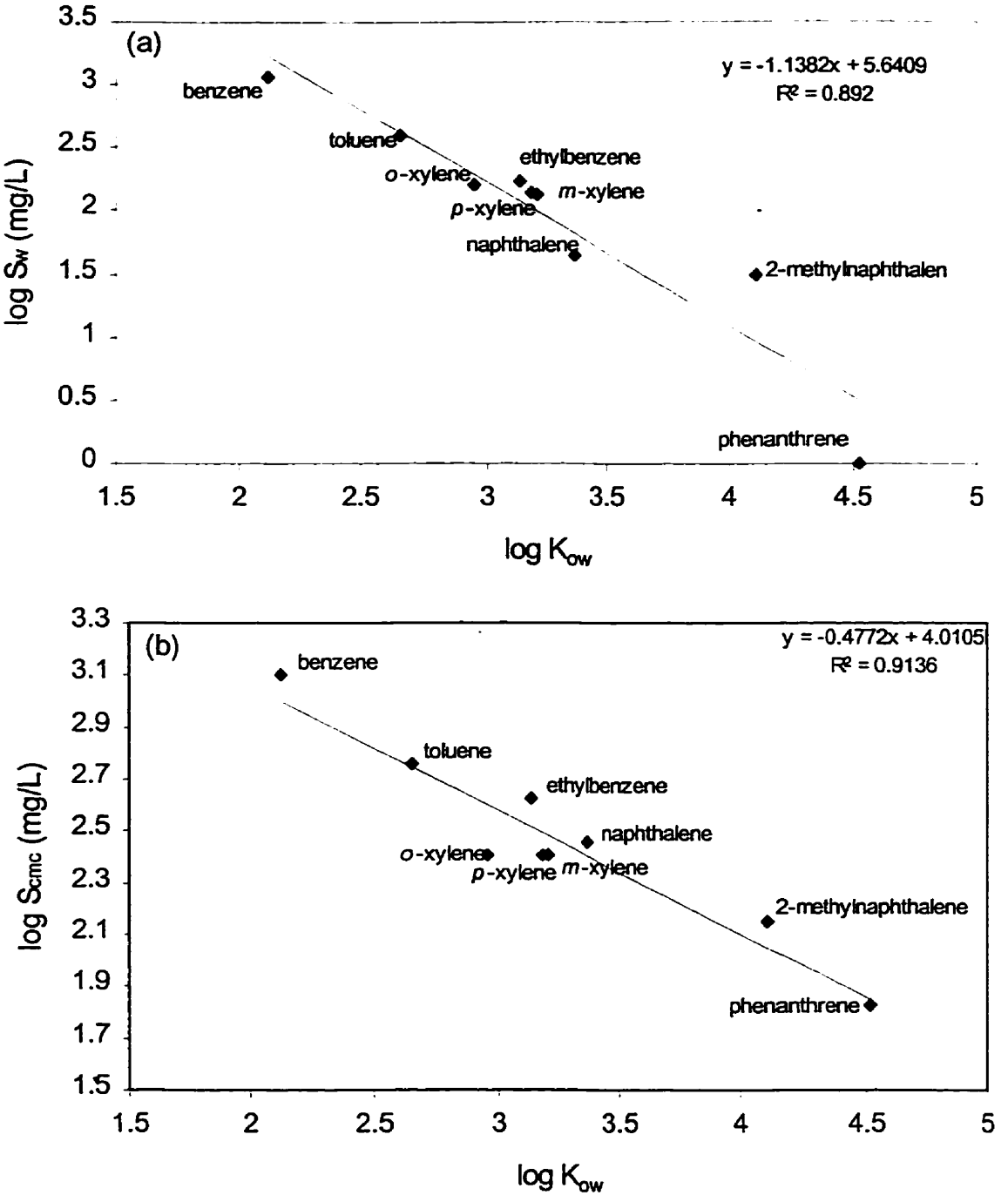

Figure 4.3 The relationships between the octanol-water partition coefficients and solubility (a) in an aqueous phase (b) in the surfactant solution at CMC.

S_w = solubility of the hydrocarbons in aqueous phase (mg/L), and

K_{ow} = octanol-water partition coefficient (dimensionless).

In addition, the linear relationship ($r^2 = 0.91$) between the hydrocarbon solubility in the surfactant solution and the K_{ow} is given by

$$\log S_{cmc} = -0.4772 \log K_{ow} + 4.0105 \qquad (4.2)$$

where

S_{cmc} = solubility of a hydrocarbons in surfactant solution (mg/L), and

K_{ow} = octanol-water partition coefficient (dimensionless).

By using the K_{ow} of organic compounds available in the literature in equations 4.1 and 4.2, the solubilities can be predicted. Table 4.2 lists the octanol-water partition coefficient (from the literature), the solubility (from the literature), the measured solubility, and the solubility predicted using equations 4.1 or 4.2.

A comparison of solubilities obtained by experiment, from the equations, and from the literature shows that the values of solubility are very similar. Therefore, if the K_{ow} of a hydrocarbon compound is known, the two equations can be used to predict the solubility of hydrocarbons in either aqueous phase or in the surfactant solution. Since the K_{ow} for many organic compounds are available in the literature, the solubility of an organic compound can easily be calculated by the above two equations.

Table 4.2 Summary of Solubility (S) and K_{ow}

Compounds	Log K_{ow}	Log Solubility (mg/L)				
	*	Aqueous			At CMC	
		*	experiment	predicted	experiment	predicted
benzene	2.12	3.24	3.06	3.23	3.10	3.00
toluene	2.65	2.71	2.60	2.62	2.76	2.75
ethylbenzene	3.13	2.18	2.24	2.08	2.63	2.52
p-xylene	3.18	2.30	2.14	2.02	2.41	2.49
m-xylene	3.20	2.20	2.13	2.00	2.40	2.48
o-xylene	2.95	2.18	2.20	2.28	2.41	2.60
naphthalene	3.36	1.48	1.65	1.82	2.46	2.41
2-methylnaphthalene	4.11	1.39	1.49	0.96	2.15	2.05
phenanthrene	4.52	0	0	0.50	1.83	1.85

*From Knox *et al.* 1993

4.1.4 Relationship between K_{mic} and K_{ow}

The relationship between the micelle-water partition coefficient (K_{mic}), determined in Section 4.1.3, and the octanol-water partition coefficient (K_{ow}), available from the literature, is shown in Figure 4.4. The hydrocarbon compounds shown in Figure 4.4 include benzene, toluene, ethylbenzene, three isomers (*para-*, *meta-*, *ortho-*), naphthalene, 2-methylnaphthalene, and phenanthrene. The results show a strong linear relationship (r^2 = 0.96) exists between K_{mic} and K_{ow} with the equation

$$\log K_{mic} = 0.5605 \log K_{ow} + 2.2004 \qquad (4.3)$$

where

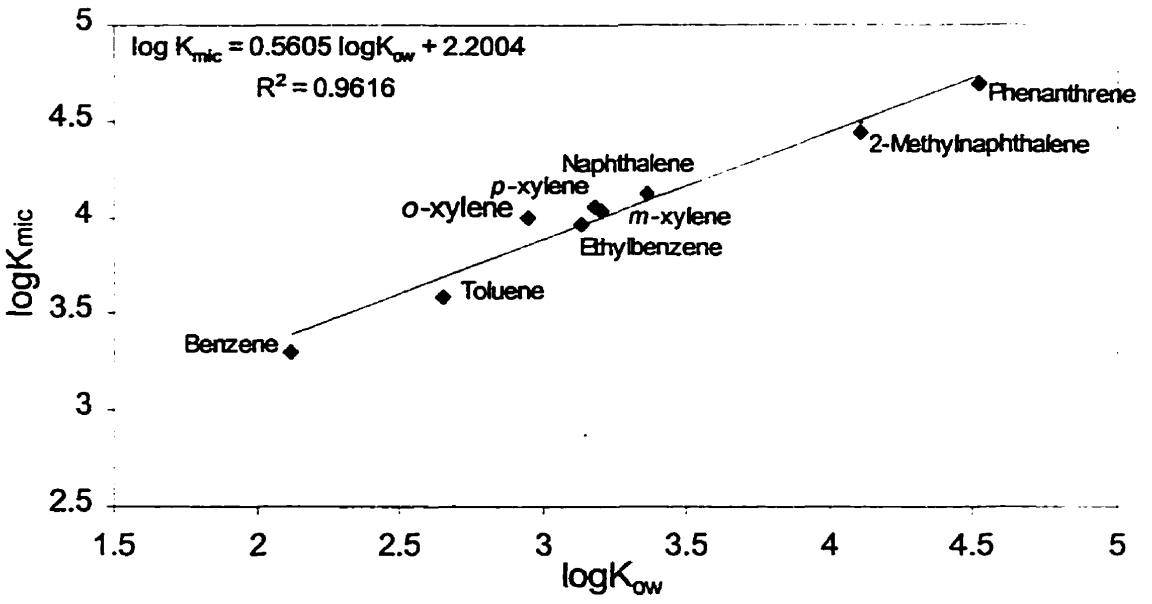

Figure 4.4 The relationship between the micelle-water partition coefficients of CTAB, from the experiments, and the octanol-water partition coefficients, from Knox *et al.* (1993).

K_{mic} = mole fraction-based micelle-water partition coefficient (dimensionless), and

K_{ow} = the octanol-water partition coefficient (dimensionless).

The calculated K_{mic} from MSR experiments as shown in Table 4.2, and predicted K_{mic}, from equation 4.3, are listed in Table 4.3. Table 4.3 also lists the octanol-water partition coefficients of BTEX and three selected PAHs obtained from the literature.

Table 4.3 The micelle-water partition coefficient (K_{mic}) and the octanol-water partition coefficient (K_{ow})

Compounds	Log K_{ow}	Log K_{mic}	
	(Knox *et al.* 1993)	Experiments	Predicted
benzene	2.12	3.30	3.39
toluene	2.65	3.59	3.69
ethylbenzene	3.13	3.96	3.95
p-xylene	3.18	4.05	3.98
m-xylene	3.20	4.03	3.99
o-xylene	2.95	4.00	3.85
naphthalene	3.36	4.12	4.08
2-methylnaphthalene	4.11	4.44	4.50
phenanthrene	4.52	4.69	4.73

4.1.5 The relationships between K_{oc} and solubility and between K_{oc} and K_{ow}

A number of empirical expressions have been proposed to describe the relationship between the organic carbon-water partition coefficient (K_{oc}) and either the octanol-water partition coefficients (K_{ow}) or the water solubility (S_w). The various expressions result

from the use of different chemicals and materials such as different soils (Lyman 1992). The relationship between the organic carbon-water partition coefficient K_{oc} and the water solubility S_w is given by Kenaga and Goring (1980) (Domenico and Schwartz 1990)

$$\log K_{oc} = -0.55 \log S_w + 3.64 \qquad (4.4)$$

where

K_{oc} = organic carbon-water partition coefficient (L/kg), and

S_w = water solubility (mg/L).

The aqueous solubility, which expresses the hydrophobicity of the hydrocarbons, of individual BTEX and three selected PAHs were measured. Another parameter used to measure the hydrophobicity of the hydrocarbons is the K_{ow}. To establish a relationship between K_{oc} and K_{ow}, equation 4.1 and equation 4.4 can be combined to develop a linear relationship given by

$$\log K_{oc} = 0.63 \log K_{ow} + 0.54 \qquad (4.5)$$

where

K_{oc} = the organic carbon-water partition coefficient (L/kg), and

K_{ow} = the octanol-water partition coefficient (dimensionless).

The K_{ow} values for most organic compounds range from 10^{-3} to 10^{7} (Kostecki and Calabrese 1993). Hydrocarbons with low K_{ow} values (<10) are considered hydrophilic

with higher water solubilities and lower distribution coefficients. Hydrocarbons with high K_{ow} values ($>10^3$) are very hydrophobic with low water solubilities and high sorption coefficients (Charabeneau *et al.* 1992). The solubility values for BTEX and selected PAHs listed in Table 4.4. are predicted from K_{ow} which is a key parameter that is used to evaluate the fate of the hydrocarbons in the environment (Charabeneau *et al.* 1992).

When surfactants, especially at concentrations above CMC, are present in the soil and water system, the amount of hydrocarbons sorbed onto the soil surface is greatly reduced and the apparent solubility of hydrocarbons in the aqueous phase is dramatically increased. Such phenomenon results in a reduction of K_{oc}, and as a result the K_{oc} must be modified in the presence of surfactants in water.

From the micelle solubilization experiments, the solubility of the hydrocarbons was measured in the surfactant solution with concentration at CMC. A linear relationship between the solubility ($\log S_{cmc}$) and the octanol-water partition coefficients ($\log K_{ow}$) was developed ($r^2 = 0.5303$) as shown in equation 4.2. To account for the presence of surfactants in the soil and water system, the modified organic carbon-water partition coefficient $K_{oc,cmc}$ and K_{ow} are developed by combining equation 4.2 and equation 4.4. This relationship is expressed as

$$\log K_{oc,cmc} = 0.26 \log K_{ow} + 1.43 \qquad (4.6)$$

where

$K_{oc,cmc}$ = modified organic carbon-water partition coefficient (L/kg), and

K_{ow} = the octanol-water partition coefficient (dimensionless).

From equation 4.5 and equation 4.6, the organic carbon-water partition coefficient and modified organic carbon-water partition coefficient ($K_{oc,cmc}$) can be calculated from the K_{ow}. Both measured K_{oc} in aqueous phase and in the surfactant solution are listed in Table 4.5 (Section 4.1.3).

Table 4.4 Summary of predicted solubility and K_{oc}

Compounds	log K_{ow}	Predicted	
	(Knox *et al* 1993)	Solubility (mg/l)	log K_{oc}
benzene	2.12	1750	1.94
toluene	2.65	515	2.18
ethylbenzene	3.13	152	2.20
p-xylene	3.18	198	2.31
m-xylene	3.20	158	3.20
o-xylene	2.95	152	2.11
naphthalene	3.36	30.0	3.11
2-methylnaphthalene	4.11	24.6	3.93
phenanthrene	4.52	1.0	4.36

4.1.6 Modified retardation factor

The retardation factor (R) is a measure of the degree of reduction in the migration of contaminants. Equation 2.17 can be used to define the retardation factor in the absence of surfactants in the aqueous and soil system. However, the presence of a surfactant results in a change in the velocity of migration of the contaminant leading to a change in

the retardation factor. The modified retardation factor can be defined by the concentration-based equation 2.18 or the mole fraction-based equation 2.19.

The equations show that the modified retardation factor is a function of the K_{oc} and K_{mic}. The K_{oc} has a linear relationship with the K_{ow} that is available in the literature. The K_{oc} also has a linear relationship with the K_{mic}. Therefore, the modified retardation factor can be characterized by the octanol-water partition coefficient (K_{ow}) as shown in Figure 4.5. In Figure 4.5, the relationships between log R and log K_{ow} are presented. The relationship of log R and log K_{ow} was developed with CTAB as the surfactant solution at various concentration ranging from below CMC to above CMC. The bulk density of 1 g/cm^3 and porosity of 63 % was obtained from experimental results. The f_{oc} and N was assumed as 0.01 and 0 respectively. The figure shows that the retardation factor greatly decreased with an increase in surfactant concentration for organic compounds with high hydrophobicity (high log K_{ow}). For organic compounds with relatively lower solubility (log K_{ow} < 2.3) such as benzene (log K_{ow} = 2.12), the presence of CTAB surfactant has very little effect on the enhancement of solubility. For organic compounds with log K_{ow} greater than 2.3, the presence of CTAB surfactant enhances the apparent solubility of compounds. When the concentration of surfactant increases, the retardation factor of a hydrocarbon with higher K_{ow}, greatly decreases. Therefore, the surfactant present in the water-soil system is affected more on the compounds with high K_{ow}, such as PAHs, during soil remediation.

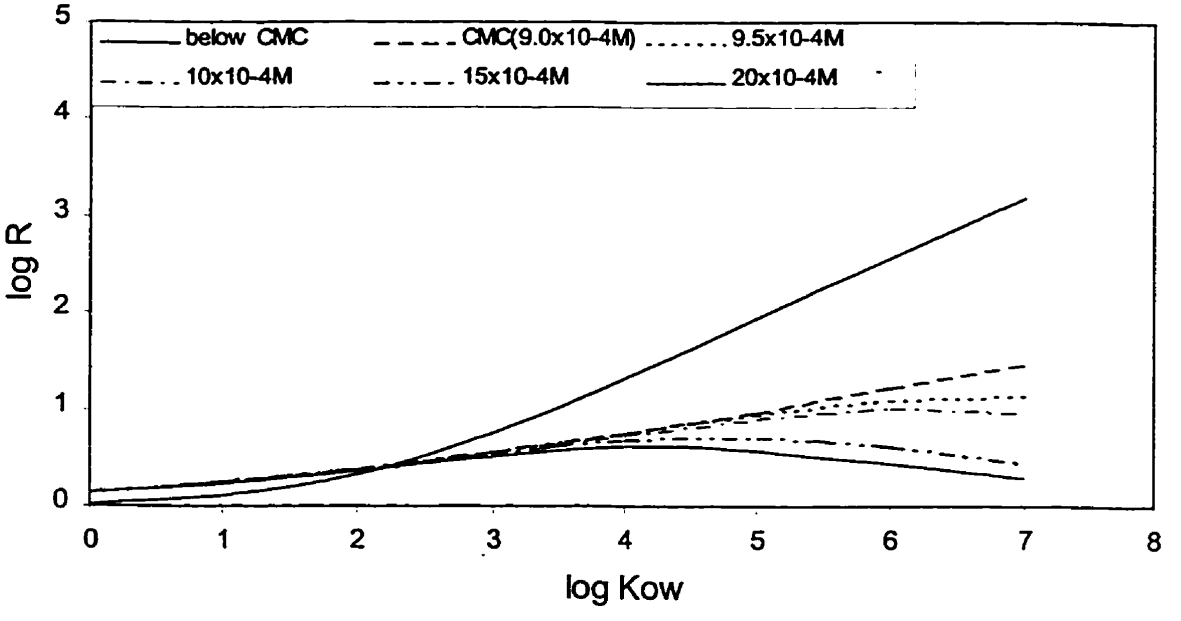

Figure 4.5 A relationship between log K_{ow} and modified log R at different concentrations of CTAB in clay soils (bulk density = 1.00 g/cm^3, porosity = 63%, f_{oc} = 0.01, N = 0).

4.2 SPME-GC-FID analysis

The solubility of hydrocarbons together in a solution is lower compared to the individual solubility of hydrocarbons. The solubility of a mixture of BTEX and three selected PAHs can be predicted based on Raoult's law. The range of concentrations which give a linear response is presented in this section.

4.2.1 Predicted solubility of BTEX and three PAHs in complex mixture

To ensure that the concentrations of hydrocarbons of interest are maintained below their solubilities during the analysis procedure, the predicted aqueous solubilities of hydrocarbons in a mixture were calculated in Table 4.5.

4.2.2 Range of concentrations giving a linear response

The linear relationships between the detector responses and concentrations were determined by the least-squares technique using the detector response from standard solutions with concentrations ranging from 0 to 50 ppm of BTEX and from 0 to 5 ppm of PAHs. The linear relationships of BTEX and PAHs are shown in Figure 4.6 and Figure 4.7, respectively.

Figure 4.6 presents the linear response for the BTEX compounds. The fitted regression lines for benzene, toluene, and ethylbenzene at concentrations less than 25ppm gave a stronger linear response. Therefore, the linear ranges for benzene, toluene, and ethylbenzene extended to 25ppm (w/v). A strong linear relationship was observed for three xylene isomers (*para-, meta-, and ortho-*), at concentrations below 50ppm (w/v).

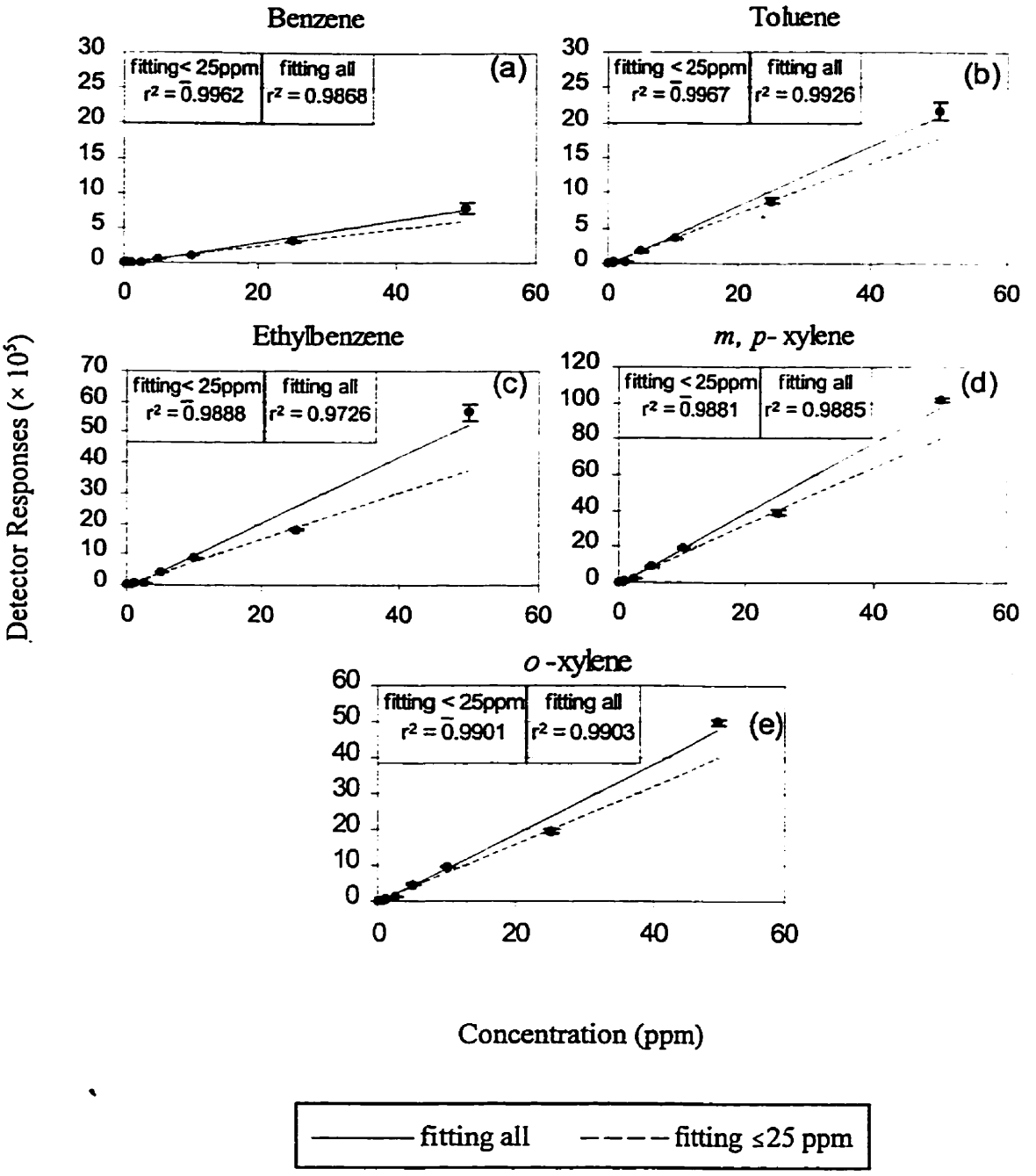

Figure 4.6 Linear relationship between the detector response and the concentration of BTEX in solutions with standard errors indicated by the error bars.

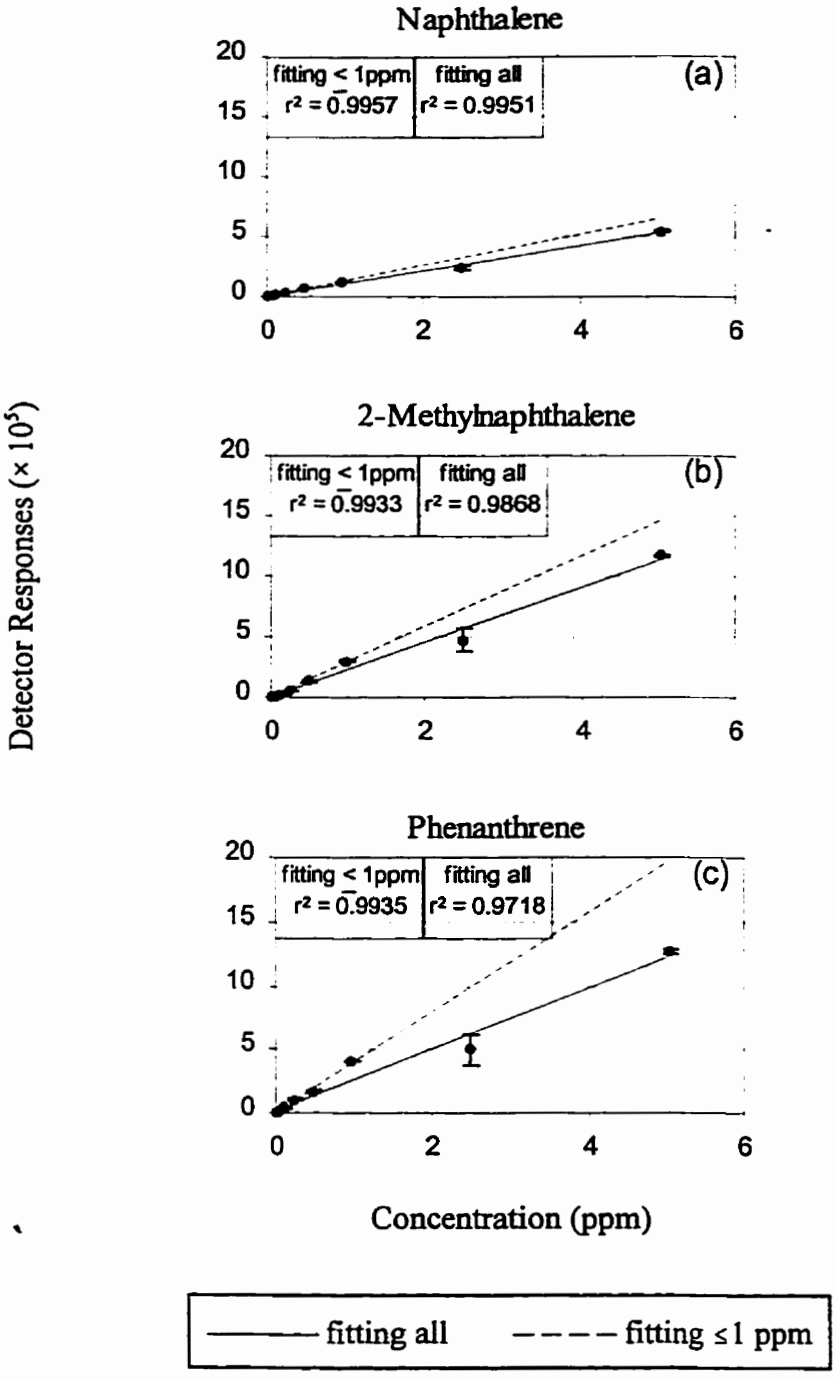

Figure 4.7 Linear relationships between the detector response and the concentration of PAHs in the solution with standard errors indicated by the error bars.

Table 4.5 Predicted solubility of BTEX and three selected PAHs in a mixture

Compounds	Aqueous Solubility(mg/L)*	Mole Fraction†	Predicted Solubility in Mixtures (mg/L)*
benzene	1159	0.16	181
toluene	401	0.13	53
ethylbenzene	175	0.12	20
p-xylene	138	0.12	16
m-xylene	135	0.12	16
o-xylene	160	0.12	18
naphthalene	45	0.10	4
2-methylnaphthalene	31	0.09	3
phenanthrene	1	0.07	0

* From experiment (Section (3.1.2.1)); † From: Knox *et al.* (1993)

Figure 4.7 presents the fitted regression lines for naphthalene, 2-methylnaphthalene, and phenanthrene showing a stronger linear response at concentrations less than 1 ppm. Therefore, for the three selected PAHs the linear ranges extend to 1 ppm.

The percentage relative standard deviation (%RSD) can be calculated by,

$$\%RSD = \frac{\text{sample standard deviation}}{\text{sample average}} \times 100\% \qquad (4.7).$$

The average percentage relative standard deviations (%RSD) were found to be 10.48%, 8.88%, 9.48%, 7.87%, 7.48%, 3.69%, 6.08%, and 8.86% for benzene, toluene, ethylbenzen, *p*- and *m*-xylene, *o*-xylene, naphthalene, 2-methylnaphthalene, and phenanthrene, respectively. Arthur *et al.* (1992a) reported that the relative standard

deviation ranged from 3% to 5% using a 56 μm methyl silicone fibre for BTEX. The relatively high %RSD for the BTEX and PAHs may have been contributed by several factors. The first factor is the evaporation of analytes, especially the more volatile organic compounds, from the fibre due to exposure to the air prior to the thermal desorption in the column. Therefore, the relative standard deviations (RSD) for the more volatile compounds such as benzene, toluene, and ethylbenzene were higher. The lack of sensitivity may also have been due to the use of an old CLOT column in the GC. In addition, equilibrium patitioning may not have been reached for ethylbenzene, the three xylene isomers, and PAHs, especially for PAHs compounds, which resulted in the high %RSD. Another reason leading to a high %RSD for phenanthrene could be thickness of the film coating on the fibre (100 μm). Arthur (1992c) indicated that it is best to use thin films to sorb the analytes with high K_f values, and thick films are used to sorb the analytes with low K_f values. Phenanthrene has a higher distribution constant due to the higher value of its octanol-water partition coefficient and was extracted by the 100 μm-thick-film fibre during the experiments possibly contributing to the higher %RSD.

4.2.3 Static and agitation extraction sorption-time profiles

The sorption-time profiles of BTEX and three selected PAHs are shown in Figures 4.8 and 4.9, respectively. Since the *m*-, and *p*-xylene isomers were not resolved on the chromatographic column they are shown together in Figure 4.8. The Duncan's multiple range test was carried out to compare the response of agitated and static extraction methods. The results of all nine selected hydrocarbon compounds are shown in Appendix I.

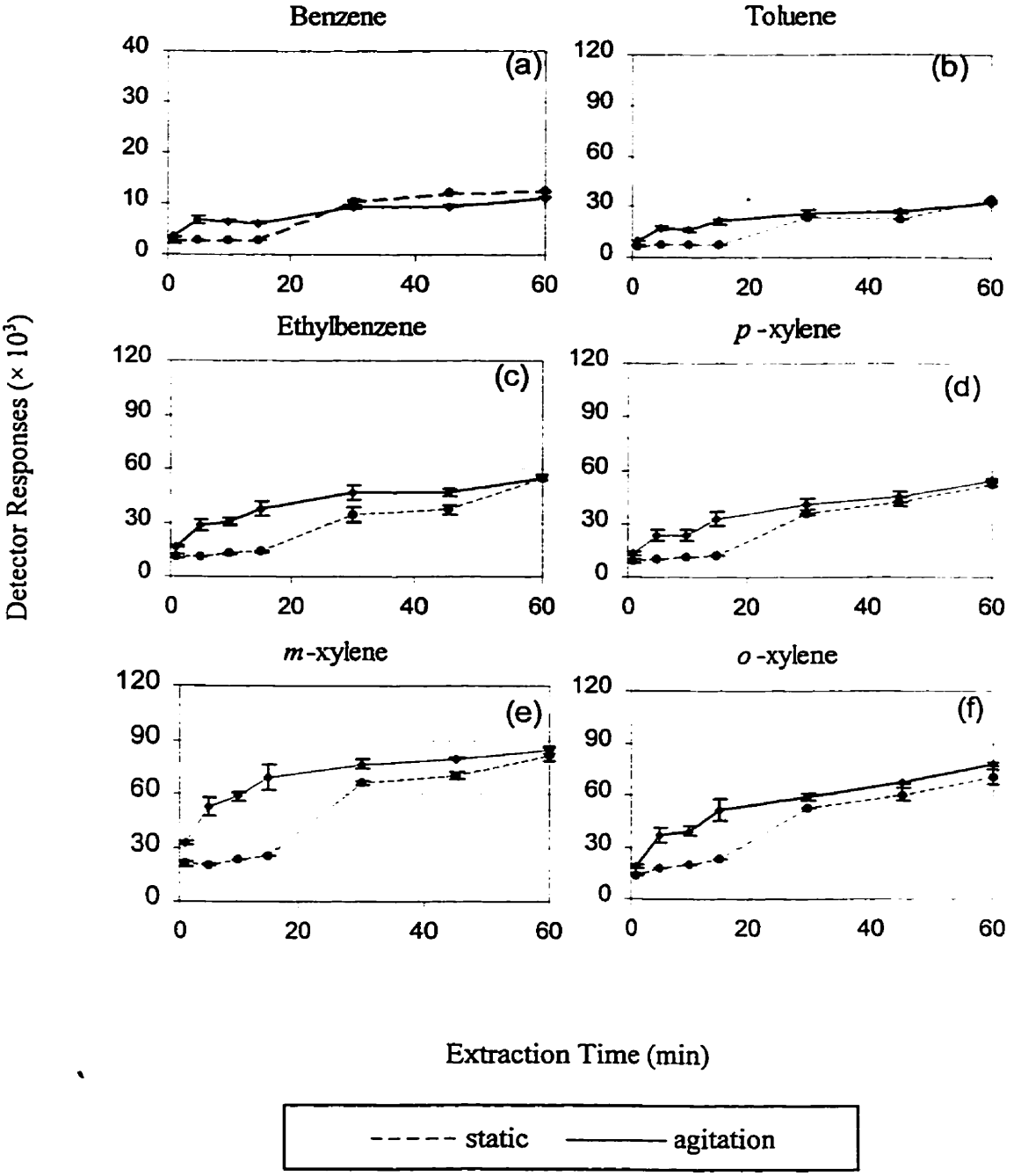

Figure 4.8 Sorption-time profiles of BTEX with standard errors indicated by error bars in both static and agitation extraction.

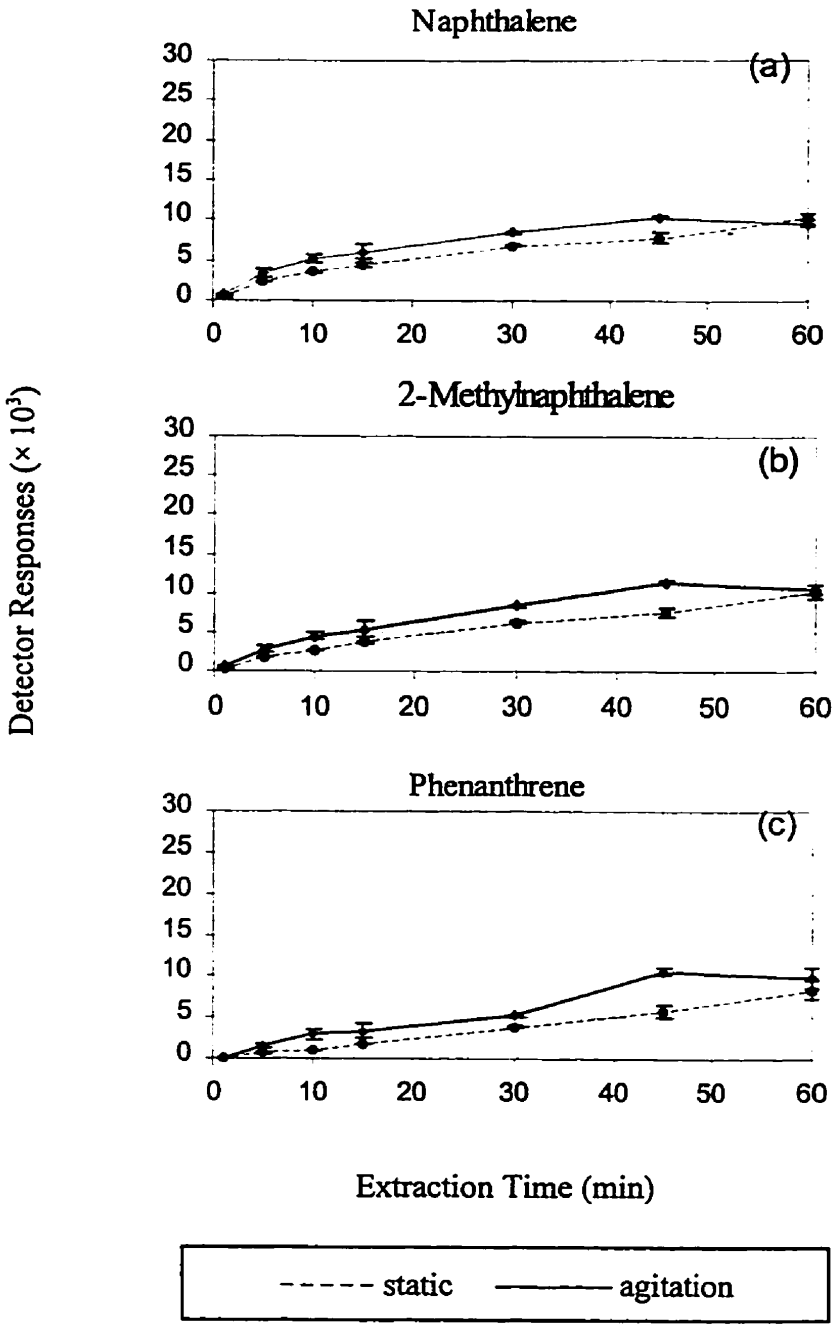

Figure 4.9 Sorption-time profiles of PAHs with standard errors indicated by error bars in both static and agitation extraction.

The results from the Duncan's multiple range test indicate that the detector response using agitation technique was significantly higher than for the static extraction for similar extraction times for the most selected compounds. Therefore, the enhanced agitation technique shows a potential to reduce the detection time and thus improve the efficiency of SPME-GC-FID analysis.

For toluene and *p*-xylene, the detector response was not significantly different in the period of time from 15 to 45 minutes and from 30 to 45 minutes in the application of the agitation and static methods, respectively. It appears that the equilibrium was reached during that time. Within the 45-min extraction time, the response was higher for the agitation method than for the static one for all selected extraction times. However, the responses were significantly increased at the extraction time of 60 min for both extraction methods. Between two methods, there were no significant differences in the responses at 60-min extraction time.

For ethylbenzene, the responses were not significantly changed in the period of time from 30 to 45 min in the applied agitation extraction. The equilibrium appears to have been reached at that time in the agitation extraction. The response within 45 min was higher for the agitation extracted than for the static one. However, the response increased at 60-min extraction time for both extraction methods.

For *m*-xylene and *o*-xylene, the equilibrium was reached at the agitation extraction time of 5 and 15 min, respectively. In the static extraction, the equilibruim was reached was reached at 30 min for both *m*- and *o*-xylenes.

For naphthalene, the equilibrium was reached when the extraction time of 5 min was applied in both extraction methods. For the 2-methylnaphthalene and phenanthrene, the equilibrium was reached at 45 min for the agitation method. It was reached at 60 min for the static extraction.

Based on the above, it can be concluded that the application of agitation results in the reduction of the equilibrium time and thus enhances the efficiency of SPME-GC-FID analysis.

Since the distribution constant of the fibre, K_f, reflects the time for equilibrium, a larger distribution constant will result in longer equilibrium times (Arthur *et al.* 1992b; Chai *et al.* 1993). When the fibre is coated with polydimethylsiloxane, the distribution constant, K_f, can be predicted based on the known octanol-water partition coefficient, K_{ow}, of the water-fibre system (Chai *et al.* 1993). Based on the K_{ow} values listed in Table 4.2, the octanol-water partition coefficients of three selected PAHs are larger than those of ethylbenzene and the three xylene isomers. Therefore, the distribution constants of ethylbenzene and the three xylene isomers are smaller than the constants for the PAHs, and the times for equilibrium of ethylbenzene and the three xylene isomers are shorter than the times obtained for the PAHs.

The increased detector responses due to the application of agitation over static extraction can be measured by (Thomas 1996a)

$$\%\text{increase} = \frac{\text{average agitation value} - \text{average static value}}{\text{average static value}} \times 100\% \qquad (4.8).$$

The percentage increases in detector response at various extraction times for BTEX and three selected PAHs are listed in Table 4.6. The average percentage increase in detector response over all extraction time was 58%, 70%, 81%, 70%, 82%, 57%, 40%, 52%, and 92% for benzene, toluene, ethylbenzene, *p*-xylene, *m*-xylene, *o*-xylene, naphthalene, 2-methylnaphthalene, and phenanthrene, respectively. The results also indicate that the extraction with agitation show at least a 40% increase, compared to the static extraction for all the selected compounds. Therefore, extraction with agitation was chosen to analyze the samples during the experiments of soil remediation.

The precision of sorption profiles, described by the percentage relative standard deviation (%RSD), was calculated using equation 4.7 and is shown in Figure 4.10. The average %RSDs for BTEX for both static and agitation were 4.6% and 8.1%, respectively. The average %RSDs for PAHs for both static and agitation were 12.2% and 14.3% respectively. The %RSDs for PAHs are slightly higher than the 10% reported for PAHs using a 15 μm polydimethylsiloxane coated fibre (Potter and Pawliszyn 1994). The slightly higher relative standard deviations may have been due to the thicker coating on the fibre.

4.2.4 Calibration and standard curves in the presence of agitation

The calibration curves were determined by the least-squares technique using the detector response as a function of concentration of analytes. The calibration curves were developed only in the presence of agitation, because the sorption-time profiles showed that the agitation extraction method was more efficient than the static extraction. Therefore, all the samples that need to be analyzed by SPME-GC-FID were run using the agitation

Table 4.6 The Percentage increase in detector responses in sorption profiles

Time(min) / compound	1	5	10	15	30	45	60	Average
benzene	28	155	138	130	-10	-22	-10	58
toluene	46	128	113	179	9	21	-5	70
ethylbenzene	49	144	140	174	35	25	0	81
p-xylene	50	139	111	162	15	6	3	70
m-xylene	56	159	153	175	15	13	4	82
o-xylene	37	109	93	127	13	11	9	57
naphthalene	95	45	48	37	24	33	-6	40
2-methylnaphthalene	111	60	63	47	33	49	3	52
phenanthrene	116	141	168	84	34	84	16	92

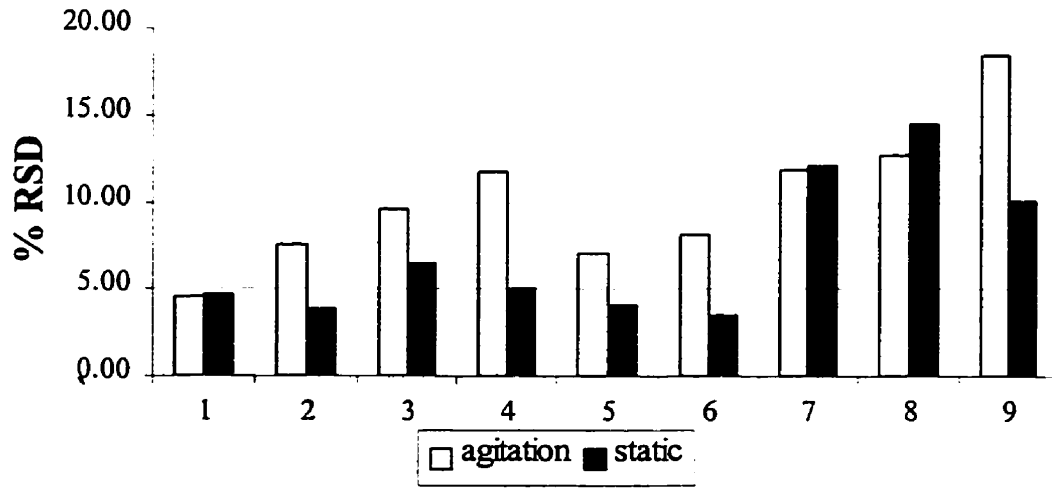

Figure 4.10 %RSD for both agitation and static extraction in the sorption profiles:

1- benzene, 2- toluene, 3- ethylbenzene, 4- *p*-xylene, 5- *m*-xylene, 6- *o*-xylene, 7-naphthalene, 8- 2-methylnaphthalene, and 9- phenanthrene.

extraction method. The calibration curves of BTEX and PAHs are shown in Figure 4.11 and Figure 4.12, respectively. The calibration curve was used to determine the concentration of analytes in the test samples based on the detector responses from SPME-GC-FID analysis. The relative standard deviations (%RSD) were 10.3%, 8.8%, 9.2%, 7.8%, 7.0%, 3.9%, 6.8%, and 10.3% for benzene, toluene, ethylbenzene, p- and m-xylene, o-xylene, naphthalene, 2-methylnaphthalene, and phenanthrene, respectively.

The standard curves developed by the least-square techniques were used to determine the number of moles of analytes in the test samples and are presented in Figure 4.13. The detector response linearly increased with an increase in the concentration of 1-μL standard solutions that were manually injected into the GC column for analysis. Most of the standard curves showed a strong linear relationship ($r^2 = 0.99$) between the amount of analyte and the detector response as shown in Figure 4.13.

4.3 Soil remediation experiments

This section presents the results of four remediation treatments that were tested. The treatments include water flushing and surfactant flushing with and without the influence of applied electrical potential difference. The flow rate, hydraulic conductivity and coefficient of electroosmotic permeability were determined in each remediation experiments. The hydrocarbon content of the treated soil columns were determined by the SPME-GC-FID analysis to evaluate the efficiency of remediation treatments.

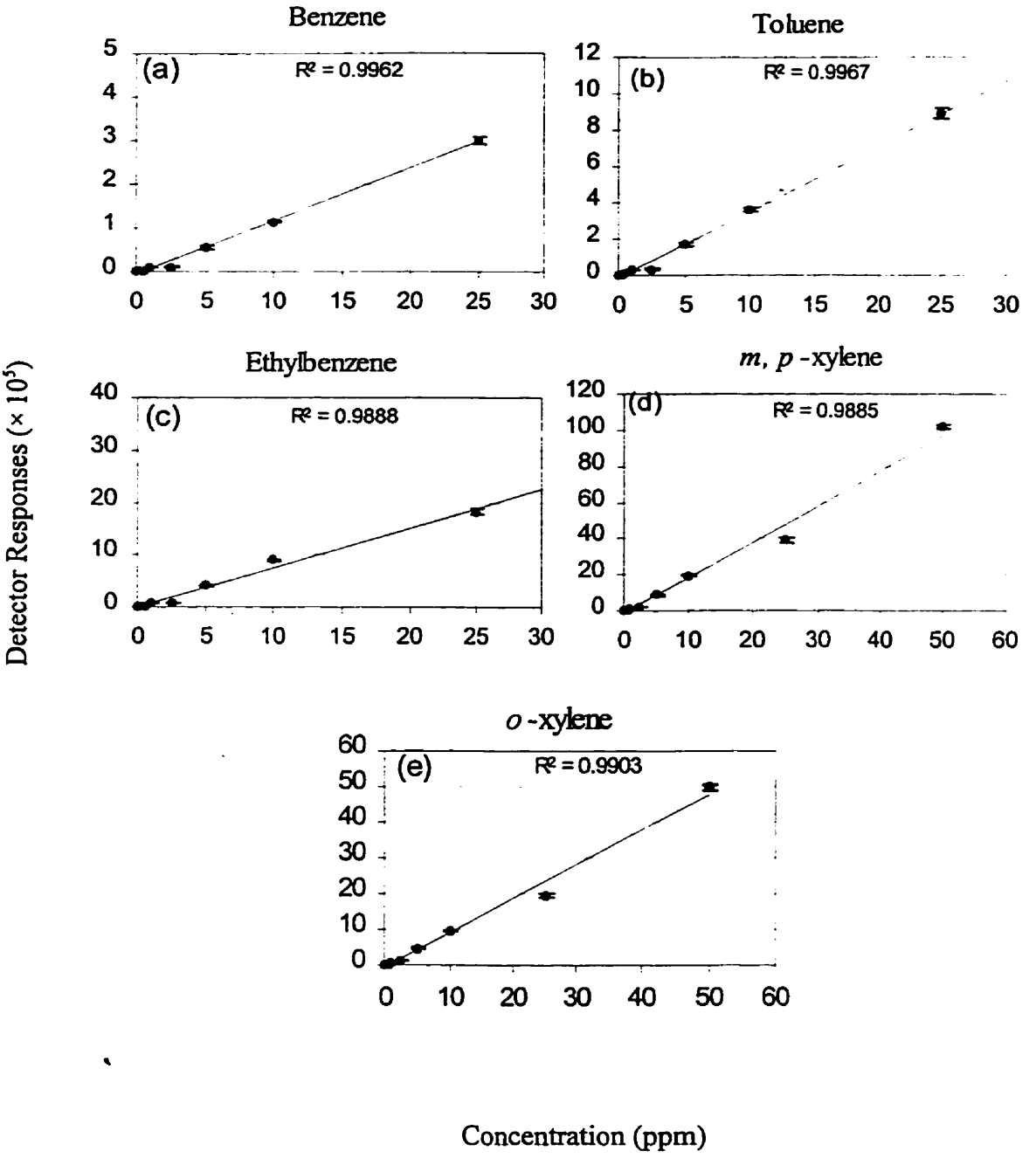

Figure 4.11 Calibration Curves of BTEX with standard errors indicated by error bars.

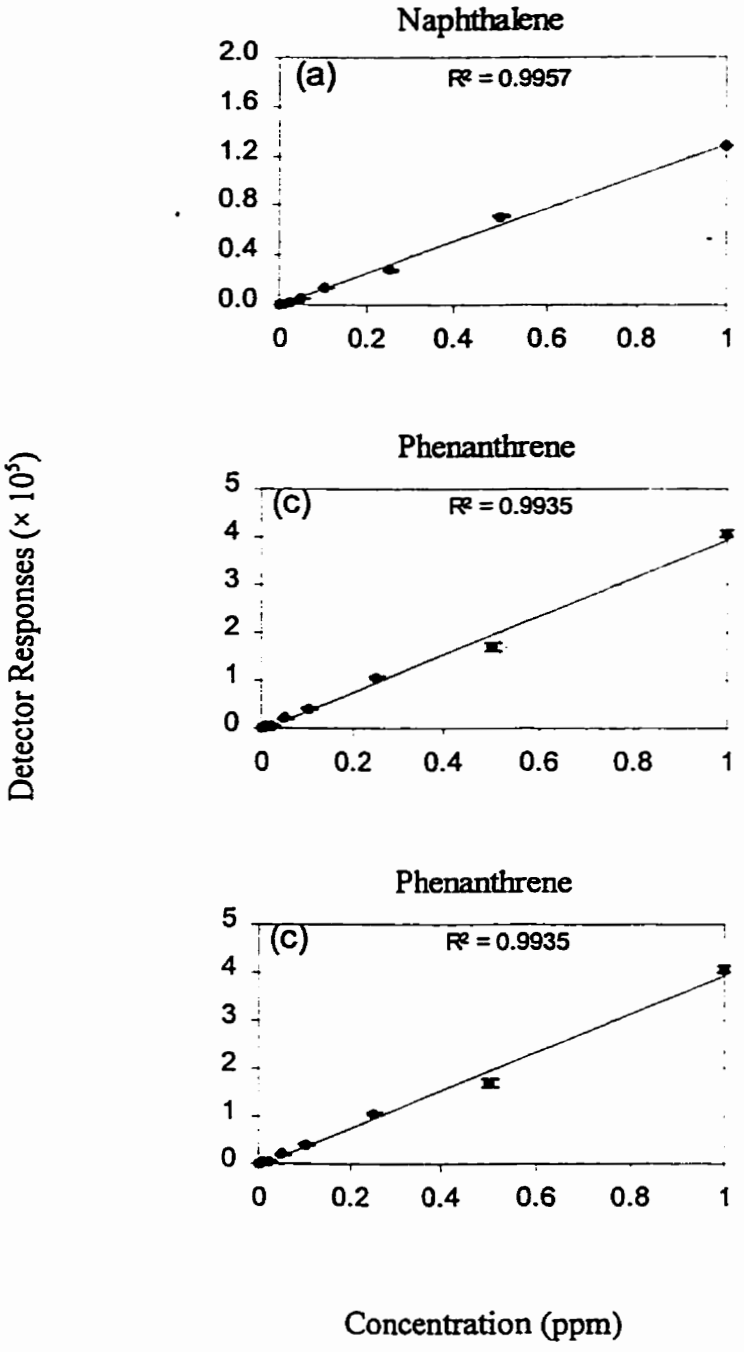

Figure 4.12 Calibration Curves of PAHs with standard errors indicated by error bars.

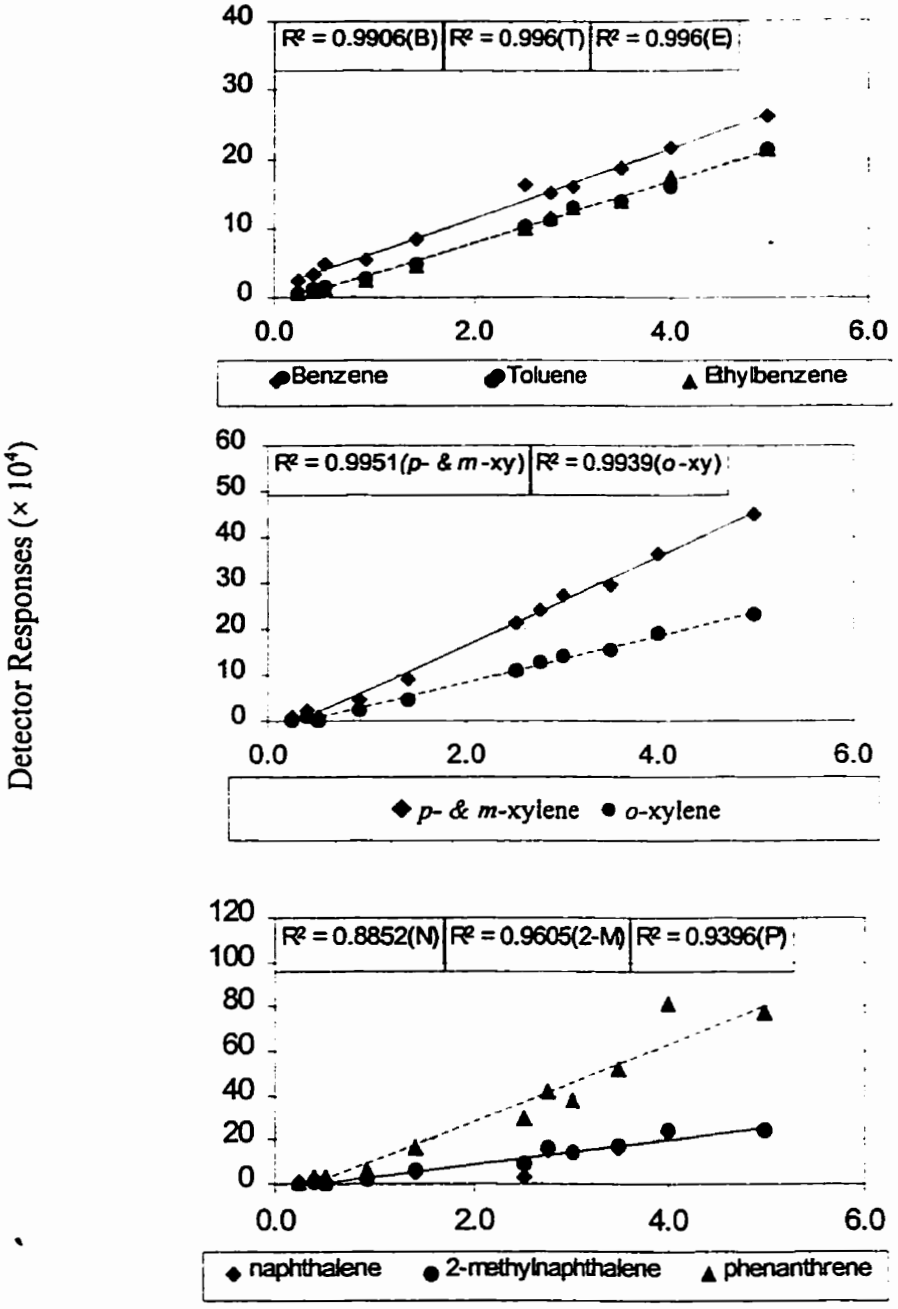

Figure 4.13 Standard curves for BTEX and three selected PAHs by using the least-squares technique.

4.3.1 Water flushing experiments

4.3.1.1 Dry bulk density of the clay

The dry bulk density of the core clay soil was found to be 1.4 (g/cm^3) (%RSD = 14.0%). The physical properties of the clay packed in the test columns, prior to the remediation treatments, were measured and are presented in Table 4.7.

Table 4.7 Physical properties of clay soils for water-flushing treatments

	Dry bulk density (g/cm^3)	Porosity (%)
Column A	0.98	63.02
Column B	1.00	62.26
Column C	0.99	62.64
Column D	0.98	63.02
Column E	0.99	62.64
Column F	0.97	63.40
Average	0.99	62.64

A, C, and F were hydraulic columns; B, D, and E were electrokinetic columns.

4.3.1.2 Flow rate, K_h and K_{eo} for the water-flushing experiments

All of the columns had been remediated with the application of a hydraulic gradient of 2.8 for 55 days. Three of the columns had been subjected to an electrical potential gradient of 0.25 ($cm^2/V.s$) referred to as electrokinetic columns.

With the application of an electrical potential difference to the soil and water system, the water is driven by the hydraulic gradient as well as electroosmosis. Since the anode is located at the inflow end, the electroosmotic flow is towards the cathode and it is

in the same direction as that due to hydraulic gradient. Therefore, the water flow rate is expected to increase due to the application of an electrical potential difference.

Throughout the remediation experiments, the effluents were collected from each column and the cumulative volume of effluent as a function of time is presented in Figure 4.14. The electrokinetic columns show an increased effluent volume compared to the hydraulic columns. Therefore, the application of the electrical potential difference seems to enhance the flow of water through the clay columns.

The hydraulic conductivity (K_h) was calculated, using Darcy's law, at different times and is presented in Figure 4.15. The results show that for the hydraulic columns, the hydraulic conductivity is stable over time with an average value of 3.5×10^{-7} (cm/s). The hydraulic conductivity is a function of the porous medium and the fluid property (Freeze and Cherry 1979). Since the hydraulic conductivity remained constant over time, the soil and fluid conditions may have not changed during soil remediation.

The total flow rate in the electrical columns are due to both the electroosmotic flow as well as the hydraulic flow. Therefore, the flow due to electroosmotic effects are determined by subtracting the flow due to the hydraulic gradient from the total flow. The coefficient of electroosmotic permeability (K_{eo}) can be calculated using equation 2.2. The calculated electroosmotic permeabilities are presented in Figure 4.15, which shows the unstable values of K_{eo} over time. Such unstable values of K_{eo} over time was also reported by Acar *et al.* (1991) and Eykholt and Daniel (1994). The coefficient of electroosmotic permeability is controlled by the chemical reaction due to the application of electricity in soil and water systems. The chemical reactions affect the properties of soil and fluid such

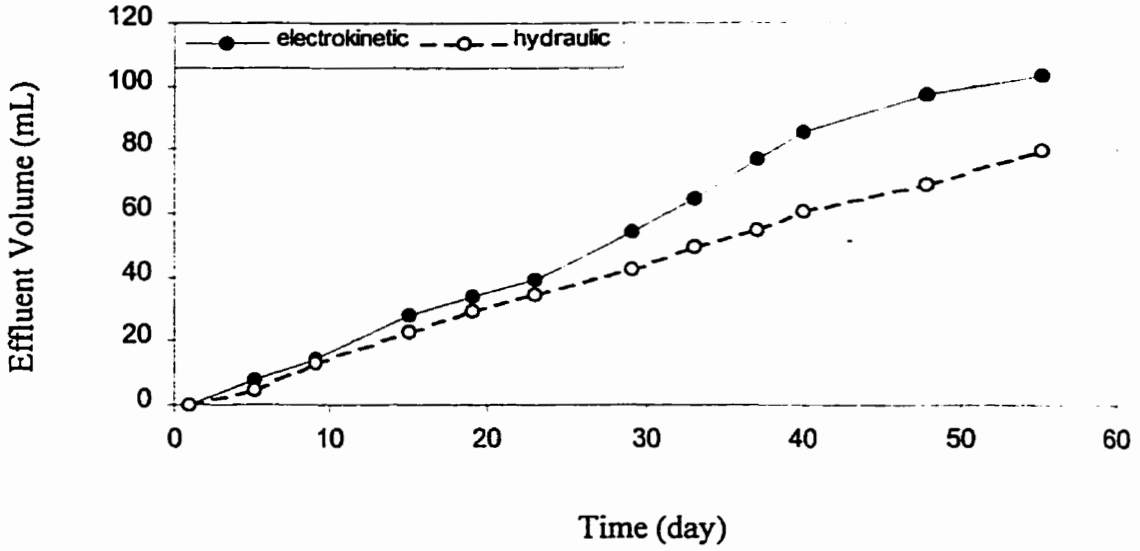

Figure 4.14 The effluent volume collected over time during water-flushing treatments.

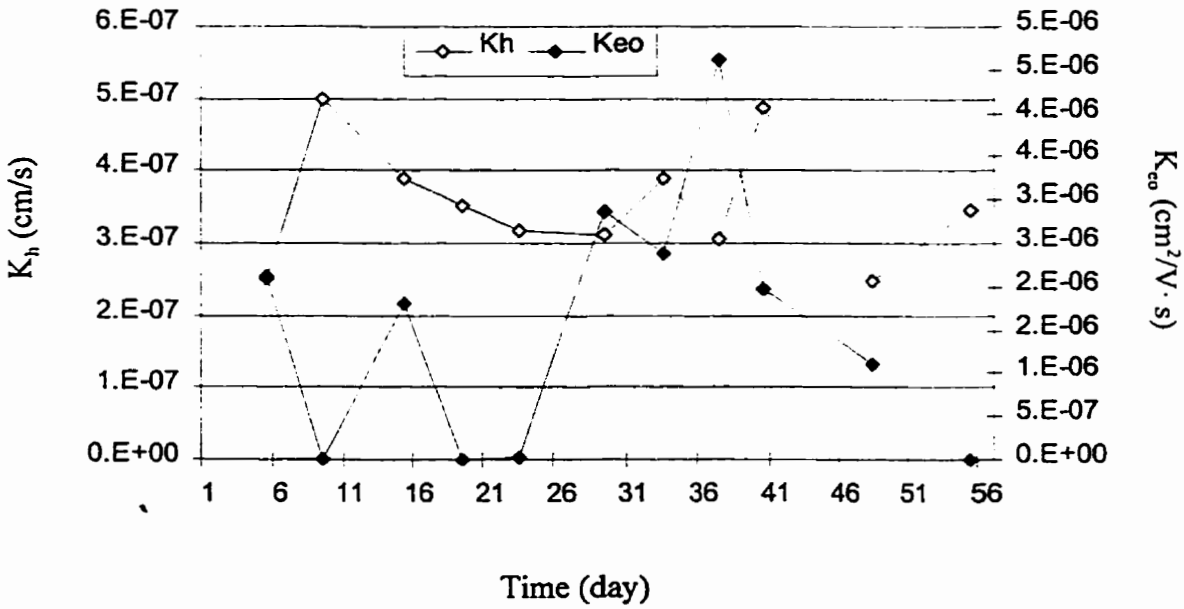

Figure 4.15 Hydraulic conductivity (K_h) and coefficient of electroosmotic permeability (K_{eo}) in water-flushing treatments.

as the zeta potential which in turn affects the K_{eo}. In general, the zeta potential decreases with a drop in pH. During the electrokinetic experiments, an acid front is generated at the anode and moves through the soil columns towards the cathode. This acid front affects the pH of the samples in the column and leads to a change in the zeta potential. Therefore, the value of K_{eo} is affected and is unstable over time during electrokinetic soil remediation. The average K_{eo} value from the experiment is 1.8×10^{-6} ($cm^2/V.s$) which is smaller than that reported by Acar *et al.* (1993a) ranging from 10^{-5} to 10^{-4} ($cm^2/V.s$). This may be due to the difference in properties of the clay soils.

4.3.1.3 Hydrocarbon extraction profiles

After the 55-day remediation of the contaminated clay soils, the columns were sectioned and all of the samples were analyzed to determine the residual contaminants in the clay soil. In addition, a portion of the samples were also analyzed to determine the water content profile and the pH profile.

The results for residual BTEX and PAHs in the remediated clay columns are shown in Figures 4.16 to 4.24. The total percentage remaining in the remediated columns are presented in Figure 4.25. Therefore, the percentage removal of benzene, toluene, ethylbenzene, *p*-xylene, *m*-xylene, *o*-xylene, naphthalene, 2-methylnaphthalene, and phenanthrene was 94.5%, 91.8%, 92.7%, 92.8%, 92.0%, 94.6%, 51.0%, 50.1%, 62.7%, respectively, for the hydraulic columns. For the electrical columns, the percentage removal of benzene, toluene, ethylbenzene, p-xylene, m-xylene, o-xylene, naphthalene, 2-methylnaphthalene, and phenanthrene was 92.2%, 94.6%, 95.2%, 96.8%, 94.9%, 96.3%, 72.1%, 72.9%, and 79.1%, respectively. The removal of BTEX did not seem to be

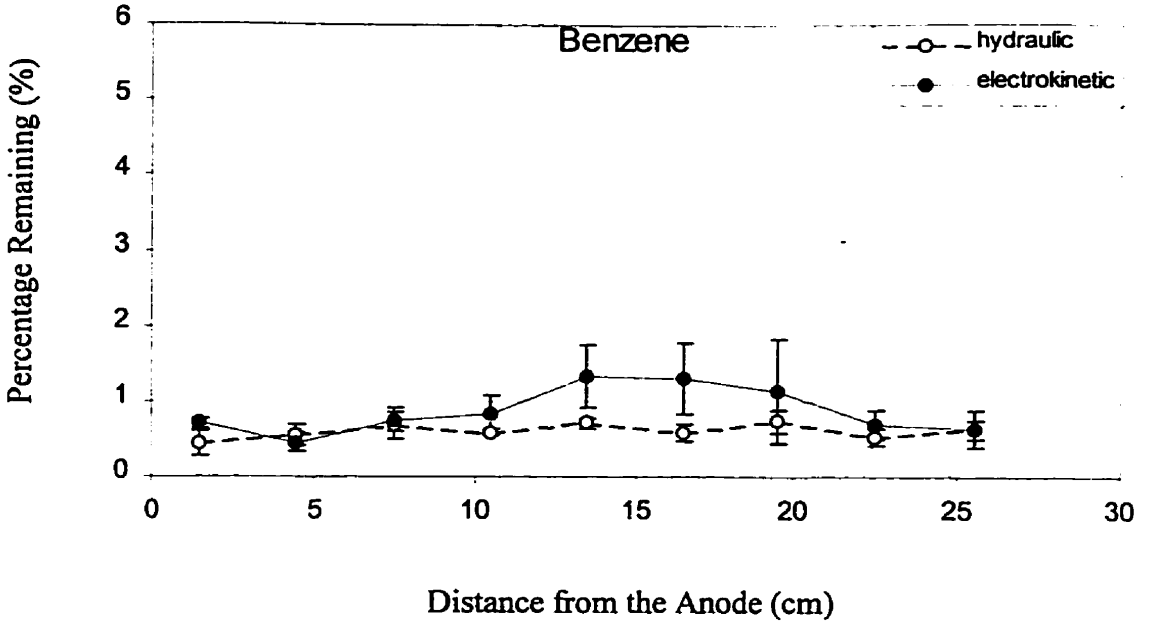

Figure 4.16 The percentage remaining, as a percent of injected amount, of benzene with standard errors indicated by error bars after water-flushing treatments.

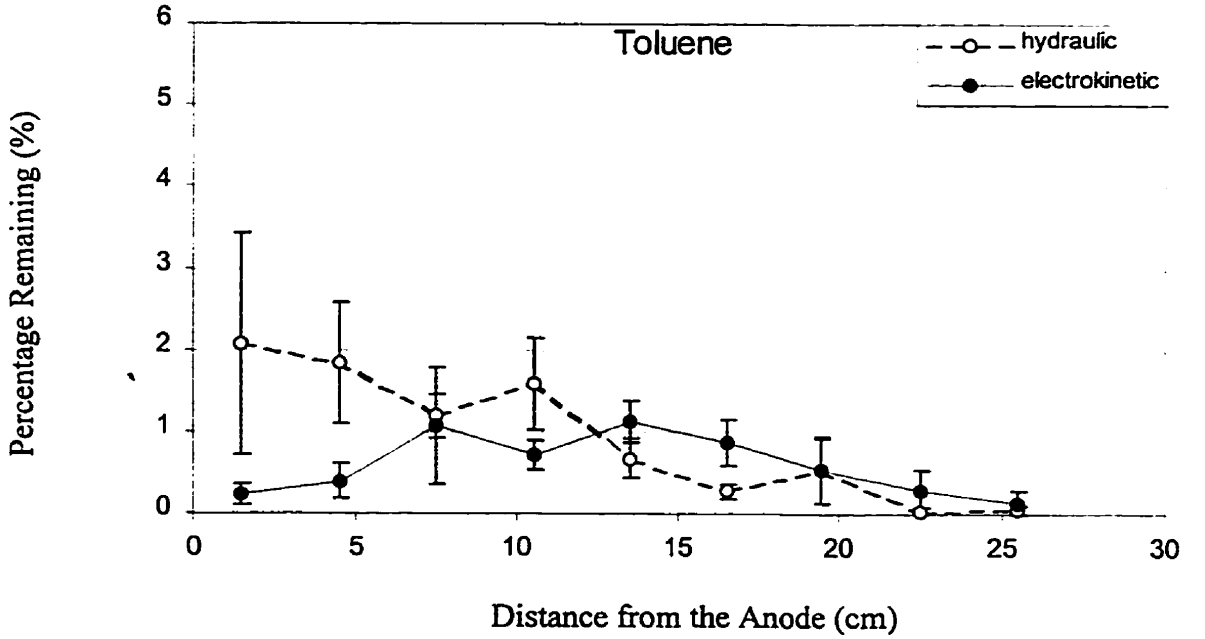

Figure 4.17 The percentage remaining, as a percent of injected amount, of toluene with standard errors indicated by error bars after water-flushing treatments.

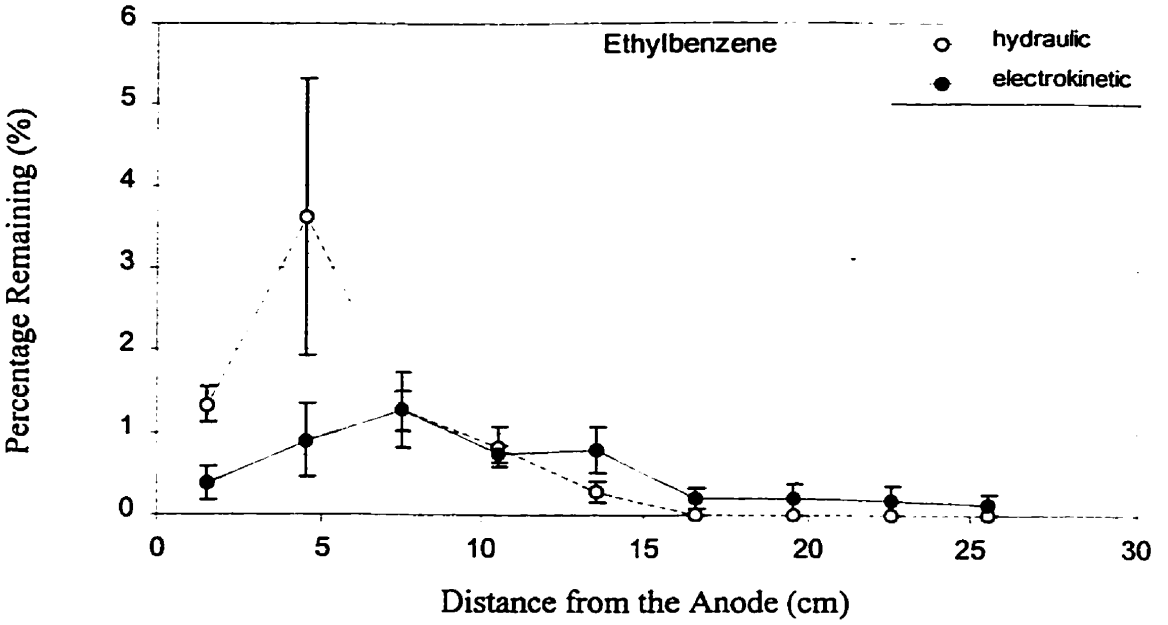

Figure 4.18 The percentage remaining, as a percent of injected amount, of ethylbenzene with standard errors indicated by error bars after water-flushing treatments.

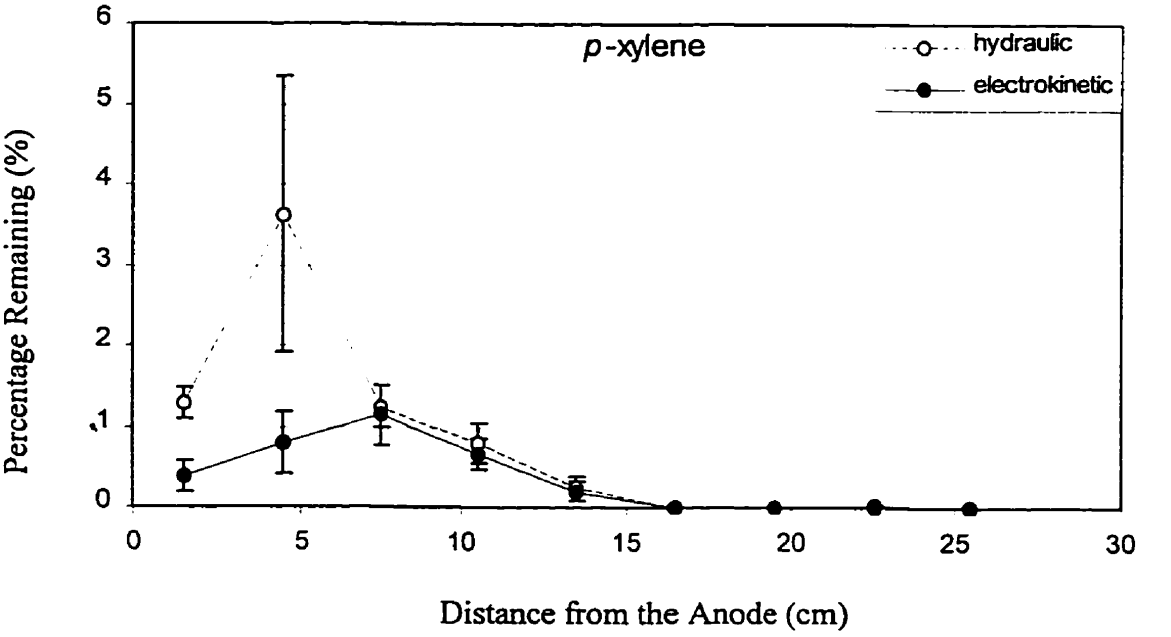

Figure 4.19 The percentage remaining, as a percent of injected amount, of *p*-xylene with standard errors indicated by error bars after water-flushing treatments.

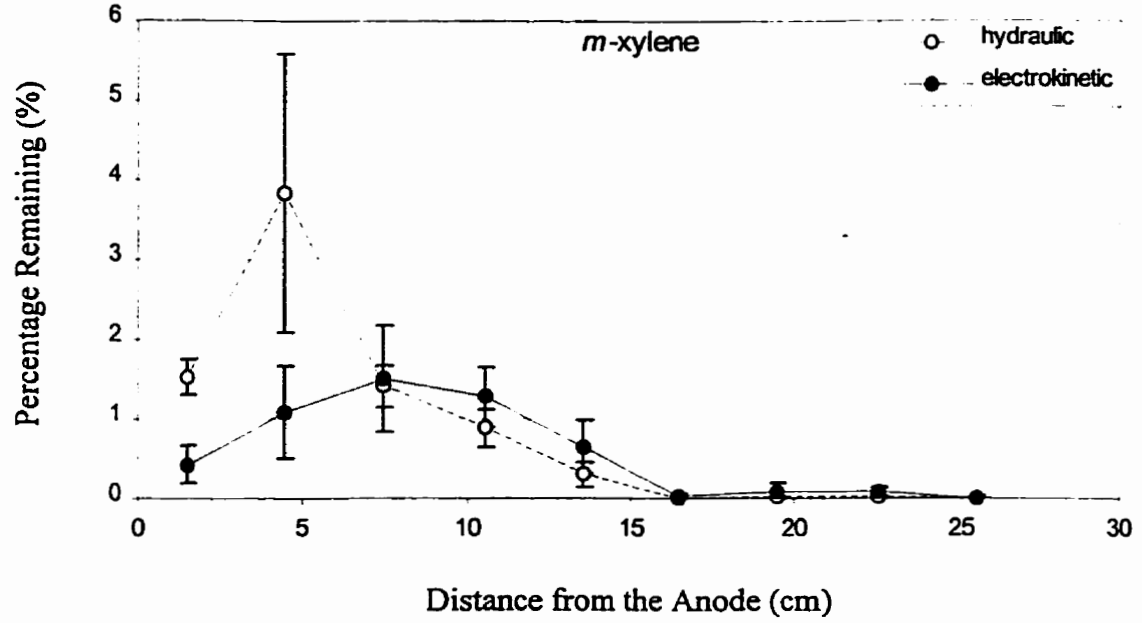

Figure 4.20 The percentage remaining, as a percent of injected amount, of *m*-xylene with standard errors indicated by error bars after water-flushing treatments.

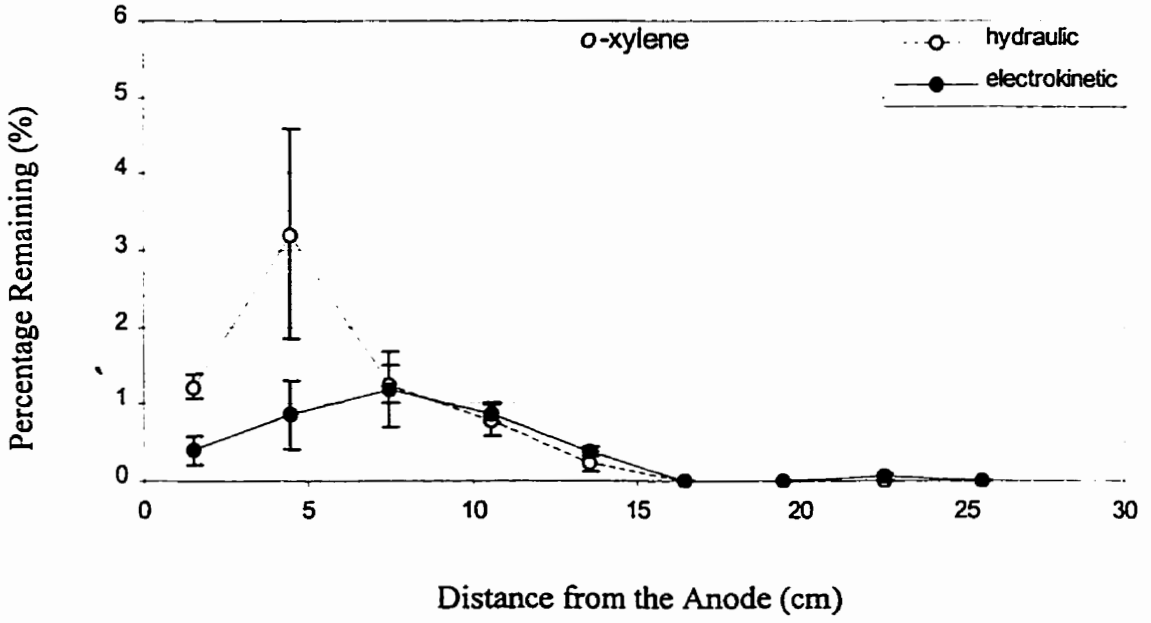

Figure 4.21 The percentage remaining, as a percent of injected amount, of *o*-xylene with standard errors indicated by error bars after water-flushing treatments.

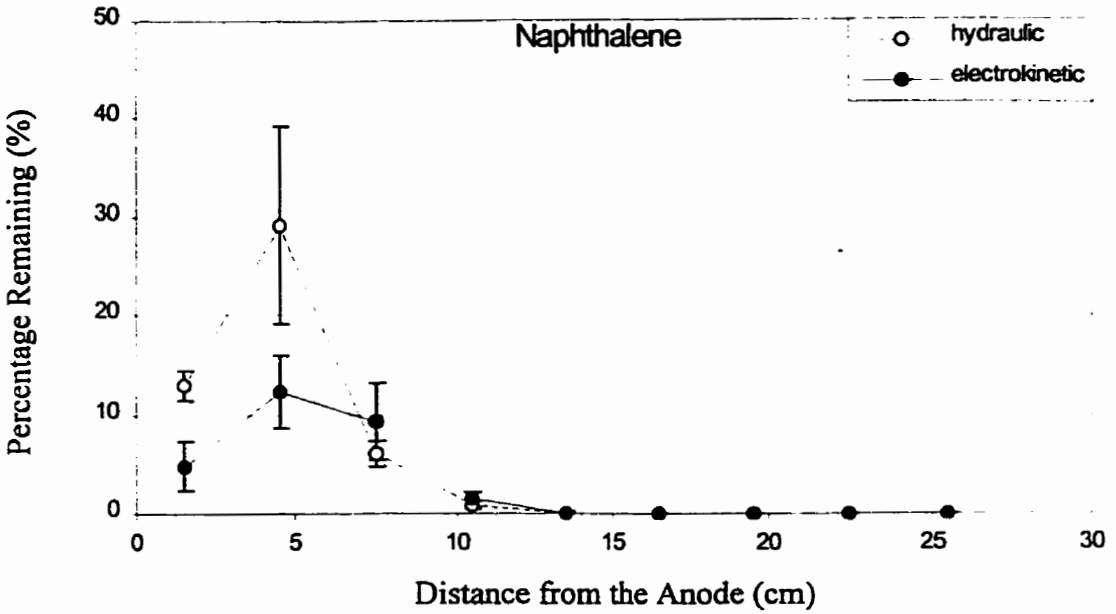

Figure 4.22 The percentage remaining, as a percent of injected amount, of naphthalene with standard errors indicated by error bars after water-flushing treatments.

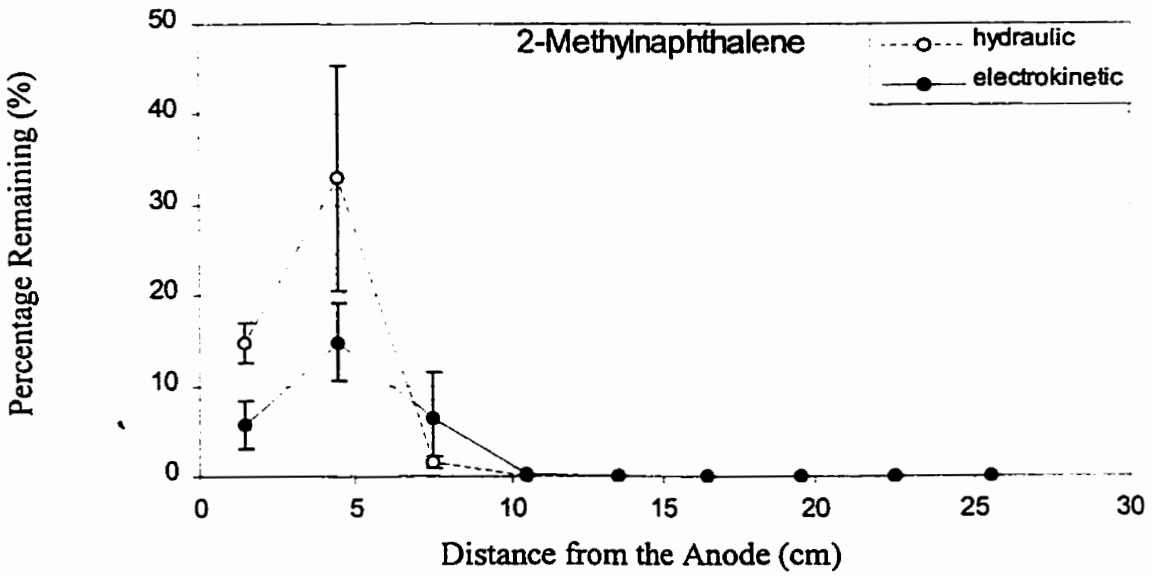

Figure 4.23 The percentage remaining, as a percent of injected amount, of 2-methylnaphthalene with standard errors indicated by error bars after water-flushing treatments.

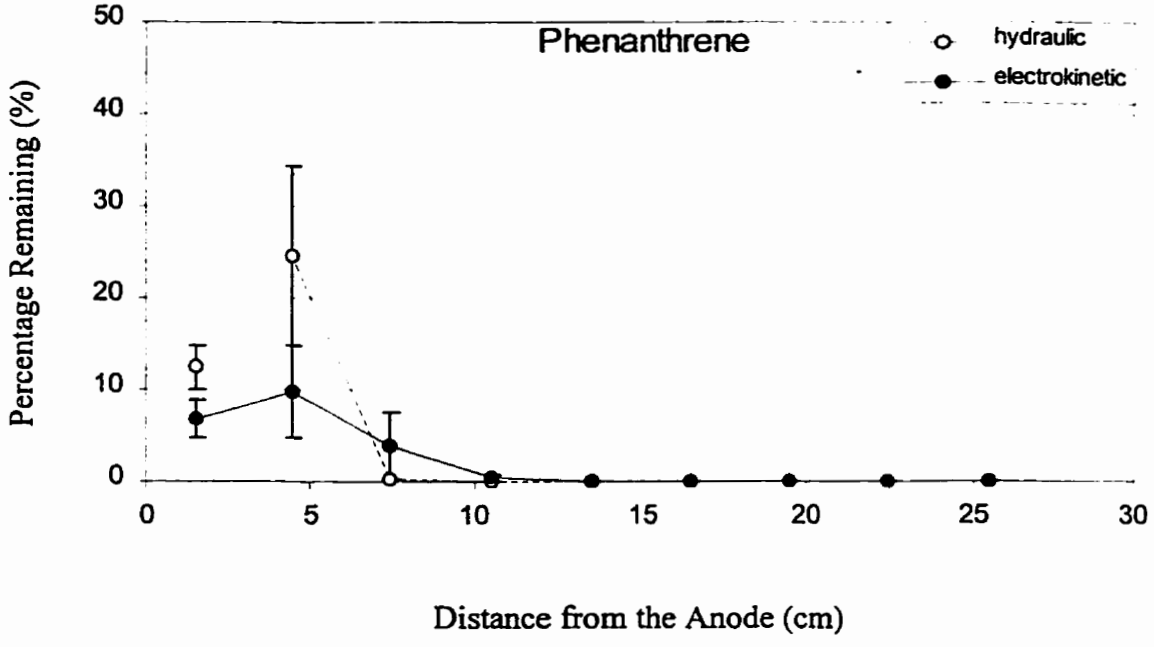

Figure 4.24 The percentage remaining, as a percent of injected amount, of phenanthrene with standard errors indicated by error bars after water-flushing treatments.

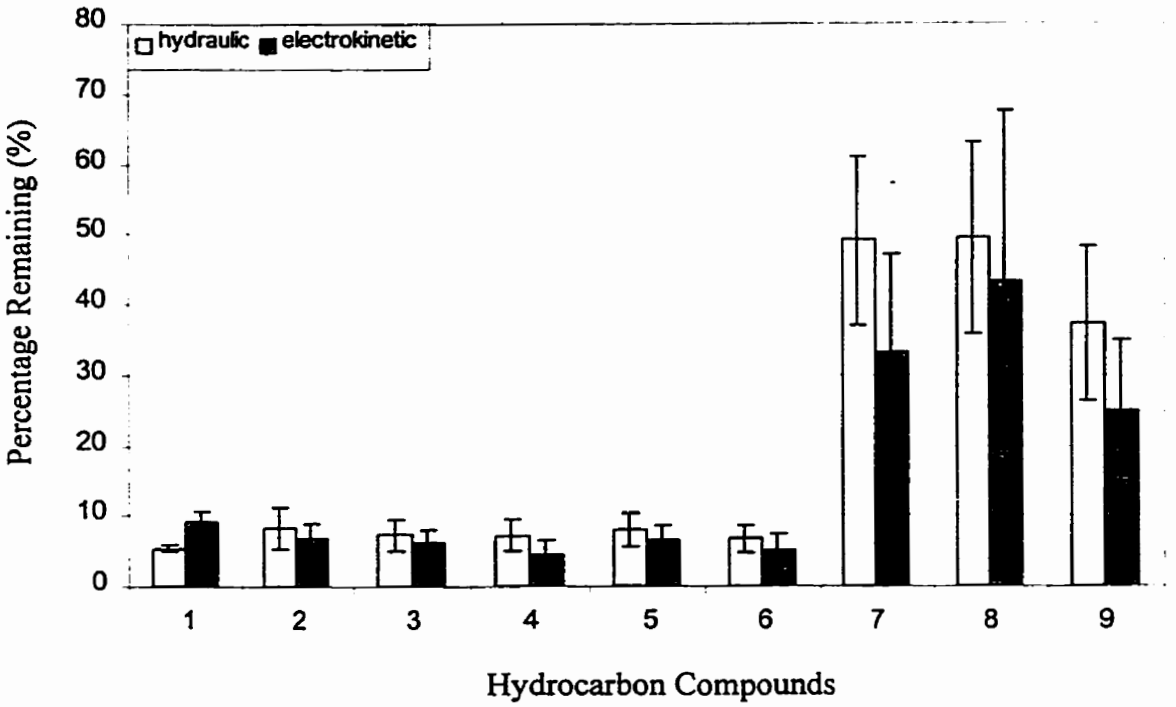

Figure 4.25 The average hydrocarbons remaining after water-flushing treatments as a percent of injected amount with standard errors indicated by error bars. In the figure, 1- benzene, 2- toluene, 3- ethylbenzene, 4- *p*-xylene, 5- *m*-xylene, 6- *o*-xylene, 7- naphthalene, 8- 2-methylnaphthalene, and 9- phenanthrene.

affected by the application of the electrical potential difference. However, the removal of the three selected PAHs, naphthalene, 2-methylnaphthalene, and phenanthrene, was enhanced by about 20% with the application of electrical potential difference. The enhancement of removal may have been due to the increased flow rate and thus increased volume of water available for the dissolution of the PAHs. Although the total removal of BTEX was not significantly enhanced with the application of electrical treatment, the peak movement of remaining BTEX was faster in the electrokinetic columns as shown in Figure 4.26. This indicates that the application of electrical potential difference has a tendency to remove the hydrocarbon contaminants faster than with hydraulic gradient alone. In conclusion, the soil remediation technique with the application of electrical potential difference is more efficient than the hydraulic treatment by itself.

The location of the residual contaminant in the test columns, based on the weighted average distance from the anode, was found to be a function of the solubility of the contaminant as shown in the Figure 4.26. The contaminant with the higher solubility shows the fastest movement over time. The location of weighted average of the contaminant from the anode was calculated by

$$D_{peak} = \frac{\sum_{i=1}^{9} D_i \%R_i}{\sum_{i=1}^{9} \%R_i} \qquad (4.19)$$

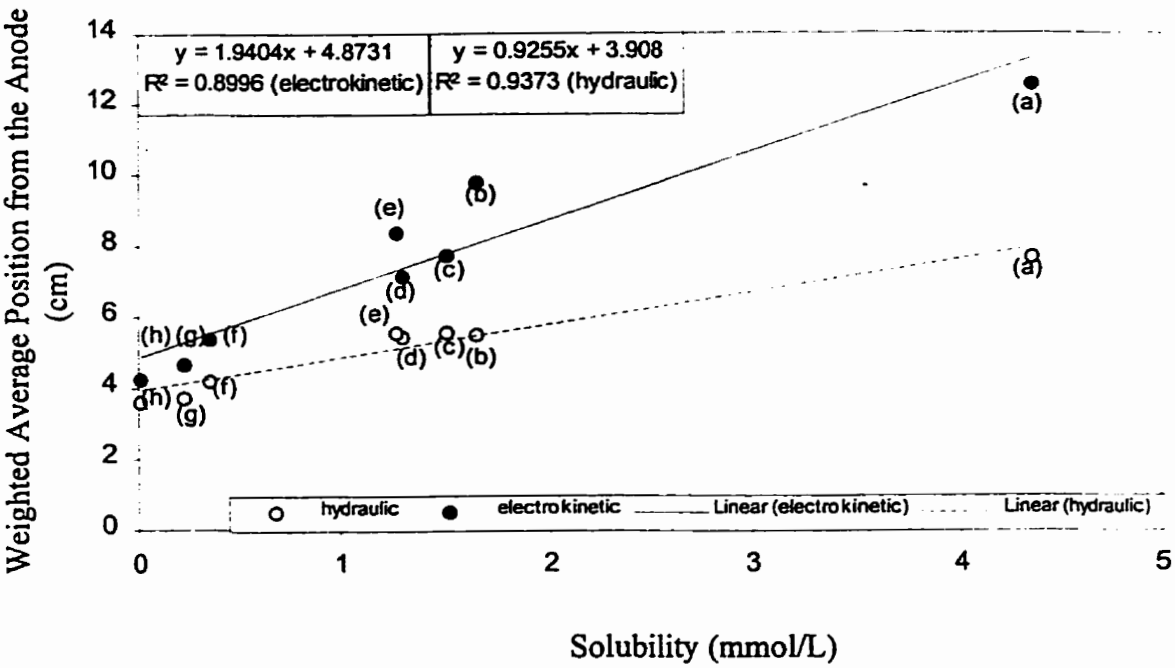

Figure 4.26 A relationship between the weighted average position of the hydrocarbon and the aqueous solubility in the water-flushing treatments. In the figure: (a)- toluene, (b)- ethylbenzene,(c)- *p*-xylene,(d)- *m*-xylene,(e)- *o*-xylene,(f)- naphthalene, (g)- 2-methylnaphthalene, and (h)- phenanthrene.

where

D_{peak} = the location of weighted average of the hydrocarbon from the anode (cm),

D_i = the distance of each section from the anode (cm), and

$\%R_i$ = the percentage remaining of the hydrocarbon in each section.

Linear relationships between location of weighted average of the hydrocarbon from the anode and its aqueous solubility were developed in the hydraulic columns ($r^2 = 0.94$) as well as in the electrokinetic columns ($r^2 = 0.90$).

4.3.1.4 The pH of effluents

The pH of the effluent was measured over time during soil remediation experiments and is shown in Figure 4.27 for both the electrokinetic and hydraulic columns. The pH of the effluent from the electrokinetic columns shows a higher value up to 13. This may be due to the production of OH^- at the cathode near the outflow end. However, the pH of the effluent from the hydraulic columns was closer to neutral (pH ~ 7).

4.3.1.5 Gravimetric water content

The water content (w/w) profiles of electrokinetic and hydraulic columns are shown in Figure 4.28. The lower water content at the inflow end indicates that the system could not supply enough water to match the electroosmotic flow rate. The average water contents of hydraulic and electrokinetic columns were 58.6% and 57.1%, respectively.

4.3.2 Surfactant-flushing treatments

4.3.2.1 Dry bulk density of the original clay samples

The dry bulk density of the clay soils, obtained from a construction area in the University of Manitoba, was 1.11 (g/cm^3) (%RSD = 2.89). After the clay soils were packed in the columns the dry bulk density and porosity are presented in Table 4.8.

Table 4.8 Physical properties of clay soils for surfactant-flushing treatments

	Dry bulk density (g/cm^3)	Porosity (%)
Column A	0.96	62.50
Column B	1.00	62.26
Column C	0.99	62.64
Column D	1.04	59.38
Column E	0.99	62.64
Column F	0.98	63.02
Average	1.00	62.26

*A, C, and E were electrokinetic columns;

*B, D, and F were hydraulic columns.

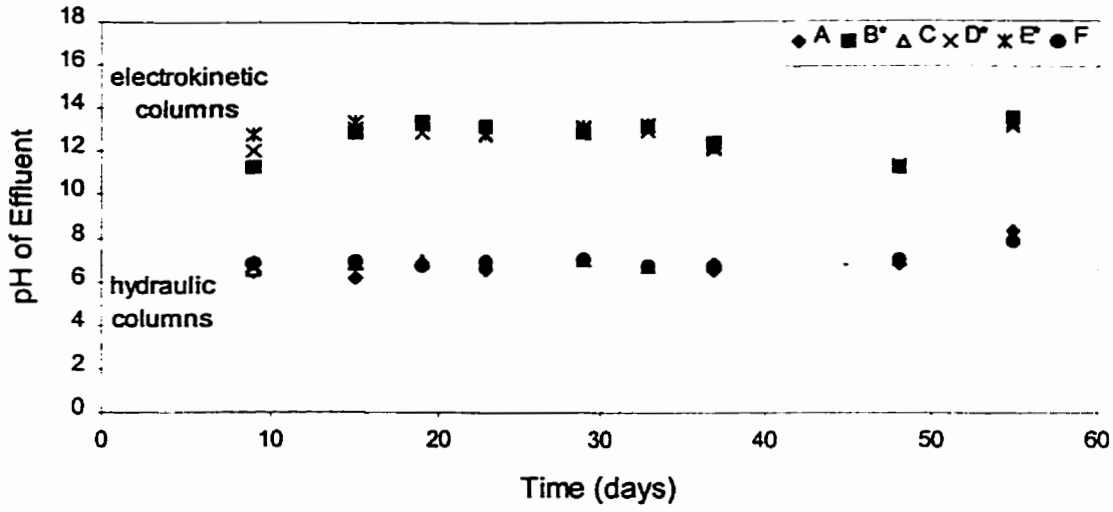

Figure 4.27 Measured pH values in collected effluents over time during water-flushing treatments. In figure, A, C, and F were hydraulic columns, and B, D, and E were electrokinetic columns.

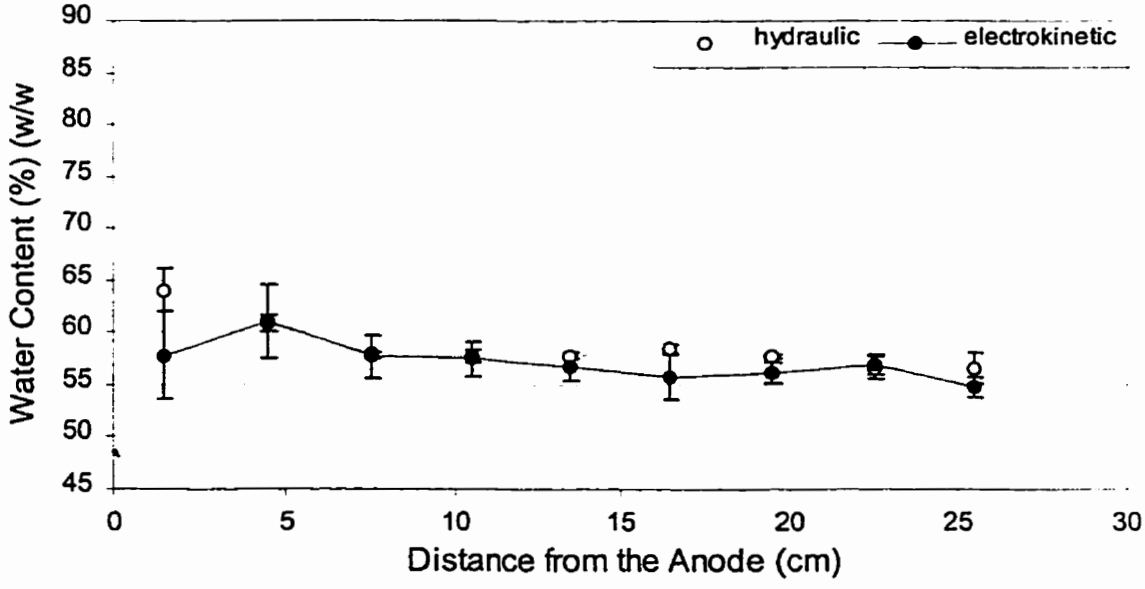

Figure 4.28 Gravimetric water content profiles with standard errors indicated by error bars after water-flushing treatments.

4.3.2.2 Flow rate, hydraulic conductivity K_h and coefficient of electroosmotic permeability K_{eo}

The experiment was conducted to evaluate the surfactant-enhanced hydraulic treatment and the surfactant-enhanced electrokinetic treatment. The conditions prevailing during the experiments were the same as for those without the surfactant. The six columns were flushed with a surfactant solution, CTAB, at a concentration of 1.5% (weight basis), which included three electrokinetic and three hydraulic columns. The effluents were collected from each column and the cumulative volume as a function of time is presented in Figure 4.29. The volume of effluent resulting from the application of electrical treatment was significantly higher than the one from the hydraulic treatment alone. The increased water movement appears to be due to the electroosmotic flow. This increased water movement is expected to enhance the migration of dissolved hydrocarbons.

The hydraulic conductivity (K_h) and coefficient of electroosmotic permeability (K_{eo}) can be calculated as described in Section 4.4.1.1 and is presented in Figure 4.30. However, the coefficient of electroosmotic permeability (K_{eo}) remained high until 50 days and then declined to almost zero at 53 days. The drop in K_{eo} could be attributed to the movement of acid front which changes the zeta potential as described in Section 4.4.1.2.

4.3.2.3 Hydrocarbon extraction profiles

The presence of a surfactant in the soil and aqueous system increases the apparent solubility of hydrocarbons. Therefore, more hydrocarbons are expected to dissolve into the aqueous phase and migrate along by advection due to the hydraulic or hydraulic coupled with electrokinetic flow. The electrophoretic flow of hydrocarbons absorbed

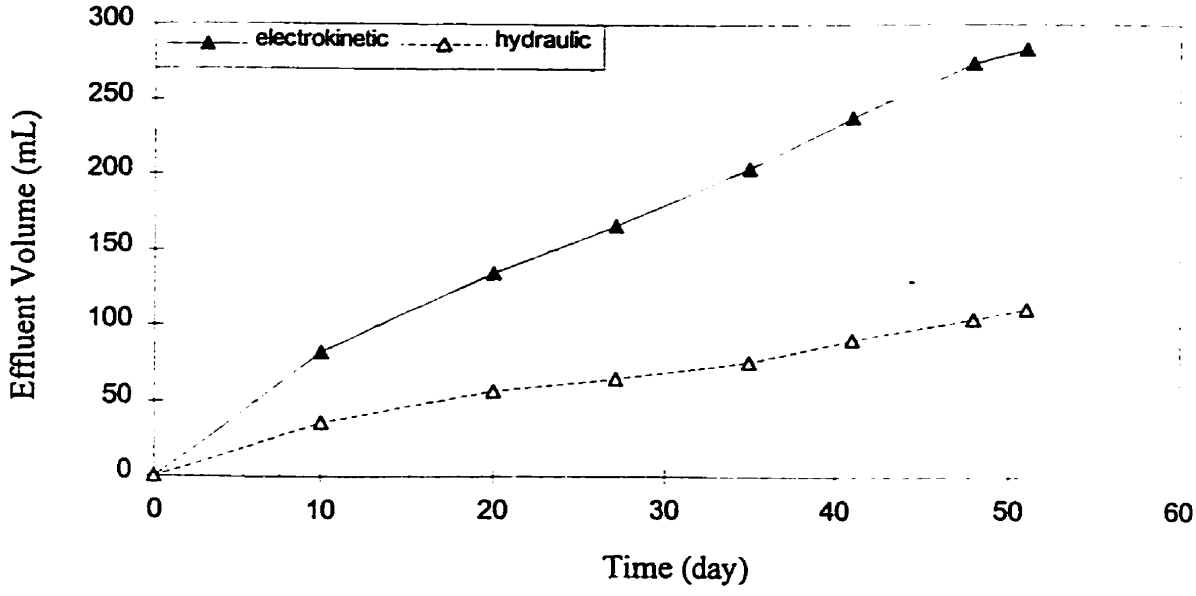

Figure 4.29 The effluent time volume collected over during the surfactant-flushing treatments.

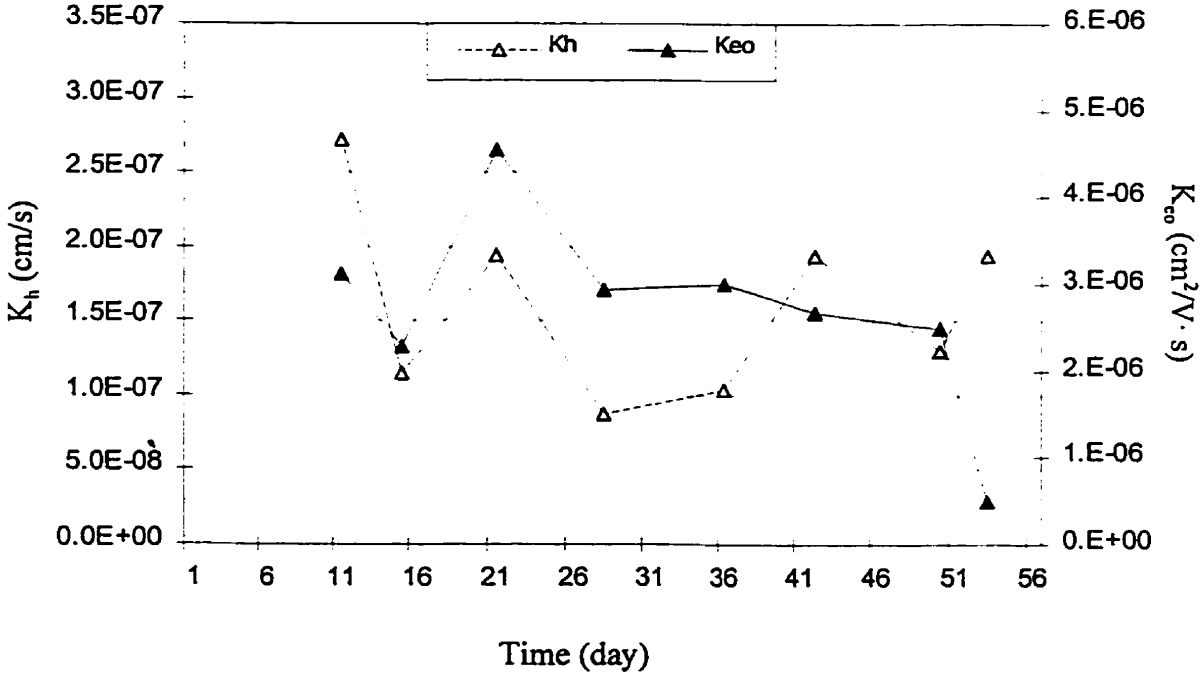

Figure 4.30 Hydraulic conductivity (K_h) and coefficient of electroosmotic permeability (K_{eo}) in surfactant-washing treatments.

within the micelles is also expected to be significant in the electrokinetic columns. Since the surfactant used in the experiments is a cationic surfactant (CTAB), the electrophoretic migration of the micelles is in the same direction of advective flow due to the hydraulic gradient as well as the electroosmotic flow. Therefore, the migration of hydrocarbons in the presence of a cationic surfactant is expected to be greater than that without the surfactant.

The residual hydrocarbons remaining in the sectioned clay samples were obtained by using SPME-GC-FID analysis. The BTEX and PAHs remaining in the remediated soil with surfactant-enhanced and with surfactant-enhanced electrokinetic treatment are presented in Figures 4.31 through 4.38. The total percentage of remaining hydrocarbons in the remediated columns are shown in Figure 4.39. Therefore, the percentage removal of benzene, toluene, ethylbenzene, *p*- and *m*-xylene, *o*-xylene, naphthalene, 2-methylnaphthalene, and phenanthrene in the hydraulic columns were 97.0%, 96.9%, 98.9%, 98.7%, 98.6%, 69.0%, 59.3%, and 58.8%, respectively. In the electrokinetic columns, the percentage removal of benzene, toluene, ethylbenzene, *p*- and *m*-xylene, *o*-xylene, naphthalene, 2-methylnaphthalene, and phenanthrene were 96.9%, 95.9%, 95.1%, 96.7%, 98.5%, 52.8%, 48.8%, and 60.4%, respectively. Overall, the electrical columns appeared to have a larger percentage of residual hydrocarbons remaining at the end of the treatment. The hydraulic columns had a better removal efficiency with 17% and 11% for naphthalene and 2-methylnaphthalene, respectively, over electrical columns. Since the micelles containing the hydrocarbons are positively charged, they may have been preferentially adsorbed onto the clay particle surfaces which are negatively charged. With

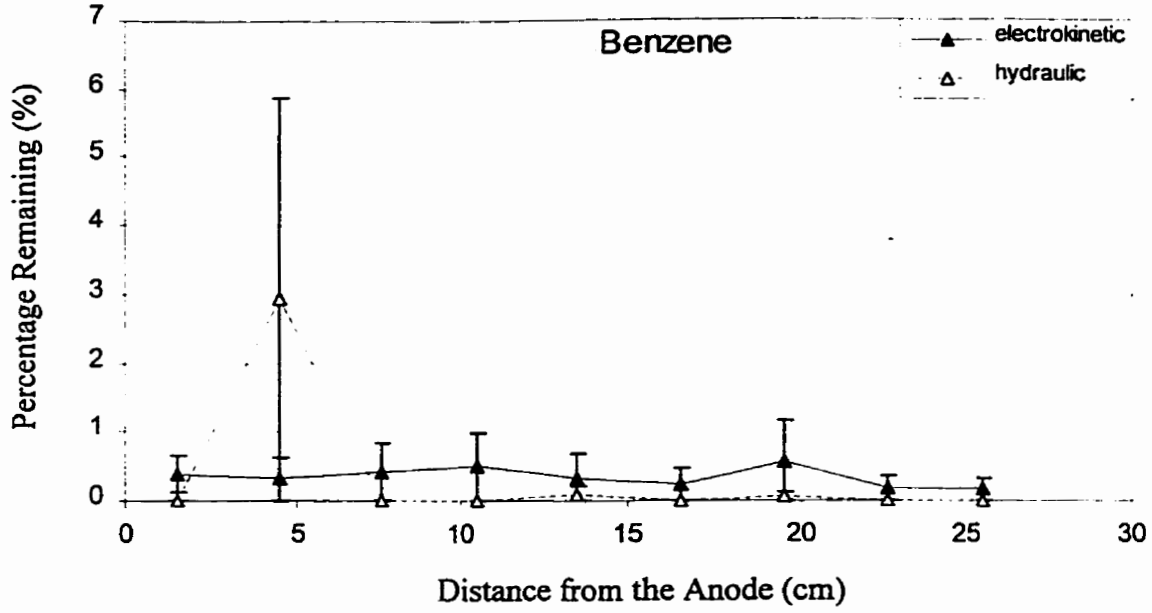

Figure 4.31 The percentage remaining, as a percent of injected amount, of benzene with standard errors indicated by error bars after surfactant-flushing treatments.

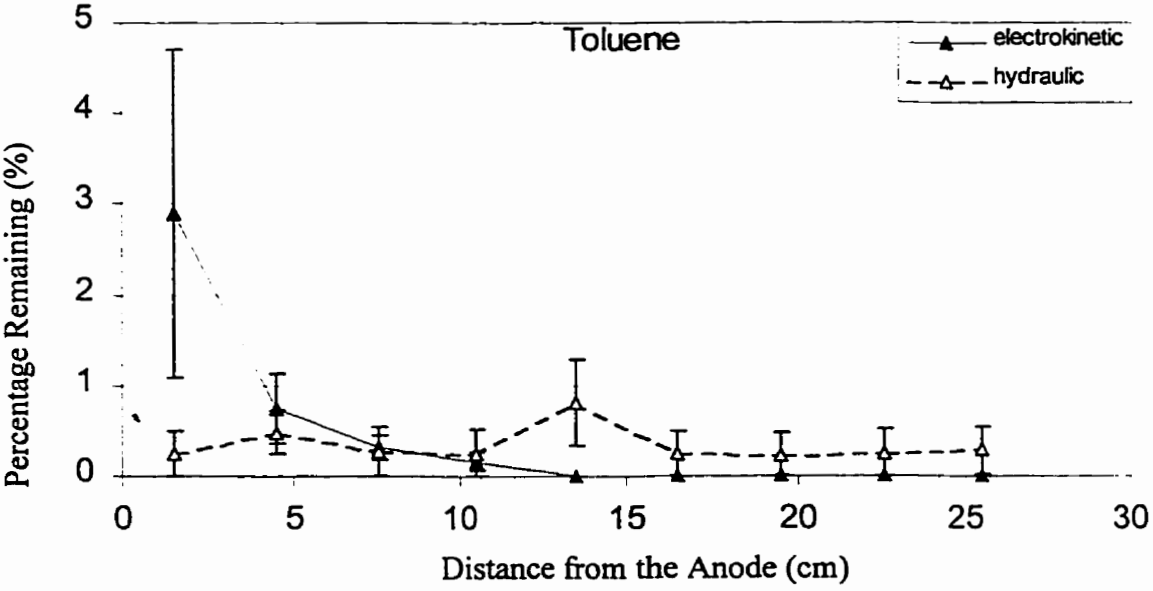

Figure 4.32 The percentage remaining, as a percent of injected amount, of toluene with standard errors indicated by error bars after surfactant-flushing treatments.

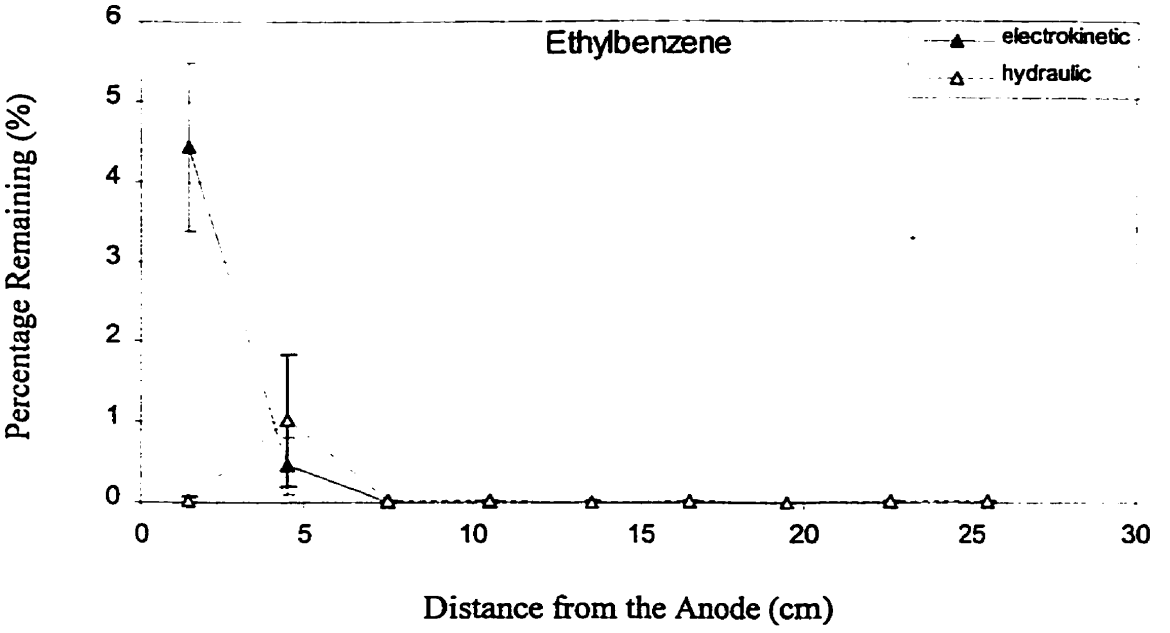

Figure 4.33 The percentage remaining, as a percent of injected amount, of ethylbenzene with standard errors indicated by error bars after surfactant-flushing treatments.

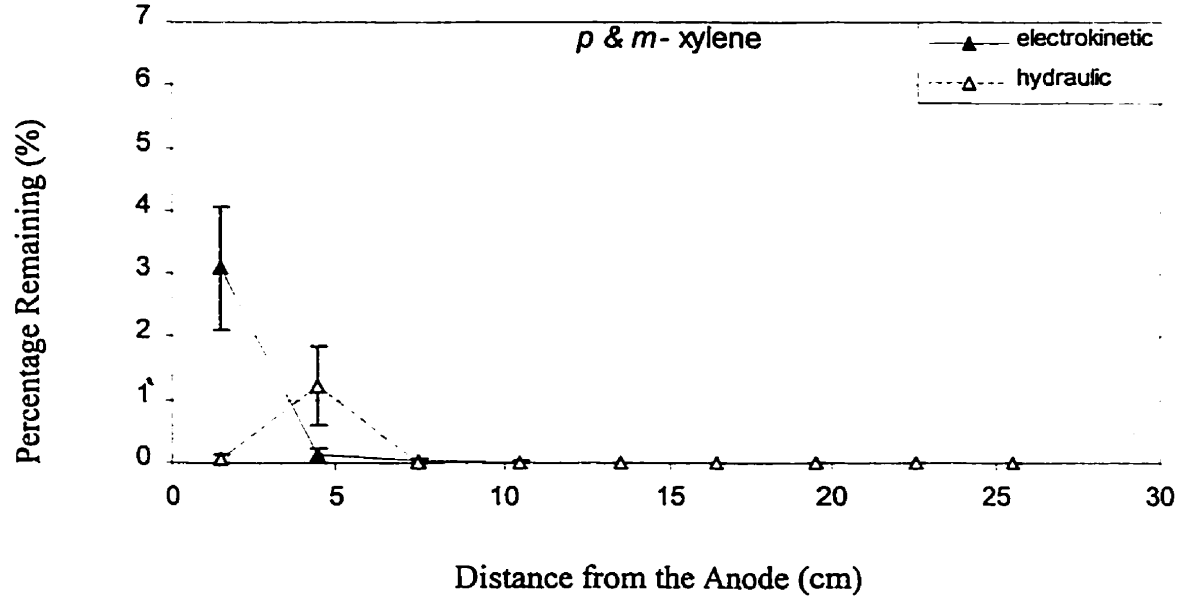

Figure 4.34 The percentage remaining, as a percent of injected amount, of *p*-, *m*-xylenes with standard errors indicated by error bars after surfactant-flushing treatments.

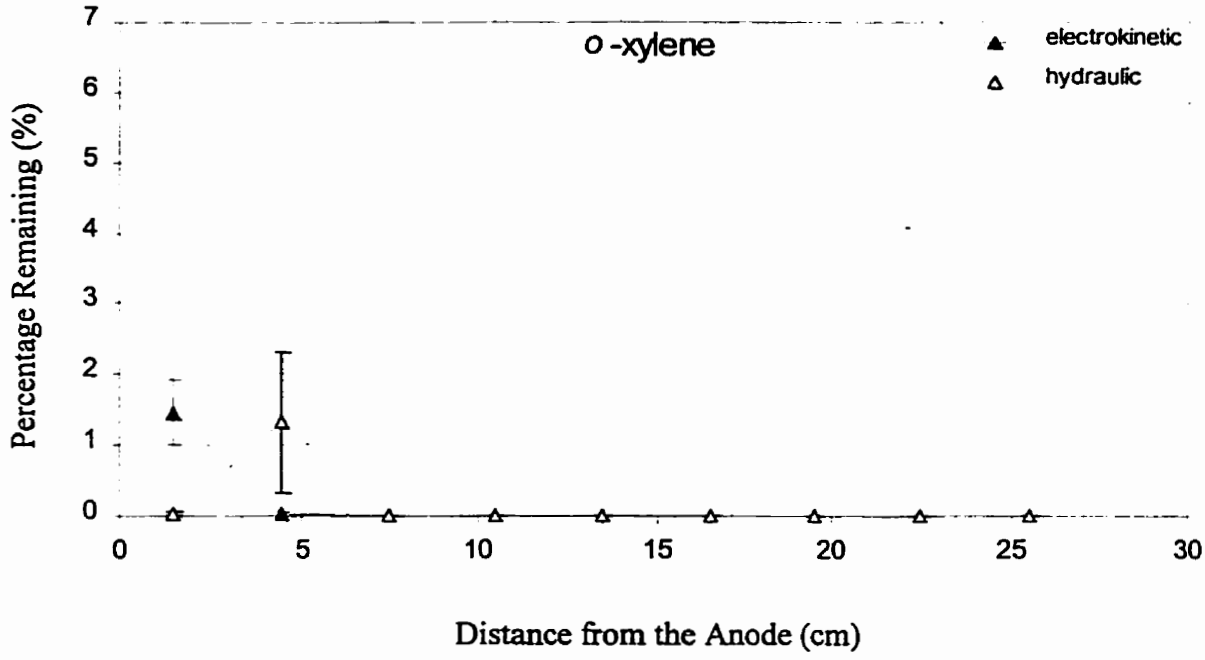

Figure 4.35 The percentage remaining, as a percent of injected amount, of o-xylene with standard errors indicated by error bars after surfactant-flushing treatments.

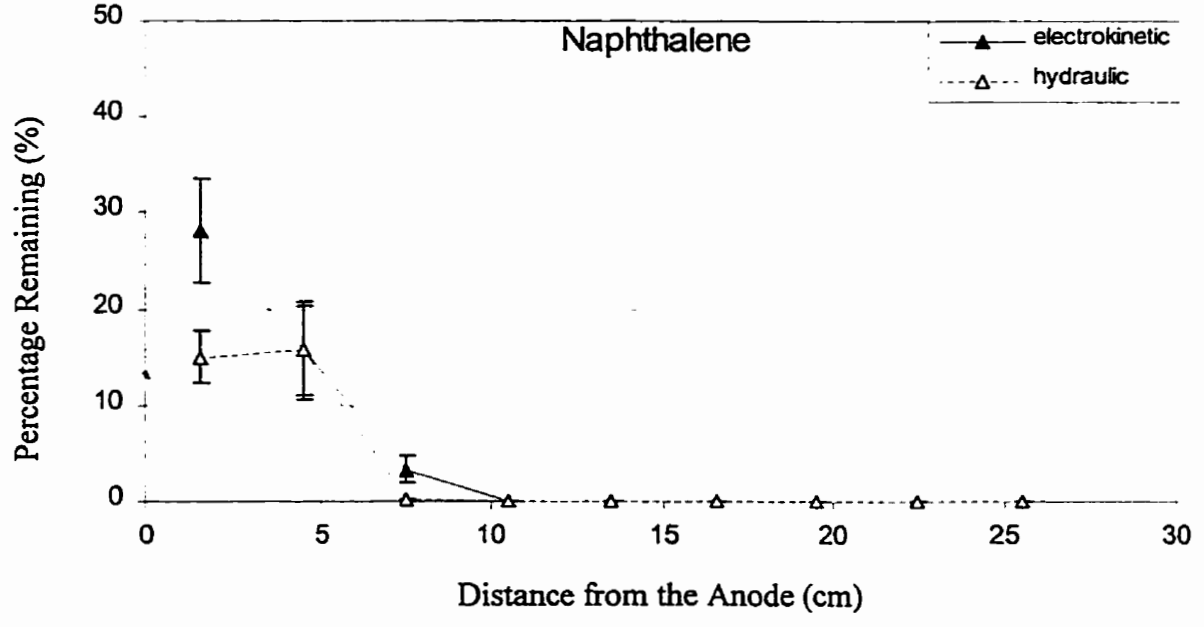

Figure 4.36 The percentage remaining, as a percent of injected amount, of naphthalene with standard errors indicated by error bars after surfactant-flushing treatments.

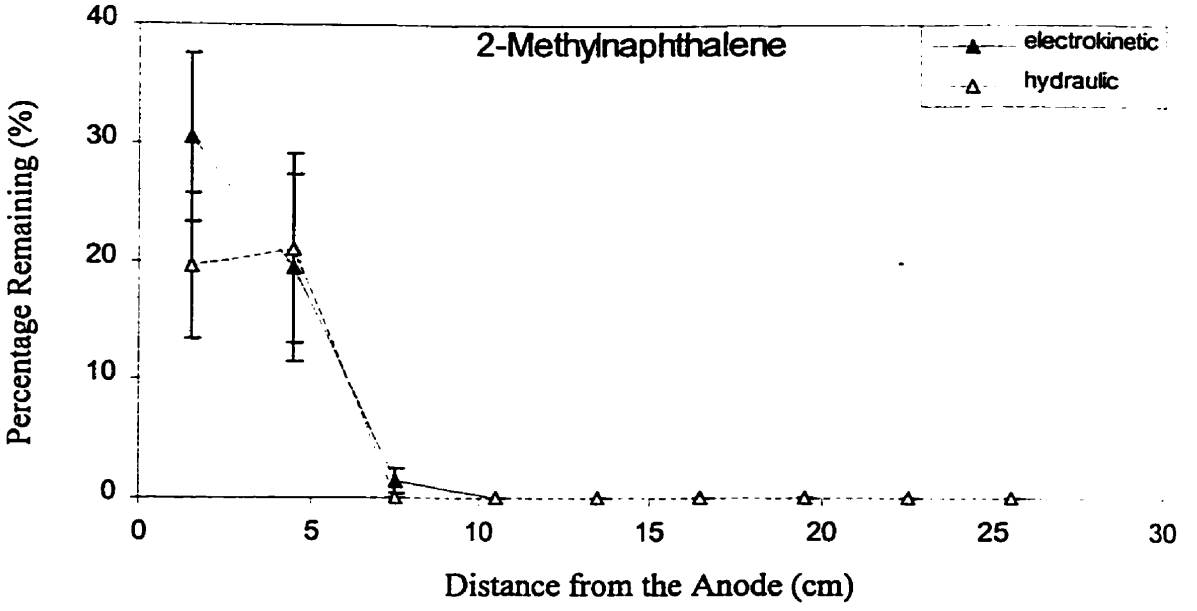

Figure 4.37 The percentage remaining, as a percent of injected amount, of 2-methylnaphthalene with standard errors indicated by error bars after surfactant-flushing treatments.

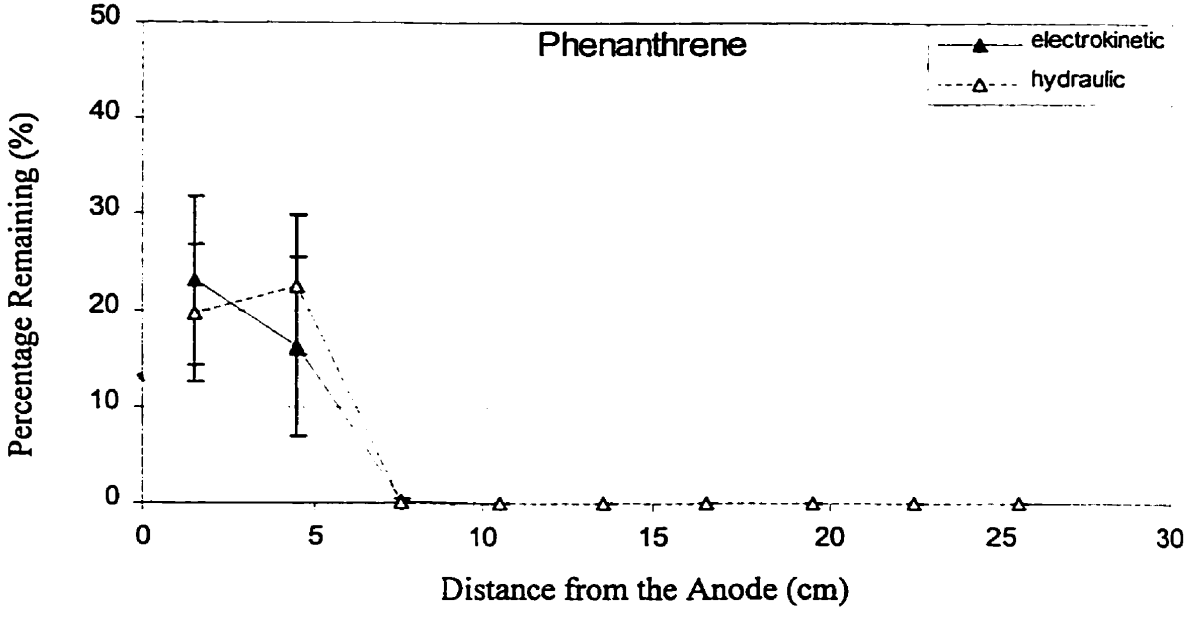

Figure 4.38 The percentage remaining, as a percent of injected amount, of phenanthrene with standard errors indicated by error bars after surfactant-flushing treatments.

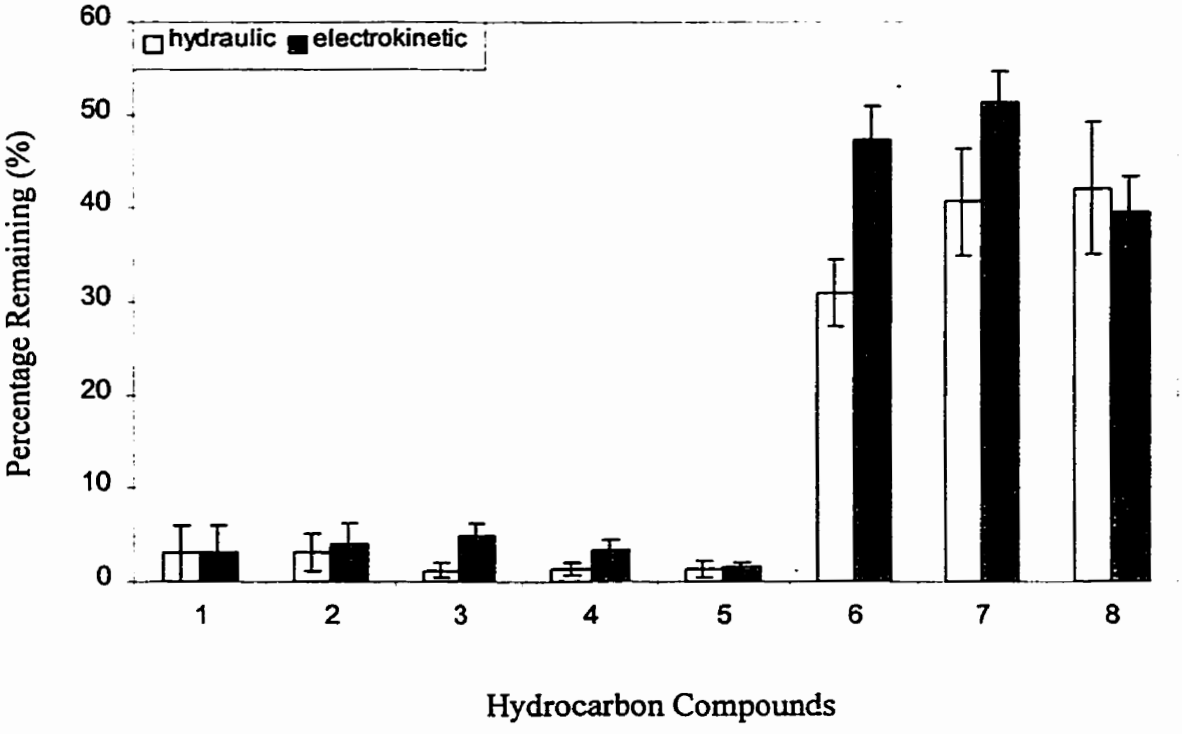

Figure 4.39 The average hydrocarbons remaining, as a percent of injected amount, with standard errors indicated by error bars after surfactant-flushing treatments. In the figure, 1- benzene, 2- toluene, 3- ethylbenzene, 4- *p*-, and *m*- xylene, 5- o-xylene, 6- naphthalene, 7- 2-methylnaphthalene, and 8- phenanthrene.

the electrokinetic treatment more of the negatively charged surfaces would have been open for absorbing the micelles. This scenario can only happen if the cations on the clay particle surfaces move towards the cathode in preference to the micelles.

The location of the weighted average residual hydrocarbon remaining in the column was found to be a function of the solubility of hydrocarbon as shown in Figure 4.40. The location of the average residue was found to linearly increase with increasing solubility of hydrocarbon ($r^2 = 0.84$) in the electrokinetic columns. In the hydraulic columns, the weighted average position was also found to be a linear function of the solubility for all selected compounds except benzene ($r^2 = 0.82$). The weighted average position was calculated using equation 4.19.

4.3.2.4 Electrical conductivity and pH measurement in the surfactant-enhanced electrokinetic remediation

The electrical conductivity of effluent with surfactant (at the cathode) was measured every five days on each electrokinetic column starting at the tenth day. The electrical conductivity of the effluent as a function of time is presented in Figure 4.41. The electrical conductivities increased linearly ($r^2 = 0.947$) over time, which is given by,

$$Y_{ec} = 0.2T - 0.57 \qquad (4.19)$$

where

Y_{ec} = electrical conductivity (ds/m), and

T = time (days).

The pH of the effluent from both the electrokinetic and hydraulic columns was measured and is presented in Figure 4.42. Since OH^- is produced at the cathode near the

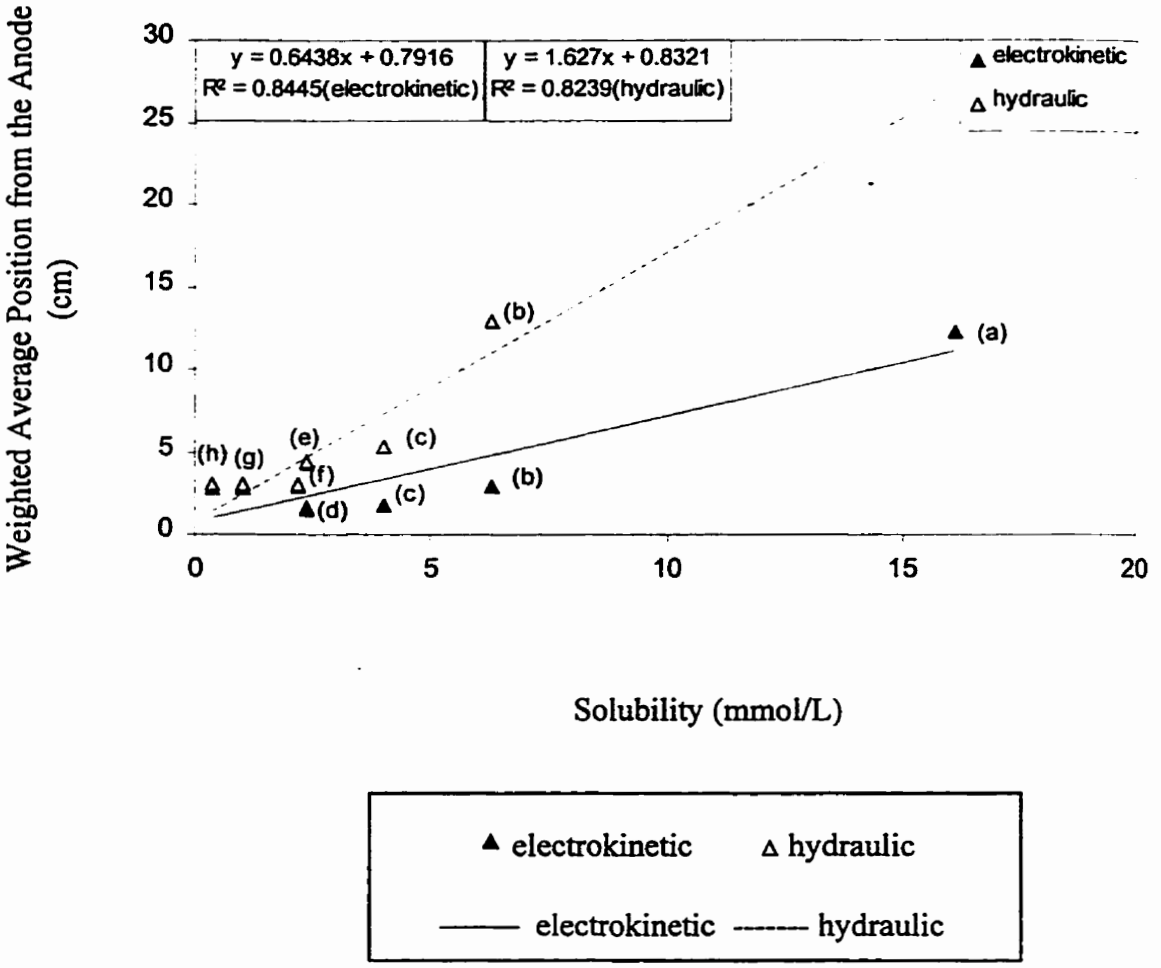

Figure 4.40 A relationship between the hydrocarbon-remaining peak and the aqueous solubility after surfactant-flushing treatments. In the figure, (a)- benzene, (b)- toluene, (c)- ethylbenzene, (d)- *p*- and *m*-xylenes, (e)- *o*-xylene, (f)- naphthalene, (g)- 2-methylnaphthalene, and (h)- phenanthrene.

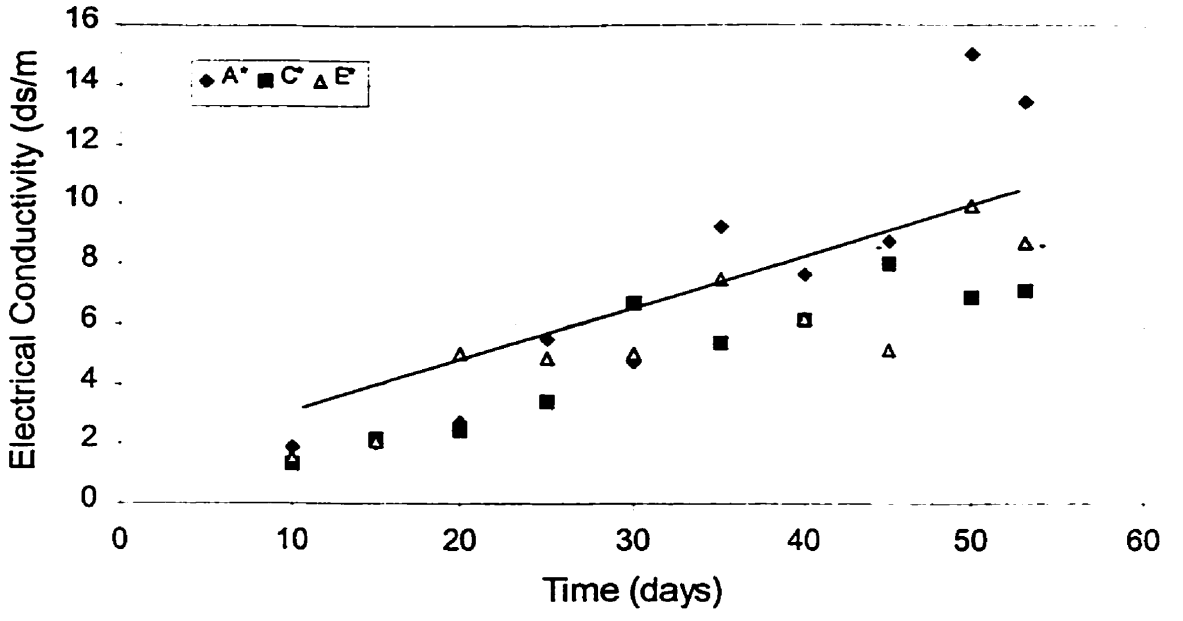

Figure 4.41 Electrical conductivities in the effluent during surfactant-flushing treatments. In the figure, A, C, and E were electrokinetic columns.

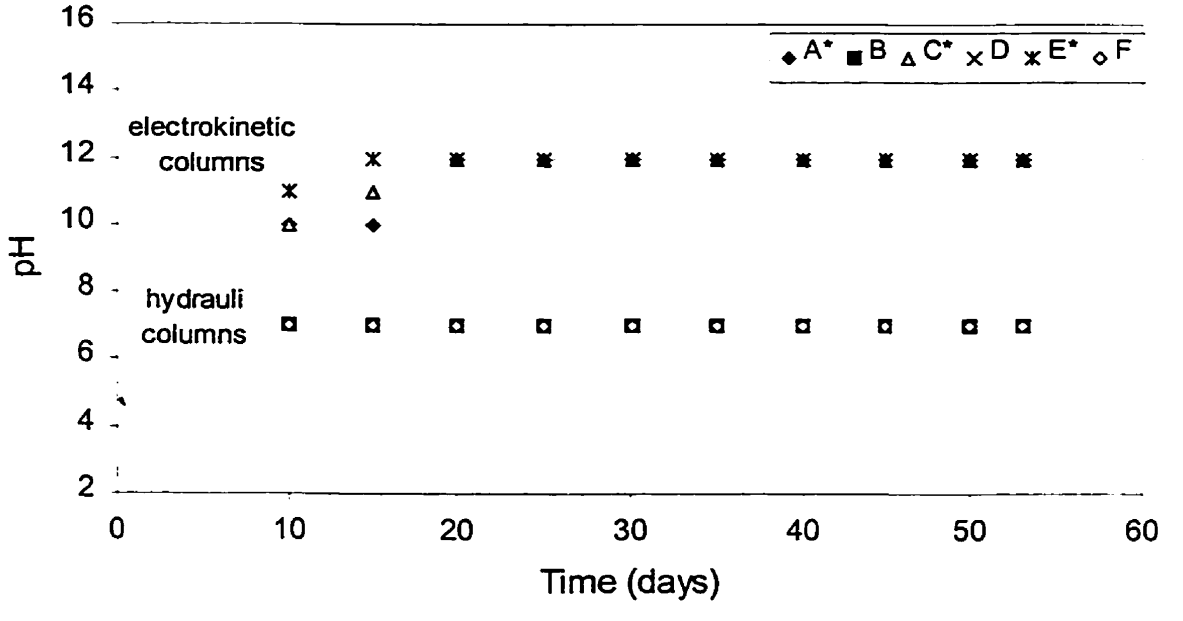

Figure 4.42 pH in the effluents during surfactant-flushing treatment. In the figure, A, C, and E were electrokinetic columns, and B, D, and F were hydraulic columns.

outflow end, the effluent will have a high pH (= 12) compared to the effluent from the hydraulic columns (= 7).

4.3.2.5 Water content profiles

The water content profiles of electrokinetic and hydraulic columns are presented in Figure 4.43. The water content of the electrokinetic column was relatively higher than that in the hydraulic column, except near the outflow end. The water content near the outflow end at the cathode was much lower compared to that in the hydraulic column. The reduction of water content at the outflow end may have been due to the electroosmotic flow. The results shown in Figure 4.43 indicate that the column had enough inflow water supporting the electroosmotic flow.

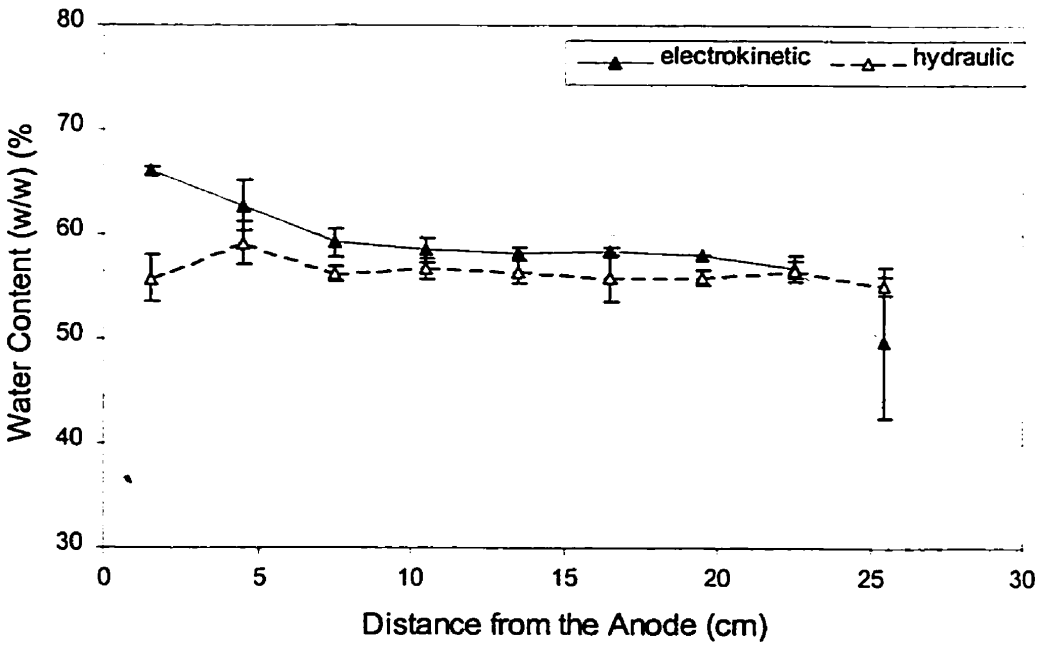

Figure 4.43 Gravimetric water content profiles with standard errors indicated by error bars after surfactant-flushing treatments.

5.0 Conclusion

Water-flushing and surfactant-flushing coupled with/without electrokinetic treatments were used for the remediation of clay columns contaminated with model diesel fuel. The efficiency of each treatment was evaluated. To accomplish the goal, SPME-GC-FID was used to determine the hydrocarbon residues remaining in the clay columns.

Three main goals, listed in Section 1.3, were addressed in this research. The selection of an efficient analytical method using the SPME-GC-FID analysis was one of the objectives. The following can be concluded from the experiments:

- The linear range of the detector response was from 0 to 25 ppm for benzene, toluene, and ethylbenzene. The linear range for three xylenes was 0 to 50 ppm. The linear range was 0 to 1 ppm for naphthalene, 2-methylnaphthalene, and phenanthrene.
- The application of agitation extraction, provided by the sample carousel agitation device, resulted in a 40% increase in detector response. The agitation extraction method reduced the analysis time by SPME-GC-FID.

The main goal of this research was to evaluate the efficiency of surfactant-enhanced electrokinetic remediation treatment by determining the removal of hydrocarbons from the clay columns contaminated with the model diesel fuel. The following can be concluded from the experiments:

- The water-flushing coupled with electrokinetic treatment slightly improved the total removal of toluene, ethylbenzene, and three xylenes from the columns compared to the water-flushing treatment alone. However, the peak of the remaining BTEX had moved

farther in the electrokinetic columns compared to the hydraulic treatment only. For the three selected PAHs, the removal was enhanced by about 20% due to the application of the electrical potential difference. Therefore, the water-flushing coupled with electrokinetic treatment has the potential to clean up more efficiently in soils contaminated with BTEX and three selected PAHs.

• The surfactant-enhanced electrokinetic treatment not only did not enhance the removal of selected hydrocarbons, but also had a larger percentage of residual hydrocarbons remaining in the columns. For some selected compounds, such as naphthalene and 2-methylnaphthalene, the hydraulic columns had a better removal efficiency with 17% and 11% over electrokinetic columns, respectively. In addition, the peak of the hydrocarbon residue was found to move less in the electrokinetic columns compared to the hydraulic treatment. Therefore, the cationic surfactant flushing coupled with electrokinetic treatment has a potential to retard the movement of selected hydrocarbon contaminants in clay columns.

Another goal of this research was to determine the factors affecting the remediation treatments. The following conclusions are based on the experimental evidence:

• In the water-flushing treatment, electroosmosis increased the amount of effluent in the electrokinetic columns. The hydraulic conductivity remained relatively stable during the remediation indicating no change in soil and pore water conditions. However, the coefficient of electroosmotic permeability (K_{eo}) was found to be unstable during the soil remediation due to the movement of the acid front through the clay columns.

• In the surfactant-flushing treatment, the volume of effluent was significantly increased due to electroosmotic flow. The hydraulic conductivity remained stable. However, the coefficient of electroosmotic permeability (K_{eo}) remained high for 51 days of the experiment and then declined to almost zero on the 53rd day at which time the experiment was stopped. The drop in K_{eo} could be attributed to the movement of the acid front which may have changed the zeta potential. The electrical conductivity of the effluent for the surfactant treatment was found to increase linearly over time. This may have been due to the accumulation of ions during soil remediation.

• The critical micelle concentration (CMC) of CTAB was found to be 9.0×10^{-4}M (0.03%), which is very close to the value from the literature.

• The apparent solubility of hydrocarbons increased at the CMC for all selected compounds.

• The molar solubilization ratio (MSR) was determined for the selected hydrocarbons. Among the nine selected compounds, ethylbenzene had the highest MSR followed by benzene, naphthalene, 2-methylnaphthalene, the three xylenes, toluene, and phenanthrene. Therefore, the surfactant-enhanced remediation may be more efficient for the removal of ethylbenzene and benzene compared to remediation without the application of a cationic surfactant.

• The micelle-water partition coefficient (K_{mic}) was determined based on the MSR. Benzene and toluene was found to have a lower K_{mic} which indicates that they are more

hydrophilic compounds compared to the compound with higher K_{mic} such as the three selected PAHs.

• The linear relationship between solubility and octanol-water partition coefficient (K_{ow}) was determined in the aqueous phase as well as in the surfactant solutions. Since the K_{ow} is available in the literature for many hydrocarbons, the solubility can be determined using the relationship either in the aqueous phase or in the surfactant solutions.

• The linear relationship between the micelle-water partition coefficient (K_{mic}) and the octanol-water partition coefficient (K_{ow}) was developed. The K_{mic} can be determined using the relationship based on the K_{ow} available from the literature.

• The relationships between the organic carbon-water partition coefficient (K_{oc}) and the K_{ow} and between K_{oc} and solubility were determined, respectively.

6.0 Recommendations

Several recommendations can be made from this research which are listed below:

- To enhance the efficiency of electrokinetic treatment with cationic surfactant, future research can focus on choosing the optimum electrical potential gradient to minimize the sorption of cationic surfactant micelles on the clay surface.
- Future research can also focus on nonionic surfactant flushing coupled with electrokinetic treatment. The presence of nonionic surfactant in the aqueous phase can improve the effective solubility of hydrocarbons, which is similar to anionic surfactant. In addition, nonionic surfactant micelles do not replace the cations sorbed on the clay surface and can migrate along with the pore-water flow.
- The choice of an optimum electrical potential gradient to retard and isolate hydrocarbon movement using cationic surfactants in clay soils.
- The amount of model diesel fuel injected into the columns to contaminate clays can be chosen to be less than 10 mL to minimize cracking of the clay columns during injection.
- The temperature effect of surfactant needs to be evaluated during soil remediation.
- To minimize the %RSD during SPME-GC-FID analysis, the thickness of the fibre coating needs to be carefully selected based on the distribution coefficient.

References

Acar, Y. B., and Hamed, J., 1991. "Electrokinetic Soil Processing in Waste Remediation and Treatment: Synthesis of Available Data." *Bulletin of Transportation Research, Record 1312*, Energy and Environmental Issues: 153-161.

Acar, Y.B., 1992. "Electrokinetic Cleanups." *Civil Engineering*, October: 58-60.

Acar, YB, Li, H., and Gale, R.J., 1993a. "Phenol Removal from Kaolinite by Electrokinetics." *Journal of Geotechnical Engineering*, 118(11): 1837-1851.

Acar, Y.B, and Alshawabkeh, A.N, 1993b. "Principles of electrokinetic Remediation." *Enviro. Sci. Technol.* 27(13): 2638-2647.

Alshawabkeh, A.N., and Acar, Y. B., 1992. "Removal of Contaminants from Soils by Electrokinetics: A Theoretical Treatise." *J. Enviro. Sci. Health*, A 27 (7): 1835-1861.

Arthur, C. L., and Pawliszyn, J., 1990. "Solid-Phase Microextraction with Thermal Desorption Using Fused Silica Optical Fibers." *Analytical Chemistry* 62 (19): 2145-2148.

Arthur, C. L., Killam, L.M., Buchholz, K.D., Pawliszyn, J., and Berg, J.R., 1992a. "Automation and Optimization of Solid-Phase Microextraction." *Analytical Chemistry* 64:1960-1966.

Arthur, C. L., Killam, L.M., Motlagh, S., Lim, M., Potter, D.W., and Pawliszyn, J., 1992b. "Analysis of Substituted Benzene Compounds in Groundwater Using Solid-Phase Microextraction." *Enviro. Sci. Technol.* 26(5):979-983.

Arthur C. L., Pratt, K., Motlagh, S., and Pawliszyn, J., 1992c. "Environmental Analysis of Organic Compounds in Water Using Solid Phase Micro Extraction." *Journal of High Resolution Chromatography* 15 (Nov.): 741-744.

Baetsle, L.H., 1969. "Migration of Radionuclides in Porous Media." Progress in Nuclear Energy, Series XII, Health Physics. Pergamon Press Ltd., London, U.K., p. 707-730.

Bear, J. 1972. "Dynamics of fluids in porous media." American Elsevier Publishing Company, Inc.

Brainard, J., and Beck B.D., 1993. "A Review of the Bioavailability of Petroleum Constituents." (From Kostecki, P.T and Calabrese E.J. 1993. "Hydrocarbon Contaminated Soils and Groundwater.").

Bruell, C. J., Segall, B. A., and Walsh, M. T., 1992. "Electroosmotic Removal of Gasoline Hydrocarbons and TCE from Clay." *J. Enviro. Eng.* 118(1): 68-82.

Canadian Council of Ministers of the Environment Secretariat (CCME), 1994. "Subsurface Assessment Handbook for Contaminated Sites." Minister of Supply and Services Canada.

Charbeneau, R.J., Bedient, P.B., and Loehr, R.C., 1992. "Groundwater Remediation." Technomic Publishing Company, Inc.

Chai, M, Arthur, C.L., and Pawliszyn, J., 1993. "Determination of Volatile Chlorinated Hydrocarbons in Air and Water With Solid-phase Microextraction." *Analyst* 118 (Dec.): 1501-1505.

Domenico, P.A., and Schwartz, F.W., 1990. "Physical and Chemical Hydrogeology." John Wiley and Sons, Inc.

Dzenitis J.M., 1997. "Soil Chemistry Effects and Flow Predication in Electroremediation of Soil." *Enviro. Sci. Technol.*31 (4): 1191-1197.

Edwards, D.A, Luthy, R.G., and Liu, Z., 1991. "Solubilization of Polycyclic Aromatic Hydrocarbons in Micellar Nonionic Surfactant Solutions." *Enviro. Sci. Technol.* 25(1): 127-133.

Eykholt, G. R., and Daniel, D.E., 1994. "Impact of System Chemistry on Electroosmosis in Contaminated Soil." *Journal of Geotechnical Engineering*, 120(5): 797-815.

Frankenburger, W.T., 1992. "The Need for a Laboratory Feasibility Study in Bioremediation of Petroleum Hydrocarbons." *Hydrocarbon Contaminated Soils and Groundwater.* Lewis Publishers, Inc.

Freeze, R., and Cherry J.A., 1991. "Groundwater." Prentice-Hall, Inc.

Gannon, O.K., Bibring, P., Raney, K., Ward, J.A., and Wilson, D.J., 1989. "Soil Clean Up by *in-situ* Surfactant Flushing. III. Laboratory Results." *Separation Science and Technology* 24)14): 1073-1094.

Gillham, R.W., and J.A. Cherry, 1982. "Contaminant migration in saturated unconsolidated geologic deposits." In: Recent trends in Hydrogeology. The Geological Society of America.

Jafvert, C. T., 1991. "Sediment- and Saturated-Soil-Associated Reactions Involving an Anionic Surfactant (Dodecylsulfate). 2. Partition of PAH Compounds among Phases." Environ. Sci. Technol. 25:1039-1045.

Jungermann, E., 1970. "Cationic Surfactants." Surfactant Science Series. Armour-Dial, Inc., New York.

Karsa, D.R., 1987. "Industrial Applications of Surfactants." Lankro Chemicals Limited, Manchester.

Kile, D.E. and Chiou, C.T., 1989. "Water Solubility Enhancements of DDT and Trichlorobenzene by Some Surfactants Below and Above the Critical Micelle Concentration." *Enviro. Sci. Technol.* 23(7): 832-838.

Knox, R. C., Sabatini, D. A., and Canter, L.W., 1993. "Subsurface Transport and Fate Processes." Lewis Publishers, Inc.

Kostecki, P.T, and Calabrese E.J. 1993. "Hydrocarbon Contaminated Soils and Groundwater." Lewis Publishers, Inc.

Lageman, R., Pool, M., and Seffinga, G., 1989. "Electro-Reclamation: Theory and Practice." *Chemistry and Industry*. p:585-590.

Lane, W.F., and Loehr, R.C., 1992. "Estimating the Equilibrium Aqueous Concentrations of Polynuclear Aromatic Hydrocarbons in Complex Mixtures." *Enviro. Sci. Technol.* 26(5):983-990.

Lorenz, P. B., 1969. "Surface Conductance and Electrokinetic Properties of Kaolinite Beds." *Clays and Clay Minetals*, 17: 223-231.

Louch, D., Motlagh, S., and Pawliszyn, J., 1992. "Dynamics of Organic Compound Extraction from Water Using Liquid-Coated Fused Silica Fibers." *Analytical Chemistry* 64: 1187-1199.

Lyman, W.J., Reidy, P.J., and Levy, B., 1992. "Mobility and Degradation of Organic Contaminants in Subsurface Environments." C. K. Smoley, Inc.

Manahan, S.E., 1993. "Fundamentals of Environmental Chemistry." Lewis Publishers.

Myers, D., 1992. "Surfactant Sience and Technology." VCH Publishers, Inc., New York, NY.

McCarty, P.L., 1990. "Ground Water and Soil Contamination Remediation: Towards Compatible Science, Policy, and Public Perception." *National Academy Press.* Washington, D.C. 1990.

Myers, D., 1992. "Surfactant Science and Technology." VCH Publishers, Inc., New York, NY.

Pamucku, S., and Wittle, J. K., 1992. "Electrokinetic Removal of Selected Heavy Metals from Soil." *Environmental Progress* 11(3): 241-250.

Parker, S.P., 1984. "McGraw-Hill, Dictionary of scientific and technical terms (third edition)." Mcgraw-hill Book Company.

Pennell, K.D., Abriola, L.M., and Weber, W.J., 1993. "Surfactant-Enhanced Solubilization of Residual Dodecant in Soil Columns." *Enviro. Sci. Technol.* 27(12): 2332-2340.

Peters, R. W., Montemagno, C.D., and Shem, L., 1992. "Surfactant Screening of Diesel-Contaminated Soil." *Hazardous Waste and Hazardous Materials* 9(2): 113-136.

Porter, M.R., 1991. "Handbook of Surfactants." Blackie & Son Ltd.

Potter, D.W., and Pawliszyn, J., 1994. "Rapid Determination of Polyaromatic Hydrocarbons and Polychlorinated Biphenyls in Water Using Solid-Phase Microextraction and GC/MS." *Environmental Science and Technology* 28(2):289-305.

Rouse, J. D., Sabatini, D.A. and Harwell, J. H., 1993. "Minimizing Surfactant Losses Using Twin-Head Anionic Surfactants in Subsurface Remediation." *Environmental Science and Technology* 27(10): 2072-2078.

Sanemasa, I.., Miyazaki, Y., Arakawa, S., Kumamaru, M., and Deguchi, T., 1987. "The Solubility of Benzene-Hydrocarbon Binary Mixtures in Water." *Bulletin of the Chemical Society of Japan* 60:517-523.

Sarna, L.P., Webster, G.R.B., Friesen-Fischer, M.R. and Sri Ranjan, R., 1994. "Analysis of Petroleum Components Benzene, Toluene, Ethylbenzene, and the Xylenes in Water by Commercially Available Solid-Phase Microextraction and Carbon-Layer Open Tubular Capillary Column Gas Chromatography." Journal of Chromatography A 677: 201-205.

Shapiro, A. P., and Probstein R. F., 1993. "Removal of Contaminants from Saturated Clay by Electroosmosis." *Environ. Sci. Technol.*, 27: 283-291.

Shirey, R.E., Wachob, G.D., and Pawliszyn, J., 1993. "Solventless Sample Preparation for Extracting Organic Compounds in Water." *Supelco Reporter* XII(4):8-11.

Soma, J., and Papadopoulos, K., 1997. "Deposition of Oil-in-Water Emulsions in Sand Beds in the Presence of Cetyltrimethylammonium Bromide." Environ. Sci. Technol. 31(4): 1040-1045.

Stelljes, M.E., and Watkin, G. E., 1993. "Comparison of Environmental Impacts Posed by Different Hydrocarbon Mixtures: A Need for Site-Specific Composition Analyses." (From Kostecki, P.T and Calabrese E.J. 1993. "Hydrocarbon Contaminated Soils and Groundwater.").

Stumm, W., and Morgan, J.J., 1981. "Aquatic Chemistry: An Introduction Emphasizing Chemical Equilibria in Natural Waters." *John Wiley & Sons, Inc.*

Thomas, S.P., 1996. "Surfactant-Enhanced Electrokinetic Remediation of Hydrocarbon-Contaminated Soils." M.Sc. Thesis in Biosystems Engineering, University of Manitoba, Winnipeg, Manitoba, Canada.

Thomas, S.P., Sri Ranjan, R., Webster, G.R.B., and Sarna, L.P., 1996b. " Protocol for the Analysis of High Concentrations of Benzene, Toluene, Ethylbenzene, and Xylene Isomers in Water Using Automated Solid-Phase Microextraction-GC-FID." *Environmental Science and Technology* 30(5):1521-1562.

Valsaraj, K.T., Gupta, A., Thibodeaux, L.J., and Harrison, D.P., 1988. "Partitioning of Chloromethanes between Aqueous and Surfactant Micellar Phases." *Water Research* 22(9): 1173-1183.

Walton, W.C., 1991. "Principles of Groundwater Engineering." Lewis Publishers, Inc.

West, C.C., and Harwell, J.H., 1992. "Surfactants and Subsurface Remediation." *Environmental Science and Technology* 26(12): 2324-2330.

Zhang, Z., and Pawliszyn, J., 1993. "Headspace Solid-Phase Microextraction." *Analytical Chemistry* 65:1843-1852.

Appendix I

Duncan's Multiple Range Test

Benzene

Analysis of Variance Procedure

Duncan's Multiple Range Test for variable: FID

NOTE: This test controls the type I comparisonwise error rate, not the experimentwise error rate

Alpha= 0.05 df= 28 MSE= 179744.1

Number of Means	2	3	4	5	6	7	8
Critical Range	709.1	745.1	768.3	784.9	797.3	807.0	814.8

Number of Means	9	10	11	12	13	14
Critical Range	821.2	826.4	830.8	834.5	837.6	840.2

Means with the same letter are not significantly different.

Duncan Grouping	Mean	N	TREAT
A	12328.3	3	60s
A			
A	12134.3	3	45s
B	11143.3	3	60v
C	10364.7	3	30s
D	9407.0	3	45v
D			
D	9336.3	3	30v
E	6830.7	3	5v
E			
E	6543.3	3	10v
E			
E	6245.3	3	15v
F	3447.0	3	1v
F			
F	2752.7	3	10s
F			
F	2710.0	3	15s
F			
F	2702.0	3	1s
F			
F	2682.0	3	5s

toluene

Analysis of Variance Procedure

Duncan's Multiple Range Test for variable: FID

NOTE: This test controls the type I comparisonwise error rate, not the experimentwise error rate

Alpha= 0.05 df= 28 MSE= 2399237

Number of Means	2	3	4	5	6	7	8	9	10	11	12	13	14
Critical Range	2591	2722	2807	2868	2913	2949	2977	3000	3019	3035	3049	3060	3070

Means with the same letter are not significantly different.

Duncan Grouping	Mean	N	TREAT
A	34190	3	60s
A A			
A	32510	3	60v
B	27203	3	45v
B B			
C B	26417	3	30v
C C			
C D	24308	3	30s
D D			
E D	22518	3	45s
E E			
E	21123	3	15v
F	17277	3	5v
F F			
F	16371	3	10v
G	10051	3	1v
G G			
H G	7686	3	10s
H H G			
H G	7576	3	5s
H G G			
H G	7558	3	15s
H H			
H	6870	3	1s

ethylbenzene

Analysis of Variance Procedure

Duncan's Multiple Range Test for variable: FID

NOTE: This test controls the type I comparisonwise error rate, not the experimentwise error rate

Alpha= 0.05 df= 28 MSE= 17207280

Number of Means	2	3	4	5	6	7	8	9	10	11	12	13	14
Critical Range	6938	7290	7517	7679	7801	7896	7973	8035	8086	8129	8165	8195	8221

Means with the same letter are not significantly different.

Duncan Grouping	Mean	N	TREAT
A	55152	3	60s
A			
A	55009	3	60v
B	46832	3	30v
B			
B	46518	3	45v
C	37876	3	15v
C			
C	37315	3	45s
C			
D C	34626	3	30s
D C			
D C	30547	3	10v
D			
D	28129	3	5v
E	16635	3	1v
E			
E	13820	3	15s
E			
E	12747	3	10s
E			
E	11520	3	5s
E			
E	11147	3	1s

p-xylene

Analysis of Variance Procedure

Duncan's Multiple Range Test for variable: FID

NOTE: This test controls the type I comparisonwise error rate, not the experimentwise error rate

Alpha= 0.05 df= 28 MSE= 14257976

Number of Means	2	3	4	5	6	7	8	9	10	11	12	13	14
Critical Range	6315	6636	6843	6990	7101	7188	7257	7314	7360	7399	7432	7460	7483

Means with the same letter are not significantly different.

Duncan Grouping	Mean	N	TREAT
A	54307	3	60v
A			
A	52701	3	60s
B	44944	3	45v
B			
B	42287	3	45s
B			
C B	41092	3	30v
C C			
C D	35596	3	30s
D			
D	32635	3	15v
E	23768	3	5v
E			
E	23755	3	10v
F	13325	3	1v
F			
F	12476	3	15s
F			
F	11238	3	10s
F			
F	9957	3	5s
F			
F	8872	3	1s

m-xylene

Analysis of Variance Procedure

Duncan's Multiple Range Test for variable: FID

NOTE: This test controls the type I comparisonwise error rate, not the experimentwise error rate

Alpha= 0.05 df= 28 MSE= 24520346

Number of Means	2	3	4	5	6	7	8	9	10	11	12	13	14
Critical Range	8282	8702	8974	9167	9313	9426	9517	9591	9652	9703	9746	9783	9814

Means with the same letter are not significantly different.

Duncan Grouping	Mean	N	TREAT
A	84708	3	60v
A A			
A	81619	3	60s
A A			
A	79600	3	45v
A A			
B A	76518	3	30v
B B			
B C	70314	3	45s
B C C			
B C	69497	3	15v
C C			
D C	66279	3	30s
D D			
D E	58480	3	10v
E E			
E	53020	3	5v
F	32589	3	1v
F F			
G F	25282	3	15s
G G			
G	23072	3	10s
G G			
G	20888	3	1s
G G			
G	20486	3	5s

o-xylene

Analysis of Variance Procedure

Duncan's Multiple Range Test for variable: FID

NOTE: This test controls the type I comparisonwise error rate, not the experimentwise error rate

Alpha= 0.05 df= 28 MSE= 21724360

Number of Means	2	3	4	5	6	7	8	9	10	11	12	13	14
Critical Range	7796	8191	8447	8629	8766	8872	8958	9028	9085	9134	9174	9208	9237

Means with the same letter are not significantly different.

Duncan Grouping	Mean	N	TREAT
A	77624	3	60v
A			
B A	70993	3	60s
B			
B C	67015	3	45v
C			
D C	60176	3	45s
D C			
D C	58977	3	30v
D			
D	52296	3	30s
D			
D	51914	3	15v
E	39302	3	10v
E			
E	37010	3	5v
F	22832	3	15s
F			
G F	20410	3	10s
G F			
G F	19280	3	1v
G F			
G F	17703	3	5s
G			
G	14087	3	1s

naphthalene

Analysis of Variance Procedure

Duncan's Multiple Range Test for variable: FID

NOTE: This test controls the type I comparisonwise error rate, not the experimentwise error rate

Alpha= 0.05 df= 28 MSE= 534780

Number of Means	2	3	4	5	6	7	8	9	10	11	12	13	14
Critical Range	1223	1285	1325	1354	1375	1392	1405	1416	1425	1433	1439	1445	1449

Means with the same letter are not significantly different.

Duncan Grouping	Mean	N	TREAT
A	10461.0	3	45v
A A	10276.7	3	60s
B A A	9629.3	3	60v
B B	8429.7	3	30v
D C C	7853.0	3	45s
D D	6795.7	3	30s
F E E	6037.0	3	15v
F F	5216.3	3	10v
H G G	4410.7	3	15s
H H	3514.7	3	10s
H I I	3417.3	3	5v
I I	2357.7	3	5s
J	764.0	3	1v
J J	391.0	3	1s

2-methylnaphthalene

Analysis of Variance Procedure

Duncan's Multiple Range Test for variable: FID

NOTE: This test controls the type I comparisonwise error rate, not the experimentwise error rate

Alpha= 0.05 df= 28 MSE= 608537

Number of Means	2	3	4	5	6	7	8	9	10	11	12	13	14
Critical Range	1305	1371	1414	1444	1467	1485	1499	1511	1521	1529	1535	1541	1546

Means with the same letter are not significantly different.

Duncan Grouping	Mean	N	TREAT
A	11387.3	3	45v
A			
A	10480.3	3	60v
A			
A	10202.0	3	60s
B	8334.0	3	30v
B			
B	7630.7	3	45s
C	6257.3	3	30s
C			
D C	5361.3	3	15v
D			
D E	4416.3	3	10v
E			
F E	3658.0	3	15s
F			
F G	2743.7	3	5v
F G			
F G	2704.3	3	10s
G			
H G	1717.3	3	5s
H			
H I	583.3	3	1v
I			
I	276.0	3	1s

phenanthrene

Analysis of Variance Procedure

Duncan's Multiple Range Test for variable: FID

NOTE: This test controls the type I comparisonwise error rate, not the experimentwise error rate

Alpha= 0.05 df= 28 MSE= 1160634

Number of Means	2	3	4	5	6	7	8	9	10	11	12	13	14
Critical Range	1802	1893	1952	1994	2026	2051	2071	2087	2100	2111	2120	2128	2135

Means with the same letter are not significantly different.

Duncan Grouping	Mean	N	TREAT
A	10708.0	3	45v
A			
B A	9792.3	3	60v
B			
B	8425.7	3	60s
C	5830.0	3	45s
C			
D C	5205.3	3	30v
D			
D E	3888.0	3	30s
D E			
D E F	3402.0	3	15v
E F			
G E F	2908.0	3	10v
G F			
G H F	1849.7	3	15s
G H F			
G H F	1581.0	3	5v
G H			
G H	1085.0	3	10s
H			
H	656.0	3	5s
H			
H	81.7	3	1v
H			
H	42.0	3	1s

IMAGE EVALUATION
TEST TARGET (QA-3)

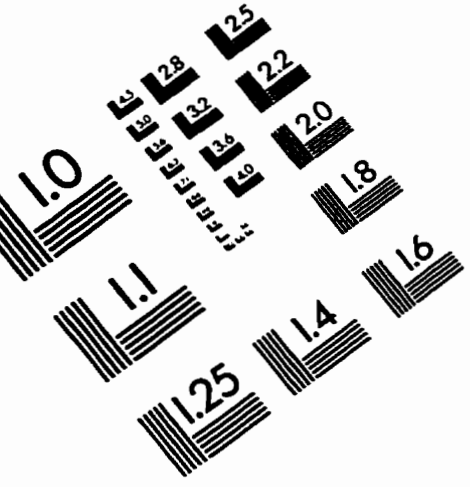

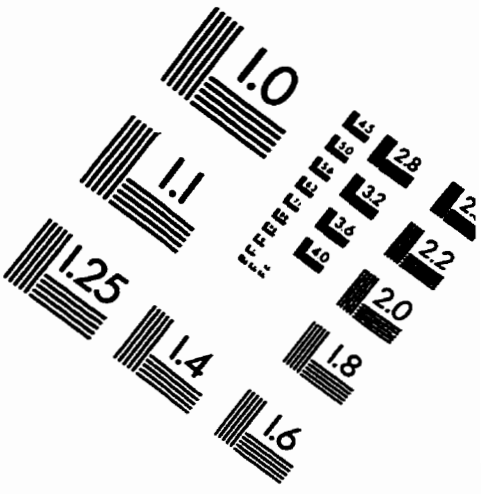

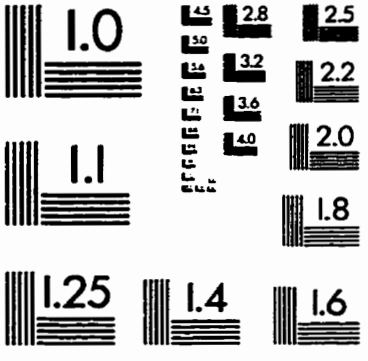

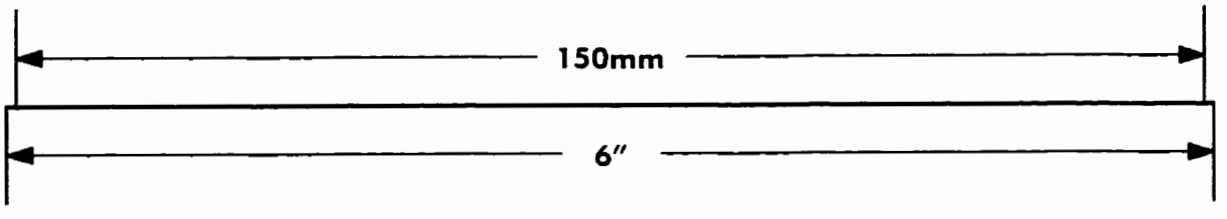

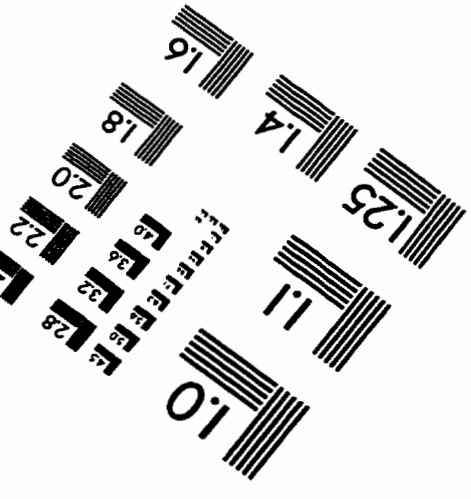

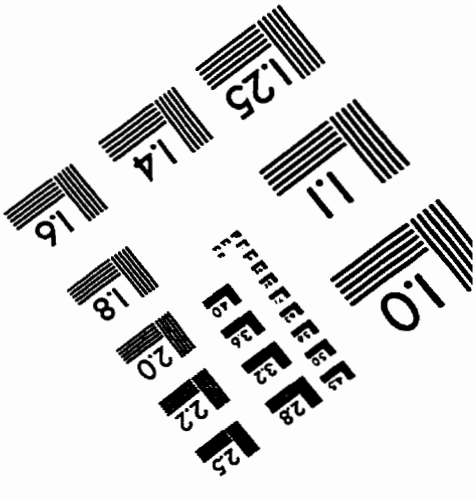

APPLIED IMAGE, Inc
1653 East Main Street
Rochester, NY 14609 USA
Phone: 716/482-0300
Fax: 716/288-5989